UNIVERSITY OF HAWAII LIBRARY
MAR 21 '62

This Issue Completes Volume 3

Journal of MOLECULAR BIOLOGY

EDITOR-IN-CHIEF: J. C. KENDREW

Volume III, Number 6, December 1961

ACADEMIC PRESS LTD., LONDON
ACADEMIC PRESS INC., NEW YORK

JOURNAL OF MOLECULAR BIOLOGY

EDITOR-IN-CHIEF

J. C. KENDREW, Peterhouse, Cambridge, England

ASSISTANT EDITOR

S. BRENNER, M.R.C. Unit, Cavendish Laboratory, University of Cambridge, England.

EDITORIAL BOARD

P. DOTY, Department of Chemistry, Harvard University, Cambridge, Mass., U.S.A.
A. F. HUXLEY, Department of Physiology, University College, London, England.
M. MESELSON, Biological Laboratories, Harvard University, Cambridge, Mass., U.S.A.
R. L. SINSHEIMER, Division of Biology, California Institute of Technology, Pasadena, Cal., U.S.A.
J. D. WATSON, Biological Laboratories, Harvard University, Cambridge, Mass., U.S.A.
M. H. F. WILKINS, Physics Department, King's College, London, England.

ADVISORY BOARD

S. BENZER, Purdue University, U.S.A.
M. CALVIN, University of California, Berkeley, U.S.A.
F. H. C. CRICK, University of Cambridge, England.
J. F. DANIELLI, King's College, London, England.
A. ENGSTRÖM, Karolinska Institutet, Stockholm, Sweden.
A. D. HERSHEY, Carnegie Institute, Cold Spring Harbor, U.S.A.
F. JACOB, Pasteur Institute, Paris, France.
A. KORNBERG, Stanford University, Stanford, California, U.S.A.
C. LEVINTHAL, Massachusetts Institute of Technology, Cambridge, Mass., U.S.A.
S. E. LURIA, Massachusetts Institute of Technology, Cambridge, Mass., U.S.A.
D. MAZIA, University of California, Berkeley, U.S.A.
P. B. MEDAWAR, University College, London, England.
L. E. ORGEL, University of Cambridge, England.
M. F. PERUTZ, University of Cambridge, England.
R. D. PRESTON, University of Leeds, England.
G. N. RAMACHANDRAN, University of Madras, India.
A. RICH, Massachusetts Institute of Technology, Cambridge, Mass., U.S.A.
G. SCHRAMM, Max-Planck Institut, Tübingen, Germany.
F. S. SJØSTRAND, Karolinska Institutet, Stockholm, Sweden.
I. WATANABE, Institute for Virus Research, Kyoto University, Japan.
R. C. WILLIAMS, University of California, Berkeley, U.S.A.

Published by Academic Press Inc. (London) Limited

Volume III, 1961: 128*s.* 6*d.* ($18.00)

Subscription orders should be sent to Academic Press Inc. (London) Limited, Berkeley Square House, Berkeley Square, London, W.1, with the exception of those originating in the U.S.A., Canada, Central America, and South America; these should be sent to Academic Press Inc., 111 Fifth Avenue, New York 3, N.Y.

Copyright © 1961, by Academic Press Inc. (London) Limited

J. Mol. Biol. (1961) **3**, 711–716

Equilibrium Sedimentation in Density Gradients of DNA Preparations from Animal Tissues

Saul Kit

Section of Nucleoprotein Metabolism, Department of Biochemistry, The University of Texas M. D. Anderson Hospital and Tumor Institute, Houston, Texas, U.S.A.

(*Received 1 June 1961*)

Experiments on the equilibrium sedimentation in CsCl density gradients of the DNA from adult mouse tissues, three tumors, mouse tissue culture cells, and from three different tissues of the monkey, the guinea-pig, and the alligator are described. The DNA banding patterns were characteristic for each species. Bimodal distributions were observed for mouse and guinea-pig DNA. The mean buoyant densities of the principal and the satellite mouse DNA bands were 1·701 and 1·690 g cm^{-3}, respectively. The mean buoyant density of the major guinea-pig DNA band was 1·697 g cm^{-3}, and that of the minor band was 1·703 g cm^{-3}. A single band was found in the case of monkey or alligator DNA but these differed in mean buoyant density and in band variance. The mean buoyant densities and the band variance were the same for the differentiated tissues of a given animal species.

1. Introduction

Equilibrium sedimentation experiments in density gradients (Meselson, Stahl & Vinograd, 1957) have revealed that the banding patterns of DNA preparations are highly characteristic for various species of bacteria (Doty, Marmur & Sueoka, 1959; Rolfe & Meselson, 1959), algae, plants, invertebrates (Sueoka, 1961), and for certain species of higher animals (Kit, 1961*a*,*c*; Sueoka, 1961). The experiments to be described provide data on the banding of DNA from a number of different adult tissues of mice, monkeys, guinea-pigs and alligators, and from the DNA of murine neoplasms and tissue culture cells. The DNA banding patterns of tissues from any given species were very similar. These results confirm and extend previous observations which have indicated that DNA preparations from adult tissues and from tumors of mice are similar with respect to average nucleotide composition (Kit, 1960*b*), chromatography on substituted anion exchangers (Kit, 1960*b*,*c*), and thermally induced hyperchromicity (Kit, 1960*d*). Anion exchangers have provided a means of discriminating between DNA molecular types on the basis of size, while optical density-thermal denaturation curves have been employed to estimate the range of heterogeneity of composition. The present centrifugation experiments were undertaken since the banding of DNA in CsCl density gradients depends upon the combined effects of heterogeneity of size and composition (Doty *et al.*, 1959; Meselson *et al.*, 1957; Rolfe & Meselson, 1959; Sueoka, 1959).

2. Materials and Experimental Methods

(a) *DNA preparation*

DNA was prepared from 0·3 to 3 g wet weight of tissues by the *p*-aminosalicylate : phenol method of Kirby (1957) with the following modifications:

(a) The aqueous tissue extracts containing the DNA were re-extracted with 0·25 vol. 90% phenol.
(b) After each precipitation step, the DNA was dissolved in a minimal volume of 4% sodium acetate containing 0·15 M-NaCl, 10^{-3} M-EDTA (ethylenediaminetetra-acetate) and 10^{-3} M-phosphate, pH 7.
(c) After incubating for 18 hr with RNase, the DNA solution was shaken with 0·25 vol. phenol and reprecipitated by the addition of 1 vol. ethylene glycol monoethyl ether.
(d) The DNA was further deproteinized with 0·5 vol. chloroform: octanol (9 : 1).
(e) Following the removal of contaminating polysaccharides by treatment with phosphate and ethylene glycol monomethyl ether (Kirby, 1957), the DNA solution (1 to 10 ml.) was dialysed for 30 hr at 4°C against 2 litres of 1% sodium acetate. The acetate solution was changed 6 times.
(f) The final DNA precipitate was dissolved in 0·15 M-NaCl, 10^{-3} M-EDTA, 10^{-3} M-phosphate, pH 7.

The physico-chemical properties of the high molecular weight DNA solutions prepared in this way have been described (Kit, 1960*a*,*b*,*d*). Approximately 90% of the DNA was extracted from the tissues by the *p*-aminosalicylate treatment and the final DNA yield was 70 to 80%.

(b) *Density gradient centrifugation*

Cesium chloride solutions of DNA (0·7 ml.) were centrifuged for 24 hr at 44,770 rev/min at 25°C in the model E ultracentrifuge equipped with RTIC temperature control and ultraviolet optics. The densities of the cesium chloride solutions were determined pycnometrically or from the refractive indices of the solutions. In the latter instance, the following equation, which relates the density of the cesium chloride solution to the refractive index at 25°C using sodium D light, was employed (Ifft, Voet & Vinograd, 1961; Sinsheimer, 1959, personal communication):

$$\rho^{25} = 10{\cdot}8601 n_D^{25} - 13{\cdot}4974$$

The buoyant densities of all animal DNA preparations were calculated relative to a *Streptomyces viridochromogenes* DNA marker (1·729 g cm^{-3}). The following equation was used to calculate the buoyant density of DNA at 44,770 rev/min:

$$\rho^{25} = \rho_0^{25} + 0{\cdot}0092\,(r^2 - r_0^2)$$

where ρ_0 equals the mean buoyant density in g cm^{-3} of the *Streptomyces viridochromogenes* DNA band and r_0 equals the distance in cm from the center of rotation to the center of the *Streptomyces* DNA band (Meselson *et al.*, 1957; Sueoka, 1961).

The Joyce-Loebl double beam automatic recording microphotodensitometer (Mark IIIB) was employed to trace all ultraviolet photographs of the DNA bands. The DNA band variance (σ_ρ) was calculated from the second moment about the mean† of the distribution by appropriate statistical methods (Arkin & Colton, 1956).

† The second moment about the mean is defined as follows:

$$\mu_2 = \nu_2 - \nu_1^2$$

where

$$\nu_2 = \frac{\Sigma f(d)^2}{N}$$

and

$$\nu_1 = \frac{\Sigma(fd)}{N}$$

ν_1 equals the first moment of a frequency distribution as measured about any arbitrary origin and ν_2 equals the second moment about an arbitrary origin.

3. Results and Discussion

(a) *Density gradient centrifugation of mouse DNA*

When DNA preparations from mouse tissue were centrifuged to equilibrium in CsCl density gradients two bands were formed (Plate I and Fig. 1). The principal mouse DNA band had a mean buoyant density of about 1·701 g cm^{-3} while the second band had a density of about 1·690 g cm^{-3}. The two characteristic DNA bands have been observed for 5 adult mouse tissues, 3 mouse neoplasms, and strain LM tissue culture cells (Table 1). The lighter DNA band accounts for approximately 8% of the

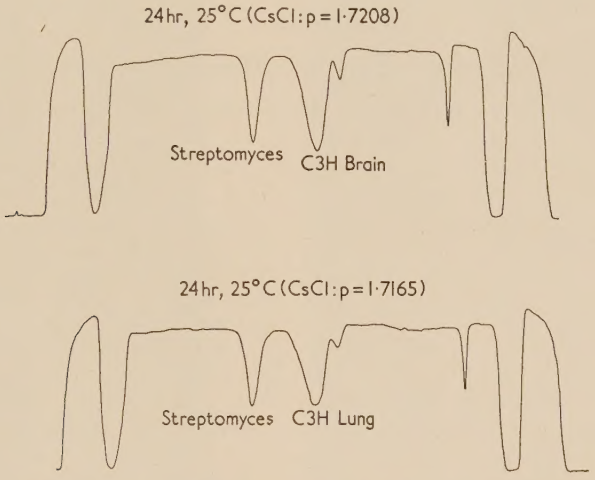

FIG. 1. Microdensitometer tracing of photograph of the banding of mouse DNA and Streptomyces DNA after density gradient centrifugation. See Plate I.

total DNA. Heat denaturation experiments suggest that the 1·690 g cm^{-3} band is double-stranded. Since a linear relationship exists between the molar content of guanine plus cytosine (G + C) of DNA preparations and their mean buoyant densities (Doty *et al.*, 1959; Rolfe & Meselson, 1959), the data of Table 1 provide an additional confirmation of the fact that the average nucleotide compositions of DNA preparations from various mouse tissues are the same (Kit, 1960*b*,*d*).

The standard deviations (σ_ρ) of all mouse DNA bands were also very similar (Table 1). Meselson *et al.* (1957) have demonstrated that the square of the standard deviation of the DNA distribution of CsCl density gradients is inversely proportional to the number average molecular weight. Molecules of uniform density are distributed in the band as a result of thermal agitation. However, if a distribution of densities is superimposed upon the molecules, the band is broadened and the variance increases. The σ_ρ values for all mouse DNA preparations ranged from 0·0042 to 0·0046 g cm^{-3}. The standard deviation σ_{GC}, expressed on a molar (G + C) scale, is approximately 10 times the value of σ_ρ (Rolfe & Meselson, 1959). Hence, an upper limit to the heterogeneity of composition for one standard deviation from the mean, σ_{GC}, may be set at about 0·043 moles (G + C). The actual value of σ_{GC} lies below the calculated upper bound because thermal motion of the DNA molecules contributes significantly to the band width.

It has been demonstrated that the total DNA band variance (σ_T^2) is equal to the

sum of the variance (σ^2_{DN}) due to density heterogeneity and the variance (σ^2_{BN}) caused by Brownian motion of the molecules (Doty *et al.*, 1959; Sueoka, 1959):

$$\sigma^2_T = \sigma^2_{DN} + \sigma^2_{BN}$$

Assuming that the number average molecular weight of the cesium salt of mouse DNA is 6,000,000 (Kit, 1960*d*; Sueoka, 1959), one may calculate that the σ_{DN} is about 0·00299 g cm^{-3}. The estimated standard deviation on the molar (G + C) scale is then 0·03. This value is of the same order of magnitude (0·028) as was calculated from the optical density-temperature curves (Kit, 1960*d*). The results contra-indicate gross differences between DNA preparations from adult tissues of the same animal or between DNA preparations from normal mouse tissues and tumors. The possibility remains,

TABLE 1

Gradient centrifugation of C3H mouse DNA in CsCl

Tissue	Band 1 ρ^{25}	Band 1 σ_ρ	Band 2† ρ^{25}
LM tissue culture cells (C3H)	1·701	0·0043	1·690
Liver	1·701	0·0042	1·690
Brain	1·701	0·0042	1·690
Kidney	1·701	0·0042	1·690
Spleen	1·701	0·0046	1·690
Lung	1·701	0·0044	1·690
6C3HED-DBA to C3H (hypotetraploid lymphoma)	1·701	0·0042	1·690
Lettre-Ehrlich‡ (hyperdiploid carcinoma)	1·701	0·0042	1·689
Ehrlich‡ (hypotetraploid carcinoma)	1·701	0·0042	1·689

All values expressed as g cm^{-3}.

Two micrograms of DNA dissolved in CsCl (density, 1·70 to 1·71 g cm^{-3}) were centrifuged for 24 hr at 44,770 rev/min at 25°C in the Spinco model E ultracentrifuge. The density of the mouse DNA band was calculated from a *Streptomyces viridochromogenes* DNA marker having a density of 1·729 g cm^{-3}.

† About 8% of the total DNA.

‡ The carcinomas were grown in Swiss albino mice. The mouse strain in which the tumors originated has not been ascertained.

however, that small differences in DNA chain length, nucleotide composition, or base sequence exist. Such differences are below the resolving power of the methods so far employed. It is worth emphasizing that the tissue culture cells and the tumors used in the present study have had a long evolutionary history and have been subjected to varied environmental selection pressures and to mutagenic agents. Profound differences have been observed between the chromosome sets of these cells and normal adult mouse cells.

(b) *DNA banding of adult tissues of other animal species*

The conclusions concerning the DNA of differentiated tissues of mice are borne out by experiments on the DNA of other animal species. Table 2 shows the results of

C3H Lung

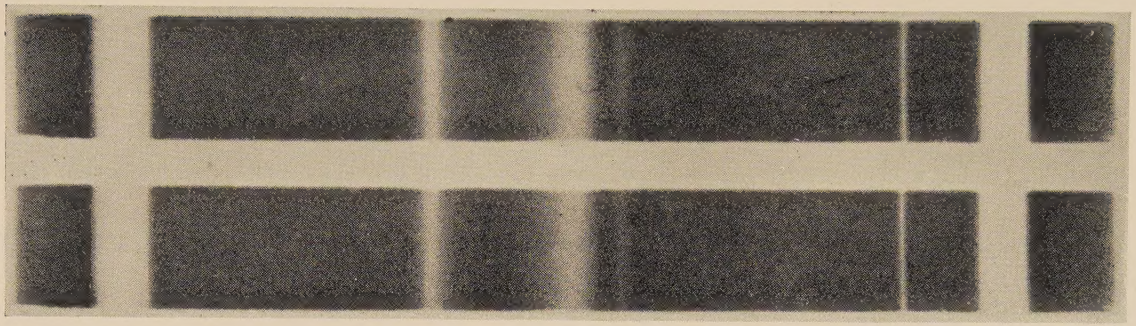

C3H Brain

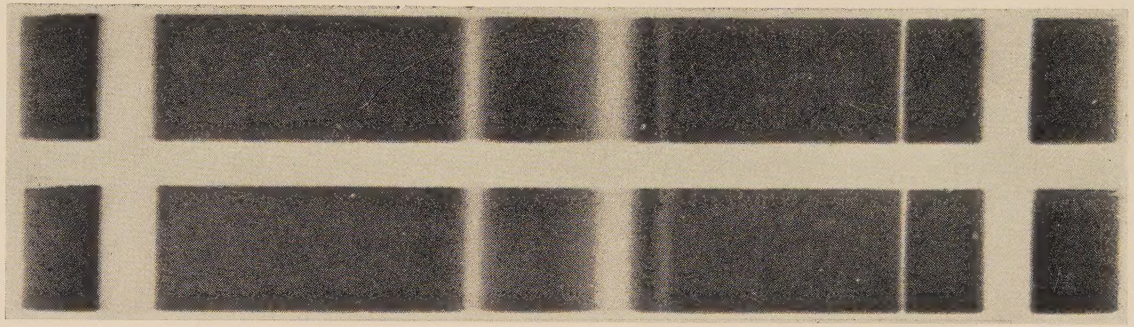

PLATE I. Resolution of *Streptomyces viridochromogenes* DNA and mouse DNA by density gradient centrifugation. The photograph was taken after centrifugation for 24 hr at 25°C and 44,770 rev/min. The *Streptomyces* band ($\rho^{25} = 1{\cdot}729$ g cm^{-3}) appears at the left. Two bands with mean densities of 1·701 and 1·690 g cm^{-3} were obtained with mouse DNA. The initial densities of the CsCl solutions were: (a) mouse brain, 1·7208 g cm^{-3}; (b) mouse lung, 1·7165 g cm^{-3}. (*Streptomyces viridochromogenes* DNA was obtained through the kindness of Doctors Julius Marmur and Carl Schildkraut.)

[*To face page* 714

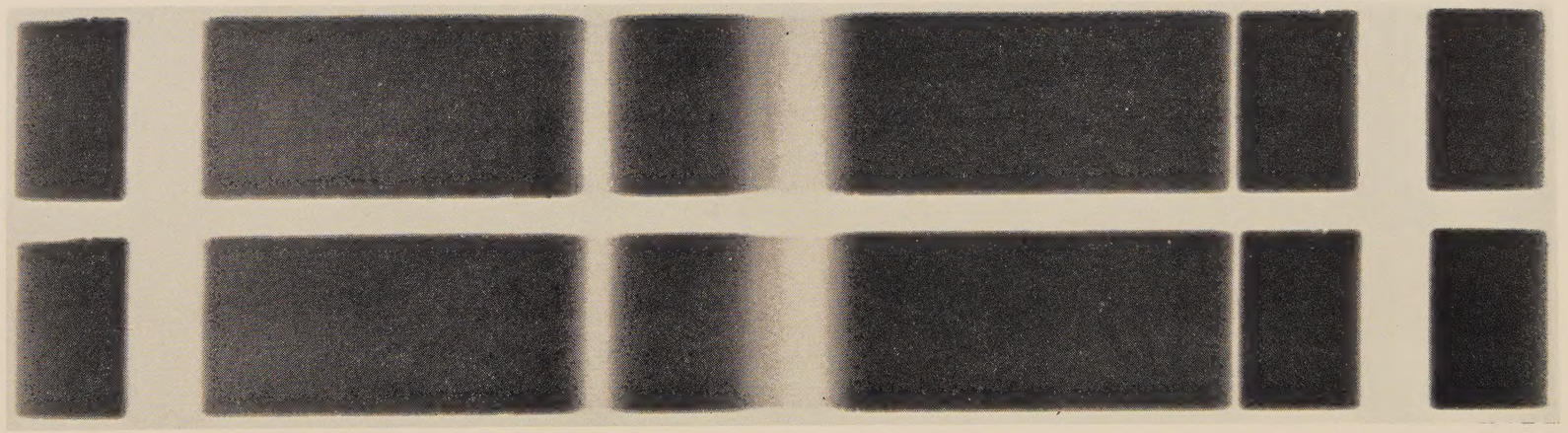

PLATE II. Resolution of *Streptomyces viridochromogenes* and guinea-pig liver DNA by density gradient centrifugation. The effective buoyant density of the *Streptomyces* DNA band at the left is 1·729 g cm^{-3}. Two overlapping bands are seen for guinea-pig DNA with mean densities of 1·703 and 1·697 g cm^{-3}. The initial density of the CsCl solution was 1·713 g cm^{-3}.

experiments on monkey, guinea-pig, and alligator DNA preparations. In contrast to the mouse DNA, only *one* DNA band was observed for monkey or alligator DNA. The buoyant densities of the DNA from monkey tissues were approximately the same as those from mouse tissues but the buoyant densities of DNA from alligator tissues were slightly greater than those from mouse tissues. The standard deviations of monkey DNA bands were approximately the same as mouse DNA (Table 2). The σ_ρ

TABLE 2

DNA buoyant densities of monkey, guinea-pig, and alligator tissues

Tissue		Band 1 ρ^{25}	Band 1 σ_ρ	Band 2 ρ^{25}
Monkey (Rhesus)	liver	1·700	0·0048	
	brain	1·700	0·0046	
	spleen	1·700	0·0045	
Guinea pig	liver	1·703		1·698
	kidney	1·704		1·697
	spleen	1·703		1·696
Alligator	liver	1·704	0·0038	
	brain	1·703	0·0035	
	spleen	1·703	0·0037	

All values expressed as g cm^{-3}.

values of rat, golden hamster, human, and rabbit DNA also approximate those of mouse or monkey DNA (Kit, 1961*b*,*d*). The standard deviation of the alligator DNA band was, however, less than that of mouse or monkey DNA (Tables 1 and 2). The

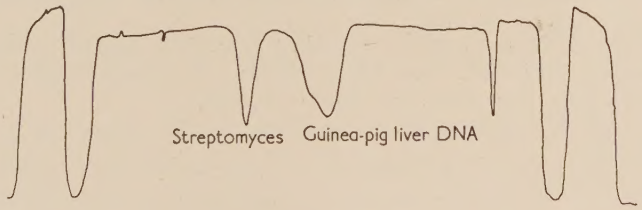

FIG. 2. Microddensitometer tracing of photograph of the banding of guinea-pig liver DNA and *Streptomyces* DNA after density gradient centrifugation. See Plate II.

σ_ρ values of frog liver DNA (0·0027 g cm^{-3}), Chinese hamster DNA (0·0037 g cm^{-3}), *Streptomyces viridochromogenes* DNA (0·0031 g cm^{-3}), and *Serratia marcescens* DNA (0·0033 g cm^{-3}) are also smaller than the σ_ρ values of murine or monkey DNA (Kit, 1961*d*). The standard deviation in all the above instances seems remarkably small when one considers that animal tissue DNA consists of a heterogeneous collection of about 3×10^5 molecular types. A number of bacterial species and animal tissues

Also many features may remain undetected if they lie in the shadow. Finally shadowing gives information only about the shape of the objects and not about the distribution of chemical groups in them. Staining in principle is not subject to these limitations and appears therefore the better approach to problems of molecular structure. For a rational design of experiments it is important to know the amount of stain necessary for visibility. Our studies are a guide in this direction.

It is known that atoms with high atomic numbers are the best electron scatterers (Mott & Massey, 1953) and so chemical groups containing them would be expected to be the best stains for use in electron microscopy. Indeed many such chemicals have been successfully used as stains in tissue sections and molecular aggregates. Recently we have found that uranyl ions form strong complexes with DNA (Zobel & Beer, 1961). In this paper we show that on staining DNA with uranyl ions its electron density becomes adequate for high resolution electron microscopy.

In our procedure, DNA molecules that had been transferred to grids covered with supporting membranes were stained by floating the grids face down on solutions of uranyl salts. After scattering polystyrene spheres on them, the grids were shadowed with platinum. DNA fibrils which lay so that they passed through the shadows cast by the polystyrene spheres were used for studying staining. Outside the shadow they were visible as in the usual shadowed preparations. From measurements in this region it was possible to determine the diameter of the DNA fibrils. The fibrils could then be followed into the shadow region where their visibility was due entirely to the density of the stain and the fibril.

2. Methods

DNA was obtained from T2 phage by phenol extraction (Mandell & Hershey, 1960). Three kinds of supporting membranes were used to cover the grids. These were: first, the grids with beryllium evaporated over formvar (marketed by the Bitter Roots Specialty Company, Hamilton, Montana); second, grids covered with the styrene-4-vinylpyridine copolymer described by Birbeck & Stacy (1959); and finally, grids covered with a film of evaporated carbon.

DNA was transferred to the grids as described previously (Beer, 1961). The grid was streaked, membrane side down, along the surface of a solution of DNA in volatile buffer. The volatile buffer used with the beryllium coated grids was that recommended by Hall & Litt (1959). This contained 0·1 M-ammonium acetate and 0·05 M-ammonium carbonate at pH 8·5. With the other grids 0·1 M-ammonium acetate/acetic acid buffer at pH 6·3 was used.

The DNA on the grids was stained by floating the grids face down for 5 to 30 min on solutions of uranyl salts with pH adjusted to 3·5 and having various concentrations. After staining they were either rinsed in anhydrous ether or dabbed dry by placing them face down on filter paper.

To avoid washing out the stain, polystyrene spheres were put on the grids dry by dabbing them in the dry powder. Excess spheres were removed, first by scraping with a fine spatula, then by blowing parallel to the surface of the grid a few gentle puffs from a rubber bulb. The distribution of spheres on the grid was easily checked in the light microscope. In the present study their diameter was usually 0·5 μ.

The grids were shadowed with platinum at an angle of 5 : 1, care being taken that the shadowing direction was perpendicular to the direction of streaking.

Several of the micrographs were taken at an electron optical magnification of 15,000 $\times$ and 30,000 $\times$ with an accelerating voltage of 50 kv on an RCA EMU 3C electron microscope with a single condenser lens and a 250 μ condenser aperture. The condenser current used was from 1·5 to 2 times the crossover value. The objective aperture in the back focal

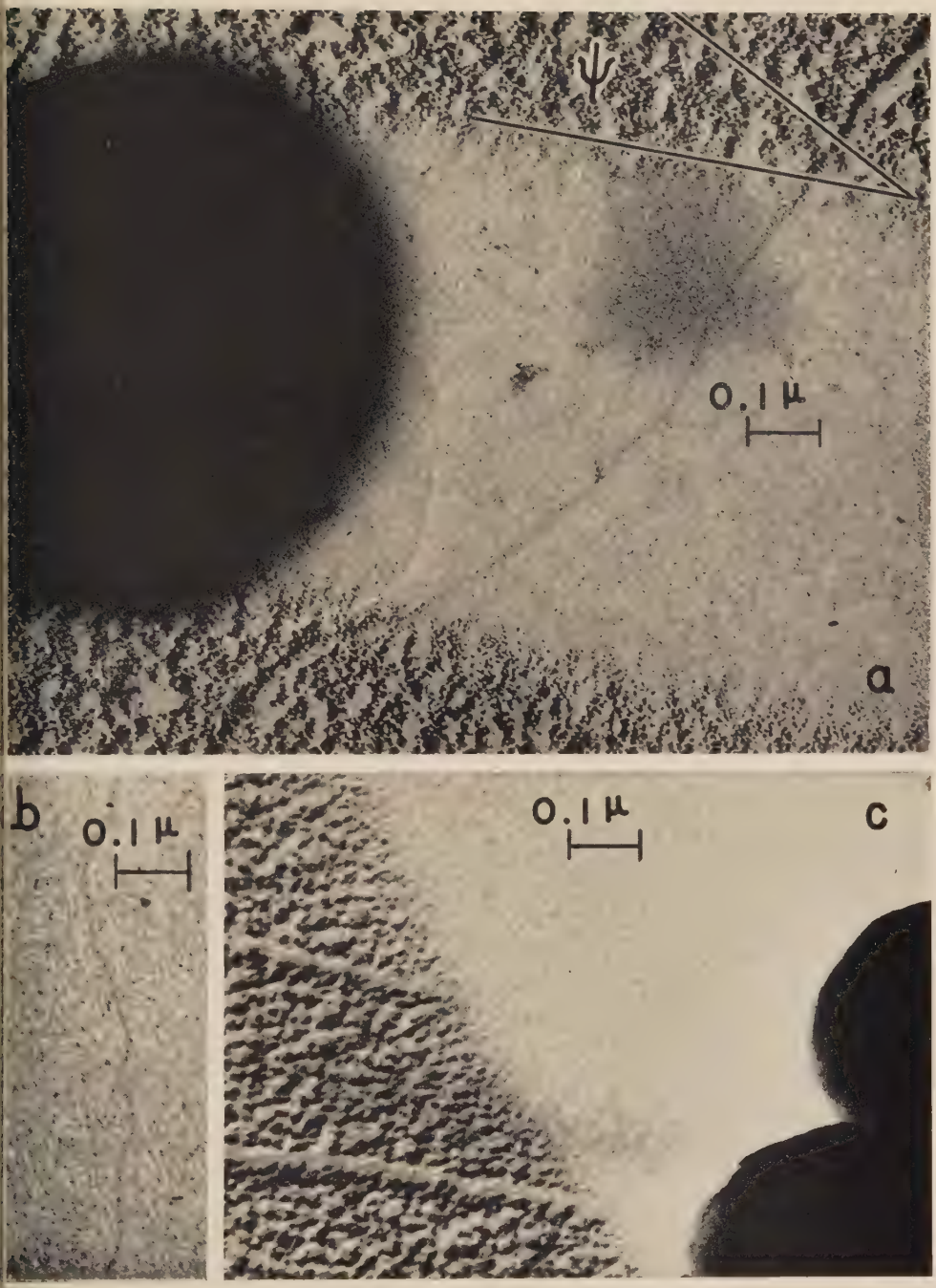

PLATE I(a). Stained DNA fibril passing through shadow cast by polystyrene sphere. The direction of shadowing deviates by the angle Ψ from the line perpendicular to the fibril. Diameter of the fibril is 50 Å showing it is an aggregate. Substrate is beryllium-coated formvar; stained in 0·1 M-uranyl nitrate at pH 3·5. ×100,000.

(b) Unshadowed DNA fibril after staining with 0·12 M-uranyl nitrate. ×100,000.

(c) Unstained DNA fibril. ×100,000.

[*To face page* 718

PLATE II. DNA molecule stained with 0·12 M-uranyl nitrate on evaporated carbon substrate. Diameter as deduced from staining as well as from dimension of shadow is about 20 Å. 380,000×.

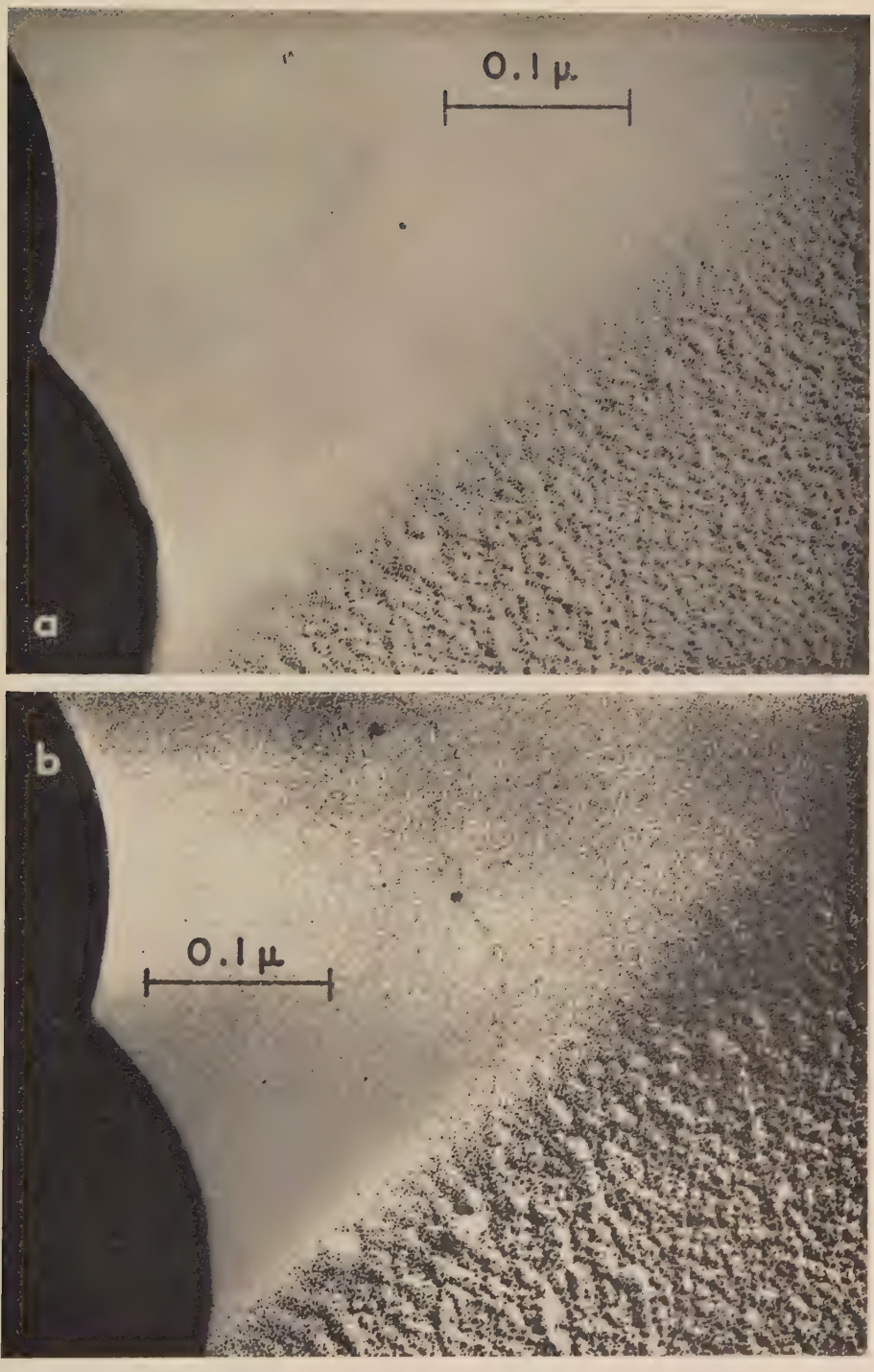

Plate III. DNA molecule stained in 0·0012 M-uranyl nitrate.

(a) Printed directly on grade 5 Kodabromide photographic paper.

(b) Printed twice in succession on intermediate Kodak contrast lantern slide plates, then printed on grade 3 Kodabromide photographic paper. ×250,000.

plane was 35 μ in diameter. The high contrast specimen holder was used so that the focal length of the objective was 4·9 mm with a numerical aperture of $3{\cdot}5 \times 10^{-3}$.

All the micrographs used in the quantitative estimation of density were taken on a Siemens Elmiskop I at 80 kv accelerating voltage using a 30 or 50 μ objective aperture and a 400 μ condenser aperture with double condenser illumination at crossover. The instrumental magnification was 80,000×.

Kodak contrast lantern slide plates were developed at 68°F for 5 min in Kodak D11 developer and were analysed on a Joyce Loebl microdensitometer. On each day of microscopy the plate characteristic was determined by taking five exposures on one plate at 4, 1, 2, 4, and 8 sec with the condenser current set far from the crossover value to minimize variation in the illumination. This variation as given by the repeated 4-second exposure was less than 10%.

Astigmatism was corrected to better than 0·1 μ by the method of O'Hara & Beer (1961). All micrographs were selected from focal series with a separation of 0·1 μ in the focal setting. Micrographs were again contact printed on Kodak contrast lantern slide plates and developed in D11 developer to obtain a plate with over twice as much contrast as the original. Then the fibril image was traced using the Joyce Loebl microdensitometer with a slit width corresponding to 5 Å on the plate.

The contrast was estimated from the height of the peak of the densitometer trace above the average background. This height was compared with the density difference $(d_2 - d_1)$ resulting from two exposures which differ by a factor of two. Since for the plate it can be assumed that the plate characteristic is linear:

$$(d_2 - d_1) = \gamma \log 2$$

also

$$h = \gamma \log (1 + K)$$

where K is the contrast as defined by Leisegang (1956)
hence

$$\log (1 + K) = \frac{\cdot 301h}{d_2 - d_1}$$

Where their contrast was low micrographs were printed twice in succession on Kodak lantern slide contrast plates. Prints obtained from the second high contrast intermediate plate had several times more contrast than when printed directly.

3. Results

(a) *Studies on DNA aggregates*

If the concentration of the DNA solution is of the order of 1 mg/ml. most of the DNA fibrils deposited on the film are too thick to be interpreted as single molecules. Their diameters as deduced from the shadowing angle and the observed shadow width are frequently as high as 50 Å. When these thick DNA fibrils are stained in 0·1 M-uranyl acetate or nitrate with the pH adjusted to 3·5 the strands become visible in the shadow of the polystyrene sphere. A typical micrograph is shown in Plate I(a). An unstained fibril of the same diameter is shown in Plate I(c).

It is clear from a comparison of the two plates that fibrils acquire great density on staining with uranyl salts. The unstained control shows no visible density and so clearly the increased contrast is a result of staining. The possibility that the density is due to scattering of platinum into the shadow is definitely disproven by the ready visibility of fibrils which have been stained but not shadowed as illustrated in Plate I(b). Thus it can be said that uranyl staining leads to increased density of DNA fibrils.

By following the shadowed portion of the unstained fibril it is possible to determine its exact location in the shadow of the sphere. By tracing across this region with a

densitometer an upper limit can be set on the contrast of the fibril. For an unstained fibril with a height of 50 Å the contrast in the unshadowed part was less than 3%.

Micrographs such as those of Plate I(a) make possible two independent measurements of the thickness of the same fibril: first, by measuring directly the average width of the dark line in the unshadowed region behind the polystyrene sphere; and second, by measuring the shadow width perpendicular to the fibril and calculating its height by using the known angle of shadowing. When the shadowing direction deviated from accurately perpendicular to the DNA fibril the measured shadow width was divided by the cosine of the angle of this deviation to give the corrected shadow width. This angle of deviation is marked Ψ on Plate I(a). Both these determinations of fibril diameter were made on twenty micrographs by three independent observers. Their results differed by less than 30% on any one measurement. The results of one of them is given in Fig. 1. The diameter determined by measuring the width of the stained fibril in the shadow of the sphere was consistently greater than that calculated

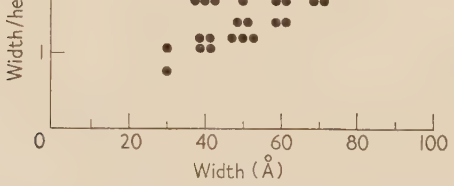

Fig. 1. Ratio of fibril width to fibril height for fibrils of different width.

from the shadow dimension with the ratio of the two apparent dimensions varying from 1 to 2. These ratios were generally higher for the thicker strands. This indicates a slight flattening of the fibrils in the plane of the film and is probably due to the adsorption of the DNA to the substrate. The apparent flattening could of course result from a consistent error in one or both methods of measuring the fibril dimension However, such errors should be less important for the large fibrils. Since these are the ones for which the ratios given in Fig. 1 are greatest, the slight spreading of the fibril in the plane of the film is believed to be real.

(b) *Dimensions of fibrils obtained from dilute solutions*

DNA fibrils when deposited on grids from solutions with DNA concentrations less than 5 μg/ml. have dimensions of about 20 Å as deduced from the shadow width When the DNA is stained in solutions of uranyl salts at pH 3·5 the contrast of the fibrils increases markedly in the shadow of the polystyrene sphere. This is clearly illustrated in Plate II. For the molecule shown the dimension of the shadow is 110 ± 25 Å. The roughness of the substrate makes a more precise measurement of the shadow impossible. Since the shadowing angle is 5 : 1 the inferred fibre dimension is about 22 ± 5 Å. The densitometer trace taken across the stained fibre is shown in Fig. 2(a). The width of the stained fibre as determined directly from the trace is about 20 ± 5 Å.

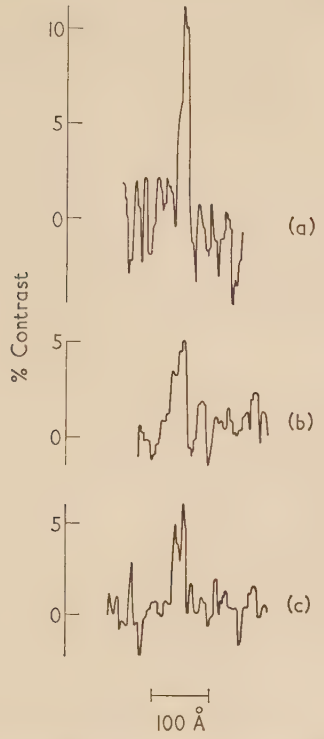

FIG. 2. Microdensitometer traces across DNA fibrils stained with uranyl nitrate solutions at pH 3·5. Concentration of stain solution was (a) 0·12 M, (b) 0·012 M, (c) 0·0012 M.

(c) *Contrast of stained DNA molecules*

The density of DNA fibres depends on the concentration of the stain solution. Plate II shows a micrograph of a fibre after staining in uranyl nitrate solution at 0·12 M concentration. Plate III(a) shows a fibre after staining in solutions with a concentration of 0·0012 M. Plate III(b) shows the same micrograph after printing twice successively on Kodak lantern slide contrast plates and obtaining the print from the second intermediate negative. The quantitative value of the contrast can be obtained by measuring the height of the densitometer trace peak. This has been done after staining with both uranyl acetate and uranyl nitrate at concentrations below 0·12 M and at pH 3·5. One set of densitometer traces for uranyl nitrate concentrations of 0·12 M, 0·012 M and 0·0012 M is shown in Fig. 2. At lower concentrations the quantitative values of the contrast become very unreliable on account of the noise of the background. The eye can discern a line in a background of dots since in effect it averages out the background. With a densitometer, however, if one uses a short slit the dots of the background become important whereas with a long slit inaccuracies arise since the molecules are often not straight. Therefore no quantitative estimates of density were made at the low contrast resulting from stain solutions below 10^{-3} M.

The results for uranyl nitrate are summarized in the curve of Fig. 3. The vertical lines represent the range of contrast obtained in a number of determinations. It is seen that at 0·12 M the contrast varies from about 6 to 12%. At the concentrations

of 0·012 and 0·0012 M the contrast values are quite reproducible and are both about 3 to 7%. Several micrographs were taken after staining with uranyl acetate at concentrations of 0·12 M, 0·012 M and 0·0012 M and adjusting the pH to 3·5. The observed densities under these conditions were very similar to those found with uranyl nitrate and need not be discussed separately.

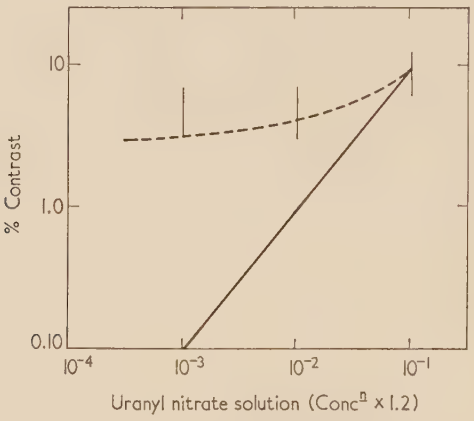

FIG. 3. Dependence of contrast on stain solution concentration. Vertical bars, as observed; —— as predicted by negative staining; - - - - as predicted by positive staining.

(d) *Comparison of supporting films*

DNA appeared to stain readily on all three substrates. Both the carbon and beryllium substrates could be washed in ether or ethanol, but the polymer film was dissolved by organic solvents.

The structures of the carbon and polymer substrates were comparable. They consisted of an irregularity of dots and lines with dimensions of the order of 10 Å and a contrast of about 3%. Both the polymer and the evaporated carbon films were smooth enough to enable the easy detection of the shadowed DNA molecules. However the beryllium-coated grids were rather too rough to enable us to see individual molecules by shadowing. Plate I(a) shows DNA on the beryllium films, Plates II and III on carbon films.

(e) *Influence of staining time on appearance of stained fibril*

Grids were variously stained from 5 to 30 min. The contrast did not appear to vary with the staining time, which suggests that the staining reaction was rapid.

4. Discussion

(a) *Comments on techniques used*

The technique of examining DNA molecules which pass into unshadowed regions appears to have two advantages. First, it is very much easier to find the molecules on the fluorescent screen if a portion of them is shadowed. Secondly, this procedure gives more information since the same fibre can be seen both shadowed and stained.

The technique of multiple printing emphasizes that much information which is present in the micrographs may be lost on account of the low contrast. This however can be regained by multiple printing on high contrast emulsions. If the first repeat printing is an enlargement the loss of detail can be kept negligibly low.

(b) *Source of density on staining*

The clear visibility of the DNA on staining (Plate I(a)) but not in the absence of staining (Plate I(c)) is proof that the visibility is due to staining. The unlikely possibility that visibility in the stained preparations is due to some scattering of the shadow material into the region of the shadow is completely ruled out by the clear visibility of an unshadowed stained DNA fibril (Plate I(b)).

(c) *Dimension of fibril*

Under our conditions preparations obtained from dilute DNA solutions gave fibrils which had a height of about 20 Å as determined from the shadow length. On staining such fibrils the densitometer traces in the shadow of the sphere had a width of about 20 ± 5 Å. The densitometry of the strand image is subject to errors because of the finite resolution of the densitometer and possible errors in aligning its slit with the image of the fibril. Both these errors would lead to an exaggerated fibril dimension. It can therefore be stated reliably that the image of the fibril is not greater than 20 ± 5 Å. On account of diffraction effects dimensions of an object near the resolution limit of the instrument may not be accurately represented by the dimensions of its image. These diffraction effects will be discussed in detail in connection with DNA in a forthcoming publication. Here the results will be anticipated, that the dimensions of the fibrils obtained from dilute solutions are not greater than about 25 Å. Thus the fibrils observed in dilute solution have a height of about 20 Å as inferred from the shadow height and a width of not more than 25 Å as inferred from the dimension of the stained molecule. These results are consistent with the hypothesis that the DNA is a double stranded Watson-Crick type helix.

(d) *Influence of staining on contrast*

The determination of the quantity of stain necessary to produce a given contrast in the electron microscope is of considerable interest. For objects near the resolution limit of the electron microscope this problem has been treated theoretically (Scherzer, 1949; Haine, 1957) but no relevant experimental results are available. The significance of our data will now be discussed in this connection.

In a previous paper we have determined the number of uranyl ions attached to DNA when in equilibrium with different stain solutions (Zobel & Beer, 1961). Those results are applicable to the stained strands studied here only if one can assume that the extent of uranyl staining of the single molecule on the dry grid is the same as in the case of bulk DNA in solution. This assumption could be questioned on two grounds: first, that after removal of the excess stain solution some of it is left on the grid and that when this dries the dissolved uranyl salt is preferentially deposited along the DNA, giving rise to additional spurious density as in "negative staining;" second, that the chemical interactions of adsorbed DNA fibrils are not the same as those of bulk DNA.

The carbon films made by our procedures were conspicuously hydrophobic. Water

and stain solutions were apparently completely withdrawn by filter paper touched to the edges. Our grids were dried after staining by placing them on filter paper face down. This it was believed removes essentially all of the stain solution from the grid. The only alternative to some drying procedure is washing the grids after staining. This was avoided since the staining reactions are known to be rapid, and so even the shortest washing procedures lead to a new equilibrium with the wash water; that is, some of the stain is removed.

A strong indication that the attached uranyl ions are not primarily the result of "negative staining"—except perhaps at the highest concentration—comes from the dependence of the density on the concentration of the staining solution. The most reasonable assumption about this residual stain solution is that the amount of it left on the grid is independent of its concentration. Then the amount of uranyl salt deposited during drying would be proportional to the concentration of the stain solution. If this were the mechanism of staining the density should be proportional to the stain concentration. This is certainly not the case. The density increases by only about a factor of two when the stain solution concentration increases by a factor of 100, from 0·0012 M to 0·12 M. This is illustrated in Fig. 3 where the vertical strokes represent the range of observed contrast and the straight line—or one parallel to it—represents the contrast dependence on stain concentration in "negative staining." Therefore it is believed that, except perhaps at the highest concentrations, deposition of stain during drying is not an important contribution to the fibre density.

This slow dependence of the contrast on the concentration is exactly what is predicted by our chemical studies. Table 1 repeats the relevant results of the earlier paper. In the first column are given the concentrations of uranyl salts used; column 2 lists the corresponding extent of staining; column 3 gives the contrast observed in the present study.

TABLE 1

Degree of staining and the observed contrast of DNA stained in uranyl nitrate at pH 3·5

Concentration of stain solution moles/l.	Extent of staining UO_2^{2+}/P	Observed contrast O-/O
0	0	1†
$1{\cdot}2\times10^{-3}$	0·5	5 ± 2
$1{\cdot}2\times10^{-2}$	0·7	5 ± 2
$1{\cdot}2\times10^{-1}$	1·5	9 ± 3

† Calculated from thick DNA fibril.

The observed contrast is the sum of contributions due to the unstained molecule and the attached stain. The contrast of the unstained molecule can be estimated from the roughly 3% contrast of the 50 Å thick unstained fibril mentioned earlier. It is a good approximation that the contrast is proportional to the height of a fibril. Then one would estimate the inherent contrast of an unstained DNA molecule to be about 1%. Subtracting this from the observed contrast one obtains the contrast contribution due to the attached uranyl ions. It is seen that the extent of uranyl attachment closely parallels their contrast contributions. This is also illustrated in Fig. 3. Here

e broken line is drawn through points whose ordinates are proportional to the number uranyl ions attached per base-pair of DNA. The contrast of proportionality was chosen that the curve should bisect the vertical stroke representing the range of served contrasts where the stain concentration was 0·12 M.

When the staining solution had a concentration of 10^{-3} M the stained fibril had a ntrast of about 5%. The chemical studies suggest an attachment of one uranyl ion every two bases. The observation that the fibrils still have a width of about 20 Å ggests that the uranyl ions lie along the polyphosphate chain. If they bridged the ses they would form a line of uranyl atoms and the fibril width would probably be s than 20 Å. This arrangement of the uranyl ions would also explain our observa- n that the melting-out temperature of DNA is not greatly affected by uranyl aining (unpublished data).

It is known from the work of Scherzer (1949) and Haine (1957) that the contrast one atom is a very sensitive function of instrumental resolution. In our work we ned at astigmatism corrections to better than 0·1 μ and had by the fringe separa- n criterion (Haine & Mulvey, 1954) a resolution of about 5 to 7 Å on the last test posure prior to microscopy. However, instrument performance deteriorates rapidly d erratically and it is not known that all the micrographs studied represent the ntrast obtained under those resolution conditions.

(e) *Implications of DNA visibility*

The line signal corresponding to the stained DNA molecule can be recognized above e irregular background of the supporting film even though the contrast of the egularity is comparable with that of the stained DNA molecule. At 0·0012 M ncentration of stain the contrast in the fibre is produced by one uranyl ion per se-pair. Assuming staining and drying do not lead to drastic changes in dimension is corresponds to one uranyl ion every 3·4 Å along the chain. Since the uranyl oms are probably spread over the two chains they are in most portions of the image en more widely spaced. Now the density produced by a point object occupies in e image an Airy disc with size equal to the resolution of the instrument. If this is the neighborhood of 5 to 7 Å in our case it can be inferred that the Airy discs of e individual uranyl atoms do not greatly overlap. Thus to a fair approximation e contrast due to one atom will be the same as that in our DNA stained in 0·0012 M- anyl nitrate. This suggests that on grounds of contrast alone a uranyl atom is sible by present detection methods.

Of course the detection of a dot signal is possible in a background of dots only if e signal exceeds the noise. This requires that the supporting films be smooth to out 1 to 2% contrast. Exploration in this direction will be reported in a subsequent blication. Nonetheless the above suggests that on a noise-free background a single avy atom should give enough contrast when used as a marker for some chemical oup. This observation suggests the possibility of determining the order of bases in cleic acids by using base-specific markers containing perhaps as few as one heavy om per base.

5. Conclusions

The first and uncontestable conclusion of this work is that DNA molecules on aining with uranyl salts at pH 3·5 have enough density when viewed in the electron

microscope to render possible high resolution studies of the configuration of DNA molecules.† The contrast observed depends on the concentration of the stain solution and varies from $5 \pm 2\%$ at stain concentrations of $1{\cdot}2 \times 10^{-3}$ M to $9 \pm 3\%$ at 0·12 M.

The second conclusion is that the thinnest fibrils observed have dimensions of about 20 ± 5 Å in the plane of the substrate as determined from densitometer traces across the stained molecule. The dimensions perpendicular to the plane of the substrate can be inferred from the shadow cast by the fibril. This also is about 20 ± 5 Å. These dimensions are most readily explained in terms of a double helix model.

The final conclusion is that DNA stained with one uranyl ion per base-pair gives rise to a contrast of $5 \pm 2\%$. This is based on the serious assumption that the chemical results on bulk DNA are directly applicable to single adsorbed molecules. The assumption is defended in the present paper on the grounds that the dependence on stain concentration in the test tube closely parallels that in the microscope.

The authors are indebted to Drs. C. A. Thomas and A. D. Hershey for their generous gifts of DNA and to Dr. F. D. Carlson for many helpful discussions. The willing and competent assistance of Miss Doris Naimark is acknowledged. This work was supported by grants from the National Institutes of Health and the National Science Foundation.

REFERENCES

Beer, M. (1961). *J. Mol. Biol.* **3**, 263.
Birbeck, M. S. C. & Stacey, K. A. (1959). *J. Biophys. Biochem. Cytol.* **5**, 167.
Gabor, D. (1948). *The Electron Microscope.* New York: Chemical Publishing Co.
Haine, M. E. (1957). *J. Sci. Instrum.* **34**, 9.
Haine, M. E. & Mulvey, T. (1954). *J. Sci. Instrum.* **31**, 326.
Hall, C. E. (1956). *J. Biophys. Biochem. Cytol.* **2**, 625.
Hall, C. E. & Litt, M. (1959). *J. Biophys. Biochem. Cytol.* **5**, 167.
Leisegang, S. (1956). In *Handbuch der Physik*, ed. by S. Flügge, **33**, 499.
Mandell, J. & Hershey, A. D. (1960). *Anal. Biochem.* **1**, 66.
Mott, N. F. & Massey, H. S. W. (1953). *The Theory of Atomic Collisions.* Oxford University Press.
O'Hara, D. S. & Beer, M. (1961). *J. Appl. Phys.* **32**, 1637.
Scherzer, O. (1949). *J. Appl. Phys.* **20**, 20.
Zobel, C. R. & Beer, M. (1961). *J. Biophys. Biochem. Cytol.* **10**, 333.

†This agrees with independent conclusions of W. Stoeckenius.

J. Mol. Biol. (1961) **3**, 727–740

Fractionation of Nucleic Acids in Aqueous Polymer Two-Phase Systems

T. Lif, G. Frick and P. Å. Albertsson

Institute of Biochemistry, University of Uppsala, Sweden

(*Received 26 June 1961*)

1. The partition coefficients of some different preparations of nucleic acid from different sources have been determined in the polymer phase systems dextran : methylcellulose : water and sodium dextran sulphate : methylcellulose : water.
2. For nucleic acids of different molecular sizes, the negative logarithm of the partition coefficient was found to increase nearly proportionally with increasing sedimentation coefficient.
3. In the counter-current experiment with thymus DNA, the distribution after each transfer changed in such a way that, according to the above-mentioned relation between sedimentation and partition coefficients, the low molecular fractions of the heterogeneous DNA moved with the top phase. Soluble RNA has also been separated from a mixture with thymus DNA and the separation was checked with a pyrimidine analysis.
4. Thymus DNA has been fractionated by the counter-current technique. After a few transfers, analysis in the ultracentrifuge showed a fractionation of the material and each tube contained DNA with a more homogeneous sedimentation coefficient distribution—the higher the tube number, the lower the coefficient.
5. In most systems, an interface layer of nucleic acid is formed. This can be used to obtain a more homogeneous thymus DNA.
6. The adsorption of nucleic acid at the interface can also be used as an analytical tool. A few per cent of high molecular RNA, in a preparation of soluble RNA, can be detected by the formation of an interface layer in a suitable polymer phase system.
7. Contaminated DNA from phage T2 was shown to deviate strongly from the main relation between the sedimentation coefficient and the partition coefficient. When the preparation was dialysed, and thus freed from parts of the contaminating substances, which are probably amines, the negative logarithm of the partition coefficient increased towards a better agreement with the main relation.

1. Introduction

Fractionation of extended macromolecules, such as nucleic acids, is a difficult problem, the usual separation methods all having disadvantages. In zone electrophoresis, as in chromatography, there is often strong adsorption on the stabilizing media and the viscous solutions of nucleic acids give very strong tailing when eluted. The analytical sensitivity of the ultracentrifuge is obscured by sharpening of the sedimenting boundary and by the dependence of the sedimentation coefficient on concentration and ionic strength. Thus the possibilities of any separation method making use of a parameter different from those hitherto used should be thoroughly investigated.

Albertsson has shown that aqueous two-phase systems can be obtained with very low concentrations of polymers such as dextran and methylcellulose or dextran and polyethylene glycol and that these polymer systems can be used to fractionate protein molecules and rather large particles of protein character (Albertsson, 1958; Albertsson & Frick, 1960). The distribution of protein particles between the polymer phases was shown to follow a relation introduced by Brønsted (1931), in which the negative logarithm of the partition coefficient is approximately proportional to the surface area of the particles.

In this paper, a similar relation is introduced for nucleic acid molecules, which, for practical reasons, is given as the partition coefficient *versus* the sedimentation coefficient instead of *versus* surface area. This relation in regard to the dimensions of the molecules will be commented upon further below.

Using this relation, we have tried to solve different practical problems of nucleic acid preparation using phase systems. With a type of simple counter-current technique, a DNA preparation may be freed from the smaller "debris" present as shown by the size distribution. If the partition coefficient does not change during the counter-current separation this is a criterion of the homogeneity of the sample. If a nucleic acid particle is contaminated, as was the case for some of the phage nucleic acid preparations described below, this will be indicated by an abnormal partition coefficient.

The method is mild and, from the experiments with DNA prepared from phage T2, it is even indicated that the polymers have a protective effect on the nucleic acid molecules.

A simple method is also described to detect, and partly separate, a few per cent of high molecular RNA from a preparation of soluble RNA. This high molecular fraction was present in such a small amount that the preparation showed the characteristics only of the main fraction.

2. Materials and Methods

(a) *Polymers*

Methylcellulose (MC) was obtained as "Methocel 4000, U.S.P. grade" from the Dow Chemical Company, U.S.A., and was dried before use at 110°C for 24 hr. The dried powder was shaken with water at 80 to 90°C and dissolved by cooling to about 4°C; the solution was then adjusted to 2% (w/w).

Polyethylene glycol (PEG) was obtained as "Carbowax 6000" and "Carbowax 20M" from the Carbide and Carbon Chemicals Company, U.S.A. "Carbowax 6000" was dissolved directly in water to give a 30% (w/w) stock solution. "Carbowax 20M" was used in a concentration procedure, which will be described below.

Sodium dextran sulphate (NaDS) made from a dextran fraction with an intrinsic viscosity of 70 ml./g and containing 15 to 18% sulphur was supplied by Pharmacia Ltd., Sweden as "Sodium dextran sulfate 2000". The dextran sulphate was dried over P_2O_5 and dissolved in water to give 6% (w/w) and 20% (w/w) stock solutions.

Dextran (D) with an intrinsic viscosity of 68 ml./g, also supplied by Pharmacia Ltd., was dissolved by wetting the powder with water, then adding the rest of the water and heating to boiling. The stock solutions contained 10% (w/w).

All aqueous polymer solutions were kept at 4°C.

(b) *Preparation of phase systems*

To prepare a phase system, stock solutions of the different polymers, NaCl, sodium phosphate buffer, and the nucleic acid solution were mixed to give the desired composition

of the system. The final concentration of the phosphate buffer was 0·01 M, pH 7·0; for phase diagrams see Albertsson (1960).

The composition of a phase system will be described by the following abbreviation:

$$NaDS_y : MC_z \ (q \text{ M-NaCl})$$

where y indicates the final sodium dextran sulphate concentration in % (w/w); z the final concentration of methylcellulose in the same units, and q the final molar concentration of NaCl. The systems with sodium dextran sulphate : polyethylene glycol and dextran : methylcellulose are described in the same way.

After preparation of the systems, the vessels were maintained at 4°C and inverted about 50 times to obtain thorough mixing. For the system sodium dextran sulphate : methylcellulose, 12 hr sufficed for good phase separation. The system dextran : methylcellulose needed 20 hr for phase separation, whereas for the system sodium dextran sulphate : polyethylene glycol, 2 hr were sufficient.

(c) *Definition of the partition coefficient*

The partition coefficient of a substance is defined as the ratio between its concentration in the top and bottom phases. The concentration of the nucleic acid is usually determined from the light absorption at 260 mμ after correction for unspecific absorption. This correction was calculated from the absorption between 330 and 400 mμ according to Heller & Vassy (1946), by plotting the values on log-log scales.

In most of the experiments reported below, a layer of nucleic acid collected at the interface. As a convenient measure of the distribution in these cases, we have used

$$K_1 = \frac{C_t}{C_b + a/V_b}$$

where C_t is the concentration of the nucleic acid in the top phase, C_b the concentration in the bottom phase, a the amount of nucleic acid at the interface and V_b the volume of the bottom phase.

(d) *Preparation of DNA*

DNA from calf thymus was prepared according to Kay, Simmons & Dounce (1952). The final product was dissolved in 0·3 M-NaCl, 0·01 M-sodium phosphate buffer pH 7·0.

DNA from phage T2 was obtained by two different methods, I and II below. The T2 phages were prepared according to Frick (1961) and, immediately before each experiment, DNA was prepared from the stock phage suspension.

Method I: The phage DNA will be released from its protein shell at a pH of about 11 (Davison, 1959). One part of phage suspension (about 5×10^{12} particles/ml.) was mixed with 6 parts of 0·001 M-NaOH. After 15 min, sodium phosphate buffer (pH 7·0) was added to a final concentration of 0·01 M with respect to the complete phase system. The base was neutralized with an equivalent amount of 0·01 M-HCl and the polymers and NaCl were then added to form the desired phase system. All operations were carried out at 4°C and with cold solutions.

Method II: The phages were treated with phenol according to Mandell & Hershey (1960). The phenol treatment was repeated three times for 3, 1·5 and 1·5 min with centrifugation after each treatment. The DNA obtained was dialysed against 0·3 M-NaCl, 0·01 M-sodium phosphate buffer pH 7·0.

(e) *Preparation of RNA*

RNA from yeast was prepared following the procedure described by Crestfield, Smith & Allen (1955). Ethanol was added to the solution containing low-molecular RNA and an RNA having a sedimentation coefficient 3·5 s was precipitated.

Soluble RNA from *E. coli* K12 was prepared according to a method developed in the laboratory of Dr. F. Lipmann and kindly supplied by Dr. H. G. Boman, Uppsala.

(f) *Ultraviolet absorption*

Absorption spectra were determined with the Beckman DU spectrophotometer.

(g) *Ultracentrifugation*

The sedimentation rates were studied in an analytical centrifuge (Spinco model E) with ultraviolet light optics. For details see Schumaker & Schachman (1957). A cell which could be filled with a broad needle was used for DNA from phages. The viscosities of the nucleic acid solutions relative to water were determined with an Ostwald viscometer.

(h) *Methods used to concentrate dilute solutions of nucleic acids*

Solutions of nucleic acids which were too dilute to be analysed in the ultracentrifuge were concentrated either by ultrafiltration and negative pressure dialysis (Laurell, 1958) or by dialysis against polymers (Soller, 1961). In the latter case, the dialysis bag was surrounded with solid "Carbowax 20M." Water passing out through the membrane was retained by the "Carbowax 20M" which dissolved. In this way, a 150 ml. solution of nucleic acid could be concentrated to 30 ml. in 8 hr using a Visking Corporation dialysis bag, diameter 2·8 cm.

(i) *Paper chromatography*

To find the relative DNA and RNA content in a mixture, in the presence of methylcellulose and traces of dextran sulphate, the relative thymine and uracil content was determined. The nucleic acid mixture was hydrolysed at 180°C for 20 hr in 6 N-HCl. The HCl was evaporated and the remaining material dissolved in water and chromatographed in an *n*-butanol : water mixture (Smith, 1960). The spots on the paper were detected by ultraviolet light and then cut out and extracted with 0·01 M-HCl. The optical densities of the extracts were measured at 265 and 258 mμ and the molecular extinction values of Wyatt (1955) used.

(j) *Column chromatography*

To detect amine-like substances, supposed to contaminate some preparations of phage DNA, chromatography was performed on a cation exchange resin, Amberlite XE-64, Na^+ form, according to Rosenthal & Tabor (1956). The dimensions of the column were $8 \times 0{\cdot}65$ cm and the elution was carried out with 0·5 and 0·9 M-Na_2SO_4 in 0·1 M-sodium phosphate buffer pH 7·05. Fractions of about 2·5 ml. were collected and tested with 2.4-dinitrophenol according to Rosenthal & Tabor (1956). The reasons given by these authors for using cyclohexane in the staining procedure were, however, not found to be valid and ethyl acetate was used throughout. Comparisons were made with known solutions of cadaverine dihydrochloride, putrescine dihydrochloride, spermidine phosphate and spermine tetrahydrochloride.

3. Experimental and Results

(a) *The size of the nucleic molecule and the partition coefficient*

(i) *Concentration dependence*

In Fig. 1 the K value in the dextran : methylcellulose system and the K_1 value in the sodium dextran sulphate : methylcellulose system are plotted for different concentrations of DNA. Whereas the K value in the former system is fairly constant in the concentration range studied, the K_1 value in the sodium dextran sulphate : methylcellulose system is dependent on the concentration, particularly at low DNA concentrations.

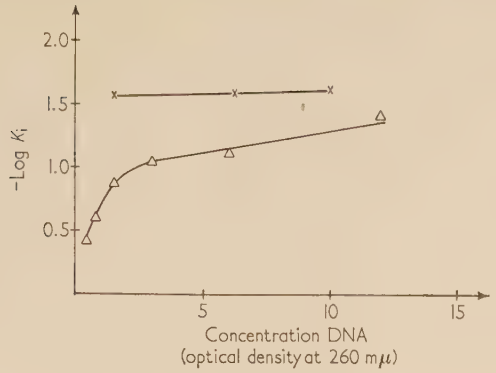

FIG. 1. The relation between the K_1 value and the concentration of DNA from calf thymus partitioned in two different polymer phase systems. ×—× is the phase system $D_{0.68}$: $MC_{0.36}$ (0·15 M-NaCl) and △—△ is the phase system $NaDS_{0.70}$: $MC_{0.25}$ (0·3 M-NaCl).

ii) *Determination of partition coefficients*

The partition coefficient was determined for RNA prepared from yeast, and for several different DNA preparations from calf thymus and phage T2. They were studied in the two following phase systems.

1. Dextran : methylcellulose. At the nucleic acid concentration tested, no interfacial adsorption was observed. It was of interest to determine the K value of nucleic acids in this system, as the K values of a number of proteins and viruses have previously been determined in the same system (Albertsson & Frick, 1960; Albertsson, 1960), thus allowing a comparison to be made between the K values of proteins and viruses on one hand and nucleic acids on the other. The K values of nucleic acids in this system are given in Table 1. In Fig. 2, the negative logarithms of the K values are plotted against the sedimentation coefficients.

TABLE 1

Sedimentation coefficient ($S_{20,w}$) *and partition coefficient* (K) *in the polymer system* $D_{0.68}$: $MC_{0.36}$(*0·15* M-*NaCl*) *for some different preparations of nucleic acid*

Nucleic acid	$S_{20,w}$ Svedberg units	K
RNA from yeast	3·5	0·49
DNA from calf thymus, preparation 1	20·5	0·024
DNA from calf thymus, preparation 2	21·8	0·020
DNA from calf thymus, preparation 3	22·5	0·020
DNA from phage T2 (method I)	35	0·002(3)

2. Sodium dextran sulphate : methylcellulose. In this phase system, adsorption of the nucleic acids takes place at the interface. The system has the great advantage that the dextran sulphate can be precipitated after phase separation. The system $NaDS_{0.70}$: $MC_{0.25}$ (0·3 M-NaCl) gives good phase separation. The volumes of the

upper and lower phases are 6 and 4 ml. respectively and no drops of bottom phase appear to remain in the top phase. The composition of this system is, however, close to the critical point in the phase diagrams and it is thus very sensitive to small

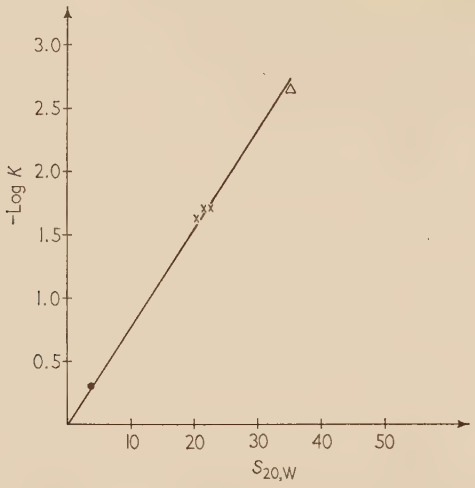

FIG. 2. The negative logarithm of the partition coefficient, K, plotted *versus* the sedimentation coefficient, S, of the various nucleic acid preparations partitioned in the phase system $D_{0.68}$: $MC_{0.36}$ (0·15 M-NaCl). ● RNA from yeast, × DNA from calf thymus, △ DNA from phage T2 (method I).

composition variations. A composition, $NaDS_{0.43}$: $MC_{0.73}$ (0·3 M-NaCl), further from the critical point was tested but the partition coefficient in such a system decreased so rapidly with increasing molecular size, that determinations became very

TABLE 2

Sedimentation coefficient ($S_{20,w}$) and K_1 values in the polymer system $DS_{0.70}$: $MC_{0.25}$ (0·3 M-NaCl) for some different preparations of nucleic acids

Nucleic acid	$S_{20,w}$ Svedberg units	K_1†
RNA from yeast	3·5	0·67
DNA from calf thymus, preparation 1	16·1	0·20
DNA from calf thymus, preparation 2	20·5	0·18
DNA from calf thymus, preparation 3	21·8	0·14
DNA from calf thymus, preparation 4	22·5	0·12
DNA from phage T2 (method I)	31·1	0·01(2)
DNA from phage T2 (method I)	31·5	0·08
DNA from phage T2 (method I)	33·0	0·02
DNA from phage T2 (method I)	35·5	0·03(2)
DNA from phage T2 (method I)	33·8	0·07(4)
DNA from phage T2 (method I)	42·0	0·02(5)
DNA from phage T2 (method II)	52·0	0·022
DNA from phage T2 (method II)	54·5	0·030

† No adsorption at the interface for RNA

difficult for some of the available preparations of nucleic acid. The K_1 values of nucleic acids in the system $NaDS_{0.70}$: $MC_{0.25}$ (0·3 M-NaCl) are given in Table 2. In Fig. 3, the negative logarithms of the K_1 values are plotted against the sedimentation coefficients. Some results, obtained for phage "DNA" prepared by method II, differed from the general trend and were found to be of special interest and will be discussed separately below.

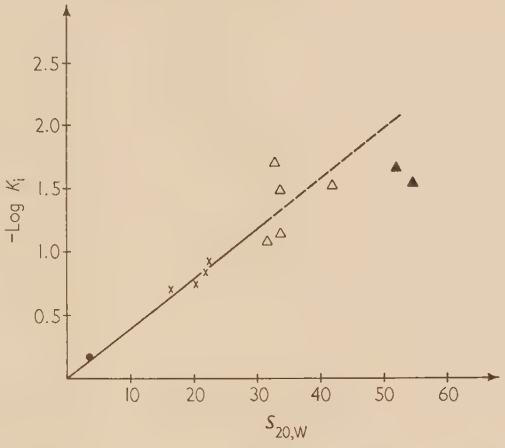

FIG. 3. The negative logarithm of the K_1 value plotted *versus* the sedimentation coefficient, S, of various nucleic acid preparations partitioned in the phase system $NaDS_{0.70}$: $MC_{0.25}$ (0·3 M-NaCl). ● RNA from yeast, × DNA from calf thymus, △ DNA from phage T2 (method I), ▲ DNA from phage T2 (method II).

In the case of DNA prepared from phage T2 according to method I, the sedimentation coefficient was determined for the DNA found in the bottom phase. In method I, the protein bags of the phage particles are still present in a denatured form and the optical density values thus have to be corrected for a rather strong unspecific absorption.

(iii) *The interface layer of nucleic acid*

As mentioned above, an interface layer of nucleic acid may appear, under certain circumstances, in the phase system. This effect depends upon the polymer system, the electrolytes present, and the concentration and molecular size of the nucleic acid. Thymus DNA in sodium dextran sulphate: methylcellulose (0·3 M-NaCl) gives a detectable interface layer at an original concentration of 0·005% in the total phase system. At this low DNA concentration no precipitation of DNA is found in polymer mixtures having the same composition as either the top or the bottom phase. This type of interfacial adsorption of DNA is obviously a result of molecular forces acting at the interface. The DNA precipitates in the absence of an interface at a higher concentration, about 0·08%, in a sodium dextran sulphate : methylcellulose mixture containing 0·3 M-NaCl, and having the same polymer composition as the top or the bottom phase of the earlier mentioned system which gave an interface layer. The layer of DNA at the interface of a phase system at higher DNA concentration is thus also due to a low solubility of DNA in the phases.

(b) *Some simple counter-current experiments*

(i) *General*

The counter-current experiments were carried out in the following way using the liquid-interface counter-current distribution technique (Albertsson, 1960). The nucleic acid was first distributed, in a tube (numbered 0), in 100 g of the system $DS_{0.70}$: $MC_{0.25}$ (0·3 M-NaCl). The volumes of the bottom and top phase were 40 ml. and 60 ml. respectively. After 12 hours phase separation, the top phase, except for a small layer above the interface, was removed by pipette and transferred to the next tube (numbered 1) with 40 ml. bottom phase. Fresh top phase, 60 ml., was then added to tube 0. The tubes were then shaken and, after phase separation, the top phase from tube 1 was transferred to a tube 2, with 40 ml. bottom phase. The top phase from tube 0 was then transferred to tube 1 and 60 ml. fresh top phase was added to tube 0. After shaking and phase separation, the same operation was repeated with the addition of a fourth tube 3.

Counter-current experiments have also been carried out with the system $D_{0.68}$: $MC_{0.36}$ (0·15 M-NaCl) and the values in Table 3 were obtained with thymus

TABLE 3

The change of the partition coefficient K *for a calf thymus DNA preparation* ($S_{20,w}$ = 20·4 S) *in the system* $D_{0.68}$: $MC_{0.36}$ (*0·15* M-*NaCl*) *during a counter-current experiment*

Transfer	*K* in tube number		
	0	1	2
0	0·024		
1	0·023	0·12	
2	0·023	0·10	0·14

DNA in this system. The nucleic acid content was determined from the optical density at 260 mμ. The results show that there is a decrease in the *K* values with transfers in the first tube, whereas an increase in *K* is found with increasing tube number. According to the relation between *K* and the sedimentation coefficient, this shows that low molecular fractions of the heterogeneous preparation of DNA have moved with the top phase with each transfer, thus making the preparation remaining in tube 0 enriched in the high molecular fractions. For confirmation see also Table 5. About 75% of the nucleic acid remains in the first tube.

(ii) *A counter-current experiment to separate low molecular RNA from high molecular DNA*

In this experiment, a mixture of 0·02% DNA from calf thymus and 0·025% soluble RNA from *E. coli* underwent a counter-current procedure in 4 tubes with 3 transfers. The usual colour reactions for DNA and RNA could not be used to follow the separations owing to the type of polymers present. The content of thymine and uracil (Chargaff, 1955; Dunn, Smith & Spahr, 1960) in the bottom phases were instead determined using the following procedure.

To avoid co-precipitation of nucleic acid, the bottom phases were diluted 5 to 10 times and then the dextran sulphate was precipitated with 4 M-KCl (Philipson, Albertsson & Frick, 1960). The precipitate was allowed to settle in the cold for 2 hr and then centrifuged down at 1000 ***g*** for 15 min. The supernatant liquid was dialysed overnight against distilled water and then evaporated to dryness; the dry powder was finally heated to 180°C in 6 N-HCl for 20 hr. This drastic treatment destroys adenine and guanine, but leaves thymine and uracil intact. The final determination was carried out as described under "Materials and Methods."

The results are given in Table 4.

TABLE 4

Separation after 3 transfers of low molecular RNA (from E. coli, $S_{20,w} = 3$ s) *from high molecular DNA (from calf thymus,* $S_{20,w} = 20{\cdot}5$ s). *Polymer system* $NaDS_{0{\cdot}70} : MC_{0{\cdot}25}$ (0·3 M-NaCl)

	Tube number			
	0	1	2	3
Thymine/Uracil	4·7	0·9(5)	0·9(3)	<0·1
% of total (DNA + RNA)	36·3	21·3	29·6	12·7

(iii) *Fractionation of thymus DNA*

The preliminary experiments, under (i) above, show that the smaller particles in a DNA preparation move from the main high molecular fraction in the first tube, leaving a more homogeneous preparation.

The results of two experiments with different polymer systems are recorded in Table 5 and Figs 4(a) and (b). One of the systems was sodium dextran sulphate : methylcellulose and the other the rapidly separating phase system sodium dextran

TABLE 5

Results of two different counter-current experiments on DNA from calf thymus with 2 or 3 transfers

Tube no.	K_i		DNA in the tubes, % of total		$S_{20,w}$ of DNA in bottom phase Svedberg units	
	a	b	a	b	a	b
0	0·012	0·063	65·5	76·6	20·6	17·0
1	0·071	0·72	24·5	15·4	17·2	13·8
2	0·21	0·87	5·3	7·9	11·2†	13·4
3	0·32	—	4·5	—	—	—

a: $S_{20,w}$ of original DNA 21·8 s. Polymer system $NaDS_{5.8} : PEG_{5.8}$ (0·3 M-NaCl). The bottom phase concentrated with ultrafiltration and negative pressure dialysis.

b: $S_{20,w}$ of original DNA 15.0 s. Polymer system $NaDS_{0.70} : MC_{0.25}$ (0·3 M-NaCl). The bottom phase DNA concentrated with the "Carbowax 20M" technique (see above).

† The content of the bottom phase in tubes 2 + 3.

sulphate : polyethylene glycol. The main relation between log K_1 and the sedimentation coefficient has not been determined for this latter polymer system, as it was difficult to obtain reproducible K_1 values in this very sensitive system. In a series of

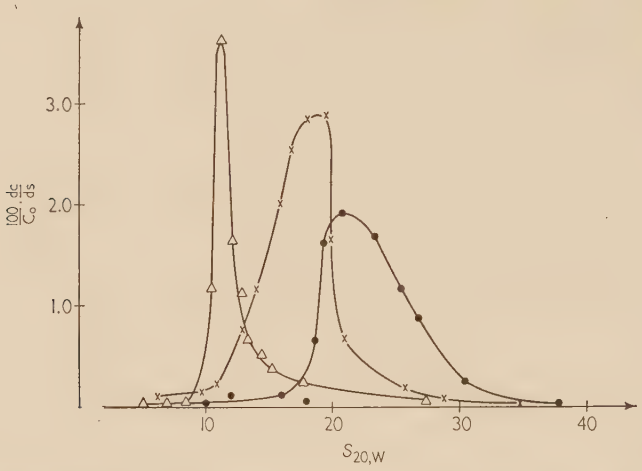

FIG. 4(a). The sedimentation coefficient distributions of DNA from calf thymus fractionated by a counter-current procedure in the phase system $NaDS_{5.8}$: $PEG_{5.8}$ (0·3 M-NaCl). ●—● bottom phase from tube 0, ×—× bottom phase from tube 1, △ — △ bottom phase from tubes 2 and 3. See also Table 5.

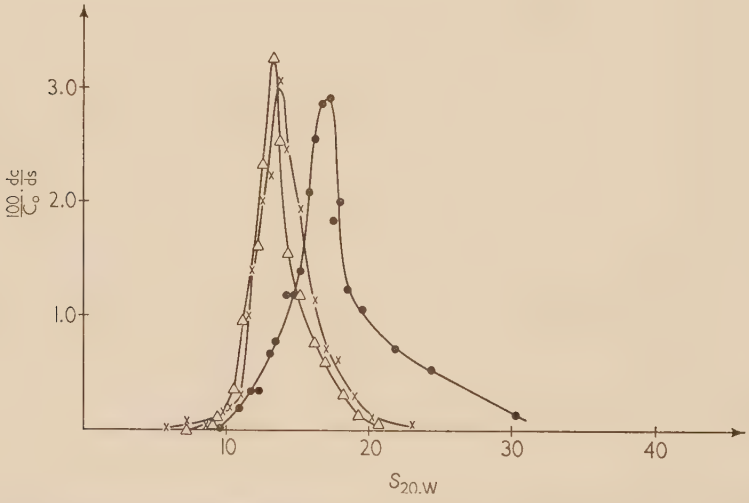

FIG. 4(b). The sedimentation coefficient distributions of DNA from calf thymus fractionated by a counter-current procedure in the phase system $NaDS_{0.70}$: $MC_{0.25}$ (0·3 M-NaCl). ● — ● bottom phase from tube 0, ×—× bottom phase from tube 1, △ — △ bottom phase from tube 2. See also Table 5.

experiments with the same batches of polymer solutions the practical result can, however, be very good and the hypothesis that partition in this system is quite similar to those more fully investigated seems to be justified by the results obtained.

The concentration of DNA in the tubes at the end of the counter-current experiment was so low that the K_1 values may increase according to the relation in Fig. 1.

The sedimentation coefficients were determined after the dextran sulphate had been precipitated. Only the bottom phases were used as the concentration of the other, non-precipitated polymer is very low in this phase, whereas the concentration of DNA is comparatively high. The directly obtained DNA solutions were, however, too dilute for ultracentrifuge analyses and were concentrated. The results are given in Table 5.

(c) *The nucleic acid interface layer*

(i) *A method to obtain a more homogeneous DNA preparation*

One part of a solution of fairly heterogeneous calf thymus DNA in 0·3 M-NaCl, 0·01 M-sodium phosphate buffer pH 7·0 and optical density (O.D.) of 20 at 260 mμ, was mixed with one part of a mixture of sodium dextran sulphate and polyethylene glycol calculated to give a final composition of $NaDS_{5\cdot3}$: $PEG_{5\cdot3}$ (0·3 M-NaCl). The DNA precipitated at the interface in tube 0, when the phases had separated after

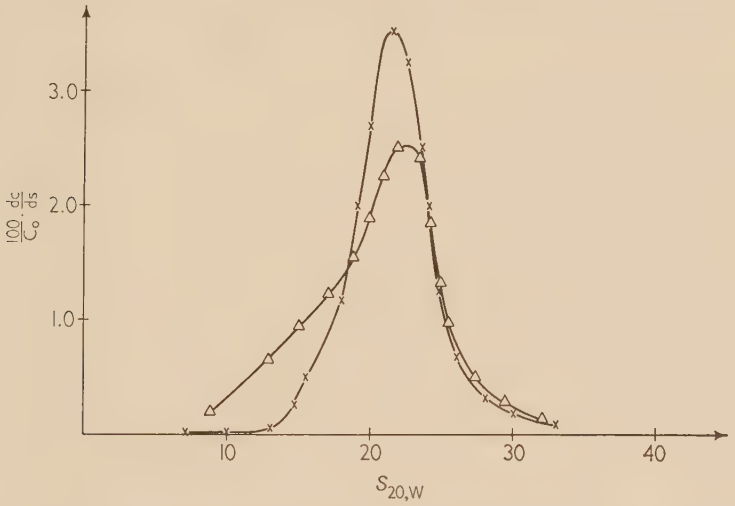

Fig. 5. The sedimentation coefficient distribution of interface DNA, in tube 0, from a counter-current procedure on a DNA preparation from calf thymus, compared with the sedimentation coefficient distribution of the original DNA preparation. ×—× interface DNA in tube 0, △— △ original DNA preparations.

3 transfers, was collected and partly freed from the other polymers by high speed centrifugation (10,000 *g*, 30 min). The DNA was then dissolved in 0·3 M-NaCl and 0·01 M-sodium phosphate buffer pH 7·0 and the solution analysed in the ultracentrifuge. The sedimentation coefficient distribution curve for the interface DNA, compared with the obviously less homogeneous original DNA preparations, is given in Fig. 5. The interface DNA forms 60% of the total DNA.

(ii) *Analytical purposes*

A few per cent of a high molecular nucleic acid in a low molecular preparation of RNA is difficult to observe in the ultracentrifuge but can easily be detected by the formation of an interface layer in a suitable polymer phase system.

One part of the low molecular RNA solution (O.D. = 20) is mixed with one part sodium dextran sulphate : polyethylene glycol to a final concentration $NaDS_{5\cdot8}$: $PEG_{5\cdot8}$ (0·3 M-NaCl). After thorough mixing, the phases are allowed to form. If an interface layer is formed, the precipitate is collected and investigated in the ultracentrifuge.

Soluble RNA from *E. coli* which sedimented with a coefficient of 3 S in the original ultracentrifugation was shown in this way to contain RNA which appeared in the interface. This RNA was less than 5% of total and possessed sedimentation coefficients of 16 and 20 S.

(d) *A deviation from the main relation between* K_1 *and the sedimentation coefficient*

The spread of the values obtained for phage DNA, prepared according to method I (weak alkali), is of little interest as this is obviously due to the difficulty in determining the DNA concentration especially in the top phase, caused by the high light-absorption of the phase polymers present.

When the phage DNA is prepared according to method II, the phenol-denatured protein is centrifuged down during the preparation and the optical densities of the DNA solutions can be determined with sufficient accuracy. In some cases, however, very much higher values were found for K_1 than expected; for two preparations with an $S_{20,w}$ of 50 and 59 S respectively, the corresponding K_1 values were found to be 0·18 and 0·21. The expected value for K_1 is at least ten times lower.

There is, however, evidence that this deviation from the main relation between size and distribution is caused by a change in the surface properties of the DNA molecule due to contamination with substances of basic character.

The following experiments were undertaken to show this:

1. Electrophoresis. Normally, DNA has many negative groups and moves fairly rapidly in the electric field. However, the main fraction of the DNA, with a high K_1 value, did not move at all. The electrophoresis was performed in a vertical tube according to Hjertén (to be published) with a suspension of agarose as the stabilizing medium.

If the DNA preparation was dialysed it gave a lower K_1 value and also started to move in the electrophoresis tube showing a continuous spectrum of mobilities.

2. Prolonged dialysis gives K_1 values closer to the expected value the longer the preparation is dialysed (Fig. 6).

3. Chromatography of the DNA preparations shows substances appearing in the fractions where putrescine and spermidine, two amines known to be present in T-phages (Ames, Dubin & Rosenthal, 1958), are expected to be found. The original phage DNA solution was made 0·3 M with HCl and the precipitated nucleic acid removed. The supernatant liquid was then neutralized with NaOH and chromatographed on a small column (8 × 0·65 cm) of a cation exchange resin Amberlite XE-64. The column was eluted with Na_2SO_4 in 0·1 M-sodium phosphate buffer pH 7·05. Fractions of 2·5 ml. were collected and treated as described under "Materials and Methods" and tested with dinitrophenol. A slight positive colour reaction was obtained at the start and a very strong reaction with the fractions expected for putrescine and spermidine. No rigorous identification was supposed necessary for the present discussion. If, however, the colour obtained with dinitrophenol is related to the mentioned amines, the concentrations of positive groups calculated would correspond to $\frac{1}{4}$ to $\frac{1}{3}$ of the polynucleotides in the original DNA.

In one case, when an abnormally high K_1 value for a DNA preparation was decreased y dialysis, as described above, the solution outside the dialysis bag was also chromato-raphed on the Amberlite XE-64 column. Colour reactions were obtained in the uate in a similar way and with the same fractions as described in the earlier experi-ent.

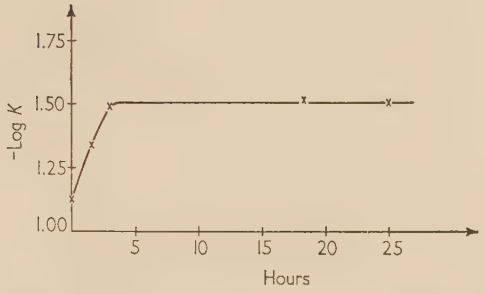

FIG. 6. The relation between the K_1 value and the time of dialysis of DNA from phage T2 repared according to method II) partitioned in the phase system $NaDS_{0.70}$: $MC_{0.25}$ (0·3 M-NaCl).

4. Discussion

The experimental results plotted in Figs. 2 and 3 can be fitted to the curve

$$-\log K_1 = kS^{\alpha} \qquad (1)$$

here K_1 denotes the partition coefficient (as defined above) of the nucleic acid olecules in the polymer two-phase system, S the sedimentation coefficient and k nd α are constants where the value of α is close to unity. The experiments further ow that this relation can be of practical significance when applied to a counter-rrent technique for separating nucleic acid molecules of different sizes. The log K_1 alue, related to a known S value for a certain preparation, can be used as a sensitive iterion of the purity of the preparation.

Until nucleic acid preparations suitable for model experiments are available and eir behaviour in the phase system is studied in greater detail, determination of the dimentation coefficient from the K_1 value is obviously not justified, except to give e order of magnitude.

When an interface layer is formed by the DNA, the distribution is dependent on e concentration of the DNA, especially at low concentrations of DNA. For a homo-neity test with the counter-current technique, one therefore has to choose a system hich does not show this dependence. The formation of an interface layer can, owever, be utilized to detect small amounts of high molecular nucleic acid in a reparation of low molecular nucleic acid. The effectiveness of the fractionation btained with the counter-current technique is probably also partly due to the collec-on of high molecular DNA at the interface.

As shown, for example, by the sedimentation coefficient distribution in Fig. 5, degradation of the DNA in the phase systems can be detected. The very large hage DNA molecules, prepared according to method II, also seem to stand the aking of the polymer system quite well.

It is difficult to compare the experimental relation found between the partition efficient and the sedimentation coefficient with other related molecular parameters.

Assuming the Brønsted relation to be valid, and the DNA molecule to be a rod with repeating equal subunits, would, for example, lead to conflict with the well known relation between the sedimentation coefficient and molecular weight given by Butler (1959). The assumptions made are obviously not valid, which is due to the complicated nature of the DNA molecule and the phase components.

This work has been supported financially by grants from the Technical and Natural Science Research Councils of Sweden.

REFERENCES

Albertsson, P. Å. (1958). *Nature*, **182**, 709.
Albertsson, P. Å. (1960). *Partition of Cell Particles and Macromolecules*. Stockholm: Almqvist & Wiksell and New York: John Wiley & Sons.
Albertsson, P. Å. & Frick, G. (1960). *Biochim. biophys. Acta*, **37**, 230.
Ames, B. N., Dubin, D. T. & Rosenthal, S. M. (1958). *Science*, **127**, 814.
Brønsted, J. N. (1931). *Z. Phys. Chem.*, Bodensteinfestband, 257.
Butler, J. A. V. (1959). *Les Nucleoproteines*, Onzième Conseil, Institut de Chimié Solvay, Bruxelles.
Chargaff, E. (1955). In *The Nucleic Acids*, ed. by E. Chargaff & J. N. Davidson, vol. 1, p. 354. New York: Academic Press.
Crestfield, A. M., Smith, K. C. & Allen, F. W. (1955). *J. Biol. Chem.* **216**, 185.
Davison, P. F. (1959). *Proc. Nat. Acad. Sci., Wash.* **45**, 1560.
Dunn, D. B., Smith, J. D. & Spahr, P. F. (1960). *J. Mol. Biol.* **2**, 113.
Frick, G. (1961). *Exp. Cell. Res.* **23**, 488.
Heller, W. & Vassy, E. (1946). *J. Chem. Phys.* **14**, 565.
Kay, E. R. M., Simmons, N. S. & Dounce, A. L. (1952). *J. Amer. Chem. Soc.* **74**, 1724.
Laurell, H. (1958). *Studies on Preparative Vertical Zone Electrophoresis*, p. 47. Uppsala: Almqvist & Wiksell.
Mandell, J. D. & Hershey, A. D. (1960). *Analytical Biochemistry*, **1**, 66.
Philipson, L., Albertsson, P. Å. & Frick, G. (1960). *Virology*, **11**, 553.
Rosenthal, S. M. & Tabor, C. W. (1956). *J. Pharmacol.* **116**, 131.
Schumaker, V. N. & Schachman, H. K. (1957). *Biochim. biophys. Acta*, **23**, 268.
Smith, I. (1960). *Chromatographic and Electrophoretic Techniques*, vol. I, p. 231.
Soller, A. (1961). *Virology*, **13**, 267.
Wyatt, G. R. (1955). In *The Nucleic Acids*, ed. by E. Chargaff & J. N. Davidson, vol. 1, p. 262. New York: Academic Press.

Mol. Biol. (1961) **3**, 741–745

Infrared Spectra of Formamide-treated Nucleic Acids

Y. Kyogoku, M. Tsuboi, T. Shimanouchi

Faculty of Science and Faculty of Pharmaceutical Sciences, University of Tokyo, Bunkyo-ku, Tokyo, Japan

AND

I. Watanabe

Institute for Virus Research, Kyoto University, Sakyo-ku, Kyoto, Japan

(*Received 26 June 1961*)

The effects of formamide treatment on the infrared absorption of sodium salts of calf thymus DNA, yeast ribosomal RNA, and yeast soluble RNA have been examined. The effects are found to be very similar to the effects of heating the aqueous solutions of these sodium salts of the nucleic acids. On the basis of the characters of the absorption bands where these effects are observed, it is concluded that the formamide treatment causes a cleavage of the base pairings, a change in the electronic structure of the base portions and a change in the molecular conformation of the phosphate and sugar portions of NaDNA.

[elmkamp & Ts'o (1961) have found recently that calf thymus DNA and pea bosomal RNA, when dissolved in formamide, show optical and hydrodynamic roperties which have been interpreted in terms of loss of their secondary structure. n attempting to obtain another type of information on their secondary structure, e have examined formamide-treated DNA and RNA by means of infrared absorption ieasurements.

Ten mg of sodium salt of calf thymus DNA was added to 10 ml. formamide. After irring overnight, a small amount of precipitate (insoluble DNA) was removed by entrifugation. To the supernatant, 1 ml. of 20% sodium acetate solution and 30 ml. thanol were added. The precipitated NaDNA was separated by centrifugation at 000 rev/min, and dissolved in water. After an overnight dialysis, the NaDNA was eprecipitated as a film on a AgCl plate by evaporating the solvent.

The infrared spectrum of the film of NaDNA thus obtained is greatly different from nat of native NaDNA (see Figs. 1 and 4). The spectrum of the native NaDNA film, hen examined in air of 75% relative humidity, shows a strong absorption band t 1700 cm^{-1}, but this is absent in the spectrum of the formamide-treated NaDNA lm. This band is assigned to C=O and C=N stretching vibrations of cytosine and denine residues that are involved in the specific pairings of cytosine-guanine and denine-thymine (Kyogoku, Tsuboi, Shimanouchi & Watanabe, 1961). Therefore, hat is observed may be interpreted as resulting from a cleavage of most of the specific ase-to-base pairings in the formamide-treated NaDNA film.

For deuterated NaDNA, a similar spectral difference is observed at 1685 cm⁻ (Figs. 2 and 3). The deuterated NaDNA films (Fig 2) were obtained by exposing th

FIG. 1. Infrared absorption of undeuterated NaDNA films in the 1800 to 1450 cm^{-1} region, observed in air of 75% relative humidity.
A: native. B: $HCONH_2$-treated.

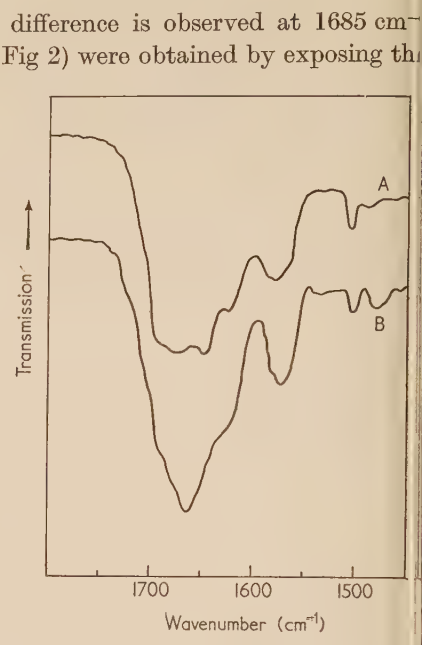

FIG. 2. Infrared absorption of deuterate NaDNA films in the 1800 to 1450 cm region, observed in air of 75% relativ humidity (D_2O vapor).
A: native. B: $HCONH_2$-treated.

FIG. 3. Infrared absorption of NaDNA in D_2O solutions. A: Before the $HCONH_2$-treatment at 30°C. B: The same, at 93°C. C: After the $HCONH_2$-treatment, at 30°C. D: The same, at 83°C

undeuterated films to D_2O vapor (75% relative humidity). The D_2O solution o formamide-treated NaDNA (Fig. 3) was obtained by repeating several times a treatment consisting of concentrating the H_2O solution of formamide-treated NaDNA

(after the above-mentioned dialysis) to about 5%, diluting with pure D_2O, and re-concentrating. In the absorption curve of the deuterated film of native NaDNA, a definite shoulder is observed at 1685 cm^{-1}, which is very faint in the absorption curve of the formamide-treated NaDNA (deuterated) film. The feature of the absorption curve of formamide-treated NaDNA (deuterated film or D_2O solution) in the 1550 to 1750 cm^{-1} region is very similar to that of NaDNA observed in D_2O solution at 93°C (Fig. 3, B) (Kyogoku *et al.*, 1961), but very different from that of native NaDNA (deuterated) film (Fig. 2, A) or from that of native NaDNA observed in D_2O solution at 30°C (Fig. 3, A). The absorptions of deuterated NaDNA in the 1550 to 1750 cm^{-1} region are wholly attributable to the C=O, C=N, and C=C stretching vibrations in the base residues (Tsuboi, Kyogoku & Shimanouchi, 1961). Therefore it may be concluded that the electronic structure of base residues of formamide-treated NaDNA is similar to that of heat-denatured NaDNA.

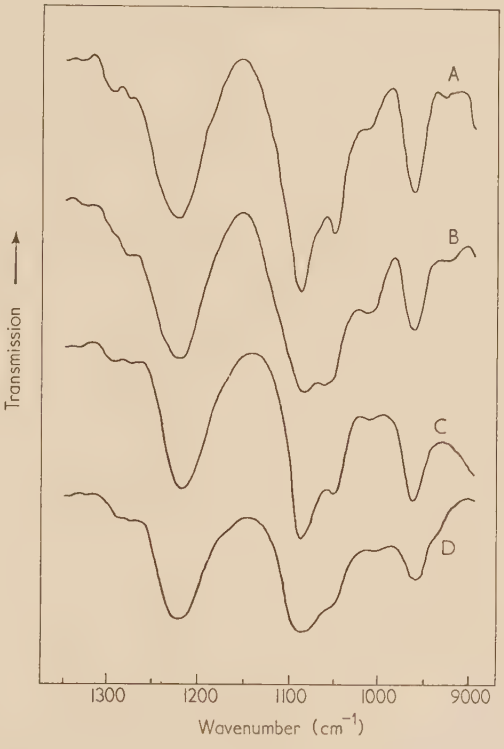

FIG. 4. Infrared absorption of undeuterated NaDNA. A: Film of native NaDNA, in air of 75% relative humidity. B: Film of $HCONH_2$-treated NaDNA, in air of 75% relative humidity. C: Native NaDNA in 5% aqueous solution, at 30°C. D: NaDNA (not treated) in 5% aqueous solution, at 95°C.

In the 1300 to 900 cm^{-1} region, the following spectral changes are observed in films (Fig. 4) when native NaDNA is treated with formamide:

(1) Disappearance of the 1292 cm^{-1} band.
(2) Weakening of the 1084 cm^{-1} band.
(3) Strengthening and high-frequency shift of the 1050 cm^{-1} band (to 1058 cm^{-1}).
(4) Strengthening of the 1015 cm^{-1} band.
(5) Weakening of the 965 cm^{-1} band.

HHH

All these spectral changes are also observed for calf thymus DNA in aqueous solution on raising the temperature from 30°C to 95°C (see Fig. 4). By an examination of dry state NaDNA film, it has been found that formamide treatment causes also a slight low-frequency shift of the 1241 cm^{-1} band (to 1234 cm^{-1}). The 1241 cm^{-1} band is assigned to the antisymmetric stretching vibration of the PO_2^- group in NaDNA (Tsuboi, 1957; Sutherland & Tsuboi, 1957). On the basis of evidence which will be detailed elsewhere, the 1084 cm^{-1} and 965 cm^{-1} bands are assigned respectively to the PO_2^- symmetric stretching and the P—O single bond stretching vibrations. The 1050 cm^{-1} band can probably be assigned to a C—O stretching vibration in the deoxyribose part of NaDNA. On the basis of these assignments, it may be concluded that the formamide treatment causes a change in the molecular conformation in the phosphate and sugar portions of NaDNA, and that the change is very similar to that induced in the NaDNA by heating an aqueous solution to 95°C.

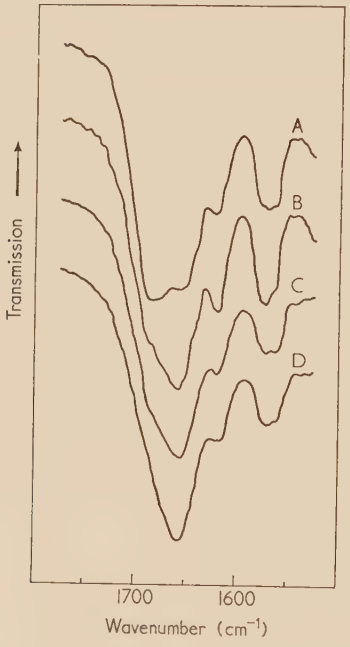

FIG. 5. Infrared absorption of NaRNA in D_2O solutions. A: Before the $HCONH_2$ treatment, at 30°C. B: The same, at 70°C. C: After the $HCONH_2$ treatment, at 30°C. D: The same, at 70°C.

Sodium salts of yeast ribosomal RNA and yeast soluble RNA have also been treated with formamide in a way similar to that described above for DNA. Infrared absorptions are practically the same for both of these two formamide-treated NaRNAs, and, when observed in D_2O solutions, are very similar to the absorptions of untreated NaRNA observed at higher temperatures (Shimanouchi, Tsuboi, Kyogoku & Watanabe, 1960) (Fig. 5). They differ definitely from native RNAs. This fact is interesting in contrast to the observation of Helmkamp & Ts'o (1961) that the RNA recovered from $HCONH_2$ solution and redissolved in water cannot be differentiated from native RNA by deviations in optical rotation. They found, however, that the ultracentrifuge pattern was similar to that of the heated RNA and markedly different from that of the native, unheated RNA. According to our observations, the formamide-treated RNA can also be differentiated from native RNA by the infrared absorptions.

This work was supported in part by grants from the Scientific Research Fund of the Ministry of Education of Japan and the Jane Coffin Childs Memorial Funds for Medical Research.

REFERENCES

Helmkamp, G. K. & Ts'o, P. O. P. (1961). *J. Amer. Chem. Soc.* **83**, 138.
Kyogoku, Y., Tsuboi, M., Shimanouchi, T. & Watanabe, I. (1961). *Nature*, **189**, 120.
Shimanouchi, T., Tsuboi, M., Kyogoku, Y. & Watanabe, I. (1960). *Biochim. biophys. Acta*, **45**, 195.
Sutherland, G. B. B. M. & Tsuboi, M. (1957). *Proc. Roy. Soc.* A, **239**, 446.
Tsuboi, M. (1957). *J. Amer. Chem. Soc.* **79**, 1351.
Tsuboi, M., Kyogoku, Y. & Shimanouchi, T. (1961). *Biochim. biophys. Acta*, in the press.

J. Mol. Biol. (1961) **3**, 746–755

The Kinetics of Parental Deoxyribonucleic Acid Replication, Deoxyguanylate Kinase Formation and ^{32}P-Inactivation of the Parental Virus in *Escherichia Coli* Infected with Bacteriophage T4†

Andrzej W. Kozinski and Maurice J. Bessman

Departments of Biology, Biophysics and The McCollum-Pratt Institute, The Johns Hopkins University, Baltimore, Maryland, U.S.A.

(*Received 20 March 1961, and in revised form 28 June 1961*)

The kinetics of deoxyguanylate kinase formation and DNA replication were compared in T4-infected bacteria. *E. coli* grown on bromouracil-containing medium were infected with ^{32}P-labeled phage and transfer of the radioactivity to high density DNA was followed as an indication of replication. At 3 min after infection, when no replication was evident, significant enzyme synthesis had occurred and by 6 min when only a small fraction of the ^{32}P had shifted to higher density, 80% of the enzyme had been formed. When ultraviolet inactivated phage were used to infect the bacteria, DNA synthesis was prevented but enzyme formation was unaffected. These results are consistent with the idea that DNA replication is not a prerequisite to enzyme synthesis in phage-infected cells.

Under the same conditions of infection, using T4 phage heavily labeled with ^{32}P, the stabilization of the parental DNA to ^{32}P decay occurred before DNA replication thus supporting the idea that the stabilization is not dependent on the prior replication of DNA.

1. Introduction

When *E. coli* is infected with the T-even bacteriophages (T2, T4, or T6) there is an immediate cessation of DNA synthesis (Cohen, 1947, 1948*a*; Cohen & Arbogast, 1950*a*) and then a resumption 6·5 to 10 min later (Cohen, 1947; Hershey, 1953; Vidaver & Kozloff, 1957). During this interval, in which there is no apparent synthesis of DNA, several interesting metabolic events take place, two of which will be examined in this paper.

First, several new enzymatic activities appear soon after infection (Flaks & Cohen, 1957; Bessman & Van Bibber, 1959; Kornberg, Zimmerman, Kornberg & Josse, 1959; Somerville, Ebisuzaki & Greenberg, 1959; Keck, Mahler & Fraser, 1960; Koerner, Smith & Buchanan, 1960; Bello, Van Bibber & Bessman, 1961). Secondly, the stabilization of ^{32}P-labeled phage to radioactive decay also occurs very soon after infection (Stent, 1955).

Since both these phenomena occur during the early period of the infection, it has been inferred that neither the synthesis of these enzymes nor the stabilization of the

† This work was supported by grant no. G-15076 from the National Science Foundation and grant no. C-4088 from the National Cancer Institute, U.S. Public Health Service. Publication no. 336 of the McCollum-Pratt Institute.

parental phage DNA to ^{32}P decay requires the prior replication of parental DNA. But some replication of the phage DNA could occur in the absence of net synthesis in the infected cell at the expense of the host DNA (Cohen, 1948*b*; Kozloff & Putnam, 1950; Evans, 1953; Kozloff, 1953) and as such would not be measurable as an increase in diphenylamine-reactive material, as an uptake of ^{32}P-labeled inorganic orthophosphate from the medium, or as an appearance of hydroxymethylcytosine in DNA. Also, the elegant experiment of Stent (1955) using ^{32}P-labeled phage to infect ^{32}P-labeled bacteria in a ^{32}P-labeled medium does not entirely rule out the involvement of host DNA as a factor in the stabilization of the parental phage DNA since a multistranded DNA (Cavalieri & Rosenberg, 1961) could be formed at the expense of host material which would have a greatly decreased sensitivity to ^{32}P decay.

In this paper the time course of DNA replication is compared both to the synthesis of deoxyguanylate kinase, an enzyme induced by phage infection (Bessman, 1959; Kornberg *et al.*, 1959), and also to the stabilization of parental phage DNA to ^{32}P decay. The measurement of DNA replication employed does not depend on net synthesis and in fact measures contributions from either host DNA and/or small molecular weight precursors (Kozinski, 1961). In addition, the independence of DNA synthesis and either enzyme formation or DNA stabilization inferred from independent experiments using different organisms and different growth conditions in different laboratories was tested directly by measuring the kinetics of these events with the same organism under the same growth conditions.

2. Materials

Deoxyguanosine monophosphate and 5-bromodeoxyuridine were products of the California Foundation. ^{32}P-labeled deoxyguanosine monophosphate was isolated from ^{32}P-labeled *E. coli* as described previously (Lehman, Bessman, Simms & Kornberg, 1958). *E. coli* B was used in all experiments and the infecting phage was an osmotic shock-resistant mutant ($T4BO_1^r$) originally isolated by S. Brenner. The TCG medium of Kozinski & Szybalski (1959) was used to grow the bacteria. When supplemented with 5-bromodeoxyuridine (200 μg/ml.), this medium is referred to as TCG-5-BU medium. L-tryptophan (20 μg/ml.) was added to all media except where indicated otherwise. ^{32}P-labeled bacteriophage were prepared according to Kozinski (1961).

3. Methods

The fractionation of DNA by centrifugation in a CsCl density gradient (Meselson, Stahl & Vinograd, 1957) and estimation of acid-insoluble ^{32}P were described in detail elsewhere (Kozinski, 1961). The measurements of inactivation of infective centers and bacteriophage were estimated according to Stent (1955). The infected bacteria and parental phage were diluted in 3XD medium (Fraser & Jerrel, 1953) and stored in liquid nitrogen until assayed.

Enzyme assay: deoxyguanylate kinase catalyses the following reaction:

$$dGMP + ATP \rightleftharpoons dGDP + ADP$$

The measurement of deoxyguanylate kinase activity was carried out under conditions described for deoxynucleotide kinase by Lehman *et al.* (1958). Briefly, this method measures the conversion of a phosphatase-labile substrate (^{32}P-labeled deoxyguanosine monophosphate) to a phosphatase-resistant product (^{32}P-labeled deoxyguanosine polyphosphate). The reaction mixture contained (in 0·25 ml.) 20 μmoles of tris (2-amino-2-hydroxymethylpropane-1:3-diol) pH 7·5; 3 μmoles of $MgCl_2$; 1 μmole of ATP; 160 mμ

moles of dGM^{32}P (0·5 to $1·5 \times 10^5$ cts/min/μmole); and 0·03 to 1 unit of enzyme. After 20 min at 37°C the reaction mixture was heated in a boiling water bath for 2 min, chilled and treated with serum phosphatase to dephosphorylate unreacted deoxyguanylate. The remaining deoxyguanosine polyphosphates were adsorbed on charcoal which was then washed, plated and counted in a thin window gas-flow Geiger counter having an efficiency of approximately 50% for ^{32}P. A unit of enzyme is that amount which phosphorylates 100 mμmoles of deoxyguanylate/hr under these conditions.

4. Experimental

(a) *Incorporation of ^{32}P into DNA after infection*

As a comparison to studies in more conventional growth media, the incorporation of ^{32}P into the DNA of cells infected with T4 in the bromodeoxyuridine medium used throughout these experiments was measured.

Cells were grown in TCG-5-BU to a density of 3×10^8/ml. and infected with 3 phage particles/bacterium. ^{32}P was added immediately and samples were removed at intervals after infection and analysed for DNA-^{32}P according to Schmidt & Thannhauser (1945) as applied by Hershey (1953). From the specific activity of the medium, the

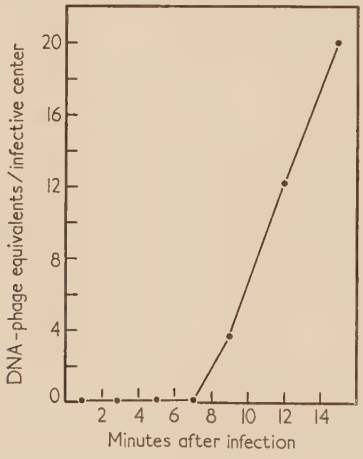

Fig. 1. Incorporation of ^{32}P into DNA after infection with T4. At zero minutes, a culture of *E. coli* (3×10^8/ml.) grown in TCG-5-BU was infected with T4 (multiplicity = 3) and inorganic ^{32}P was added to the medium. At the indicated times, samples were removed and assayed for the incorporation of ^{32}P into DNA as described by Hershey (1953).

number of phage-equivalents of DNA-P incorporated was calculated using 2×10^{-11} μg of P per infective phage particle as measured by Hershey, Dixon & Chase (1952). The curve in Fig. 1 shows that the incorporation of ^{32}P from the medium into DNA takes about 7 to 9 min, results essentially equivalent to those of Hershey (1953).

(b) *Replication of DNA and formation of dGMP kinase in T4-infected* E. Coli

In this experiment, *E. coli* grown in TCG-5-BU medium (thus containing high-density DNA) were infected with ^{32}P-labeled or unlabeled T4 bacteriophage. At intervals after infection, samples were removed and subjected to density gradient centrifugation to measure transfer of parental DNA (as measured by radioactivity)

to bromouracil DNA (as measured by increased density). At each time interval, a sample was also used for the measurement of dGMP kinase.

The conditions of the experiment were as follows: *E. coli* B were grown at 37°C with bubbling in 300 ml. TCG-5-BU medium containing 0·025 μmoles of L-tryptophan and 7 μmoles phosphorus/ml. When the cell population increased to 3×10^8 bacteria/ml. as measured by direct count in a Petroff-Hauser chamber, 100 ml. of culture were transferred to each of two bottles. Bottle "A" was infected with ^{32}P-labeled phage (specific activity = 60 μc/μmole), and bottle "B" was infected with unlabeled phage from the same stock.† The ratio of phage to bacteria in each bottle was 3.

The radioactive bacteriophage were prepared the day before the experiment and 78% were viable as estimated by ^{32}P content and plaque formers. Immediately after infection, 2·5 ml. suspension was taken from bottle A for measurement of DNA replication and 5·0 ml. from bottle B for enzyme assay. These represented the zero-time samples and were chilled to 0°C. Three minutes later, both bottles were chilled rapidly in ice and 0·5 ml. from the radioactive infection was precipitated with an equal volume of 15% trichloroacetic acid to measure the total input of ^{32}P (this represented 100% of the added ^{32}P bacteriophage). The remainder of the chilled suspensions were centrifuged at 2°C (5000 ***g*** for 10 min) and washed once with cold TCG medium for the removal of unadsorbed bacteriophage. The cells were suspended in one-half the original volume of TCG-5-BU medium and total ^{32}P was again measured on a portion of the radioactive sample. This represented 95% of the original ^{32}P input. The bottles were put back into the water bath at 37°C. At 3 min intervals (3 to 18 min), samples were taken from both bottles for measurements of DNA replication and deoxyguanylate kinase formation. Two ml. of the unlabeled culture was chilled to 0°C and disrupted by sonic oscillation for 1 min in a Mullard Sonic Oscillator and then used for measurement of enzyme activity.

For measurement of DNA replication, 5 ml. of the labeled culture was taken at each of the given times, chilled to 0°C and centrifuged at 500 ***g*** for 10 min. The cells were washed once with 5 ml. of 0·1 M-NaCl in 0·1 M-ethylenediaminetetra-acetate pH 8·0 and resuspended in 0·5 ml. more of this same solution. The DNA was extracted from these cells in the following manner: 10 μl. of sodium lauryl sulfate (30%) were added and the mixture was maintained at 37°C for 3 min and then chilled. The cell suspension cleared, and 0·05 ml. of this lysate was added directly to 3·3 ml. of 9 molal CsCl, pH 8·3. The insoluble material was removed by centrifugation at 1000 ***g*** for 10 min, and 3·0 ml. of the solution was transferred into a nitrocellulose tube, overlaid with paraffin oil, and centrifuged in the swinging bucket head (SW 38L) of the Spinco model L ultracentrifuge for 72 hr at 35,000 rev/min. At the end of the run the bottom of the centrifuge tube was punctured and about 30 fractions of 0·1 ml. each were collected. The densities of these samples were calculated from their refractive indices (Bausch and Lomb refractometer) using a standard curve relating refractive index to the density of known solutions of CsCl. Portions of the fractions were precipitated in cold 0·3 M-trichloroacetic acid using 0·1 ml. 2% albumin as carrier, the precipitates were centrifuged at 1000 ***g*** for 10 min, supernatant fluids were discarded and the precipitates were dissolved in 0·02 M-KOH, plated and their radioactivity determined. A portion of the original CsCl solution of DNA taken before centrifugation served as a measure of the total input. Recoveries ranged from 30 to 95%. The losses were due to formation of insoluble denatured nucleoprotein which floated as a pellet on the surface of the CsCl. The losses were random rather than systematic since varying losses were incurred on centrifugation of several portions of the same solution.

The data are presented in Figs. 2 and 3. At 3 min, when no replication of DNA is evident, there is a significant increase in deoxyguanylate kinase. At 6 min, a small amount of ^{32}P has shifted to higher densities and about 80% of the total enzyme has been synthesized. When 35% of the parental DNA has been incorporated into dense DNA (9 min) the enzyme synthesis has already leveled off.

† Since the assay for deoxyguanylate kinase is based on ^{32}P, it was necessary to use unlabeled phage to infect those cultures in which enzymatic activity was measured.

(c) *Effect of ultraviolet light on replication of DNA and formation of dGMP kinase*

Flaks, Lichtenstein & Cohen (1959) demonstrated that T4 bacteriophages irradiated with ultraviolet light to about 1% survival were still able to initiate the synthesis of deoxycytidylate hydroxymethylase. Similar observations were reported by Keck *et al.* (1960) with deoxycytidylate deaminase. Kozinski (unpublished results) has observed

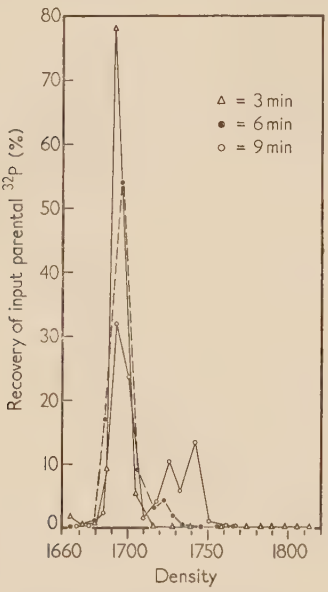

FIG. 2. The replication of DNA in phage-infected cells. Details of the experimental procedures are given in the text.

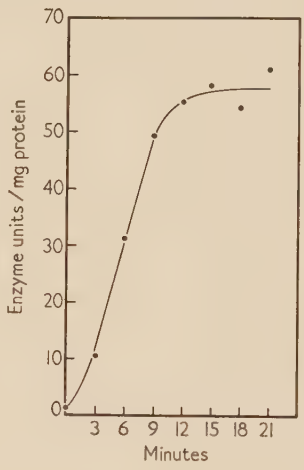

FIG. 3. The formation of deoxyguanylate kinase in phage-infected cells. At the indicated times, samples were withdrawn from the culture, disrupted by sonic oscillation and assayed for enzymatic activity as described in the text.

that transfer of parental phage ^{32}P to bromouracil DNA is inhibited by irradiating the phage with ultraviolet light. It was felt that the independence of dGMP kinase formation from DNA replication could be accentuated by using ultraviolet-irradiated phage for the infection if dGMP kinase was induced under these conditions. Accordingly, the following experiment was carried out:

E. coli B were grown in TCG-5-BU medium as in the previous experiment, and when the cell density reached 3×10^8 per ml., the culture was divided into 4 flasks. Flask A was infected with a multiplicity of 3 phage/bacterium and Flask B was infected with the same number of ultraviolet irradiated particles. These phage had been irradiated to less than 0·2% survival. Flasks C and D were treated in exactly the same way except that the phage were labeled with ^{32}P. At 0 time of infection, 0·5 ml. of culture from C and D was taken for measurement of total radioactivity added. In this experiment, the cells were not washed after 3 min as in the previous experiment.† At 2, 4, 6, 9 and 12 min, samples were

† We have consistently seen that washing the infected bacteria delays replication of DNA about three minutes. Compare Fig. 2 (washed cells) and Fig. 4 (unwashed cells). No striking effect on enzyme formation was observed.

taken for measurement of dGMP kinase formation (Flasks A and B) and for DNA replication (Flasks C and D). The results are depicted in Figs. 4 and 5. It is evident that DNA replication as measured by parental ^{32}P transfer is markedly inhibited after ultraviolet irradiation of the phage whereas dGMP kinase formation is not.

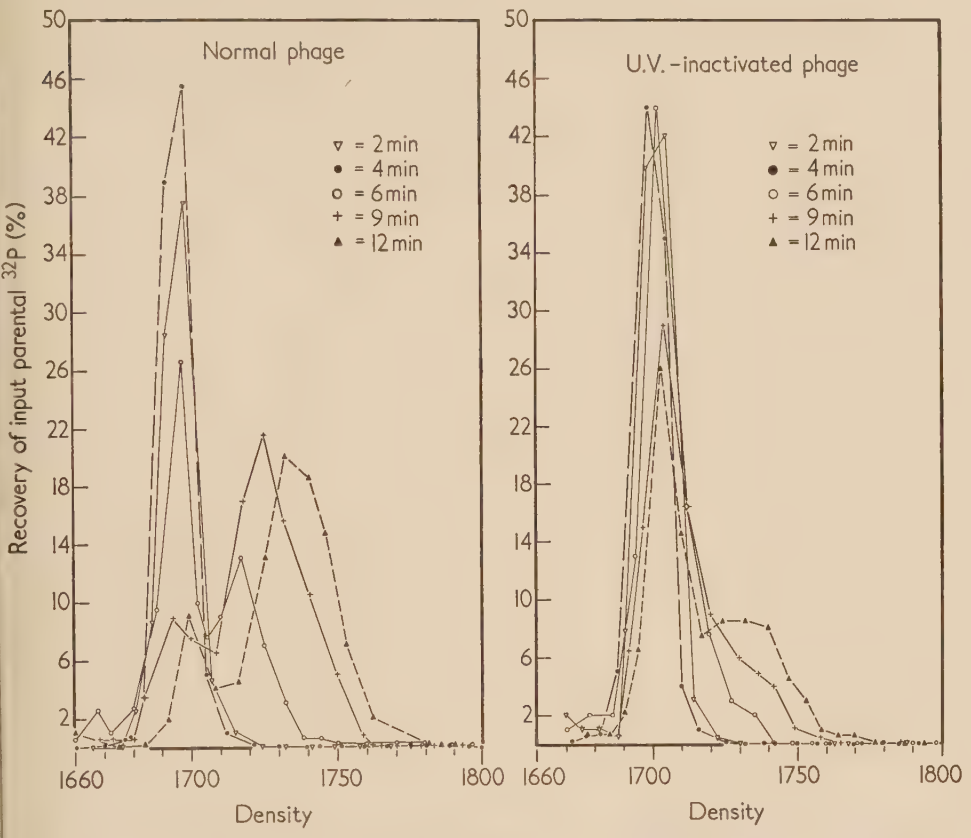

Fig. 4. Comparison of replication of DNA in cells infected with normal and ultraviolet-irradiated phage.

(d) *Kinetics of parental DNA replication and stabilization to ^{32}P decay*

E. coli were grown in TCG-5-BU medium to a concentration of about 5×10^8 cells/ml. The bacterial suspension was separated into two portions. One-half of the bacterial suspension, "A", was infected with phage heavily labeled with ^{32}P (specific activity 10 mc/μmole P) at a multiplicity of 0·01. These bacteriophage were prepared on the day of the experiment and were used as a crude lysate. The other half of the bacterial suspension, "B", was infected with phage of low radioactivity (specific activity 0·1 mc/μmole P) prepared and purified the day before the experiment. Eighty-eight per cent of this phage preparation was viable, as determined by ^{32}P content per infective phage. The multiplicity of infection was 0·1.

Three minutes after infection the bacteria in each of the suspensions were chilled in ice, sedimented by centrifugation in the cold at 5,000 *g* for 5 min, washed twice with TCG, L-tryptophan-containing medium, to remove unadsorbed phage, and resuspended in one-half the original volume of TCG-5-BU medium.

The suspensions were warmed to 37°C, and incubation was continued. Samples were taken from each of the flasks at identical times. The samples taken from "A" for the estimation of ^{32}P-inactivation of infected bacteria were frozen in liquid nitrogen. Samples

were later withdrawn from the liquid nitrogen, thawed, and plated for the estimation of surviving infective centers. The rates of inactivation of infective centers and free parental phage were compared. The death of free parental phage was followed both after dilution in 3XD medium and freezing in liquid nitrogen and after storage at 4°C.

The samples taken from "B" were used for the estimation of parental DNA replication by density gradient centrifugation as described above.

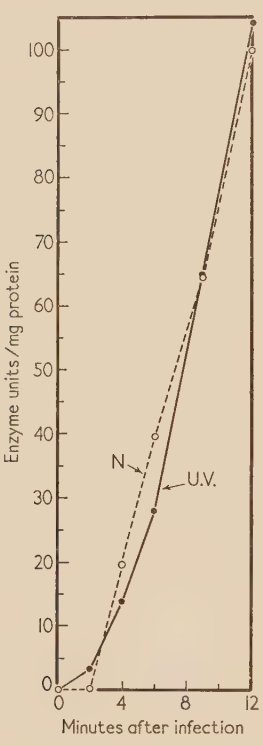

FIG. 5. Comparison of deoxyguanylate kinase in cells infected with normal (N) and ultraviolet irradiated (UV) phage.

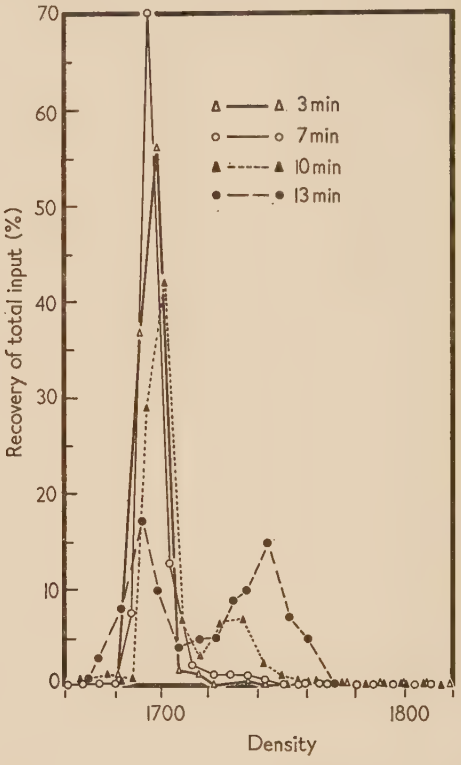

FIG. 6. Replication of DNA in phage-infected cells. The details of this experiment are given in the text. The time intervals involved are to be compared with the rate of inactivation of parental DNA in Fig. 7.

The results of the centrifugation are shown in Fig. 6. Soon after infection (3 min, 7 min) the extracted DNA bands at 1·700. This position is identical to that at which extracted parental phage DNA bands (not shown in Figure). No shift of the ^{32}P peak toward the light or heavy side of the gradient was observed. At 10 min after infection, there is a small displacement toward the heavy side. (The new peak contains about 15% of total ^{32}P.) The formation of a new, separate peak is visible at 13 min. At this later time a considerable fraction (about 50%) of the total parental ^{32}P is displaced toward the heavy side.

Figure 7 shows the rate of inactivation of infective centers by ^{32}P decay in the same cultures and at the same times post-infection used in obtaining the data presented in Fig. 6. From a comparison of the two Figures it is clear that the ^{32}P stabilization of infective centers occurs before appreciable replication (change of the parental density) is observed.

5. Discussion

The experiments with normal phage demonstrated the formation of dGMP kinase before DNA replication. The experiments with ultraviolet-irradiated phage showed an accentuation of the independence of the two processes. These results are in agreement with those of Flaks *et al.* (1959), Keck *et al.* (1960), and Murakami, Van Vunakis & Levine (1959) who demonstrated that phage-specific proteins are formed in bacteria infected with ultraviolet-irradiated phage. The inhibition of DNA replication by ultraviolet light is in agreement with its inhibition both of net DNA synthesis (Cohn & Arbogast, 1950*b*) and of formation of hydroxymethylcytosine-containing DNA (Vidaver & Kozloff, 1957).

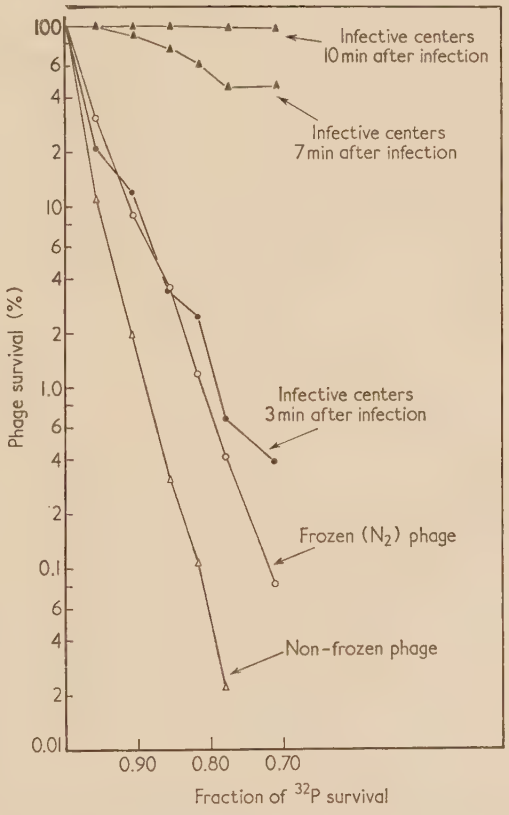

Fig. 7. Rate of inactivation of parental phage DNA by ^{32}P decay at different times after infection.

The possibility remains, however, that the mechanism promoting dGMP kinase formation is located at one end of a DNA molecule in the infecting phage and that a replication of this small region would not be detected. Any replication of less than 10% of the injected parental DNA might escape detection in these experiments. One possibility for the introduction of the capacity to synthesize dGMP kinase into the host is that the infecting DNA acts as a template for the synthesis of the specific RNA found after phage infection (Volkin & Astrachan, 1956; Astrachan & Volkin, 1959). The recent experiments of Fessler, Kelemen & Burton (1960) using adenine-

requiring mutants of *E. coli* suggest that specific enzymes can be induced by phage infection in the absence of adenine. This would mean either that the specific RNA turnover is not required for the synthesis of these proteins or that the adenine requirement is being met from some endogenous source.

In respect to the ultraviolet-irradiated phage it is of interest to mention the observations of Dirksen, Wiberg, Koerner & Buchanan (1960) who recently demonstrated that infection with such phages produces greater increases in several phage-induced enzymes than unirradiated phage. Similar results have recently been obtained by Delikas (1961); these results are especially significant since ultraviolet irradiation of the phage appears to produce a complete inhibition of DNA replication.

The stabilization of infective centers to ^{32}P decay occurs soon after infection, and is complete between 7 and 10 min. The major fraction of this stabilization is not caused by the synthesis of new DNA, since most of the stabilization occurs before there is a significant change in the density of the parental ^{32}P-containing DNA.

These results support Stent's inference (1955) that ^{32}P stabilization is not due to replication of DNA. However, they do not show whether stabilization is caused by a transfer of genetic information to a new substance, is due to preservation of information in the existing DNA structure, or is the consequence of the DNA reaching a critical site in the cell where it is confined and perhaps protected from digestion by intracellular DNase. Perhaps the DNA is maintained under conditions where scission of the molecule will not affect its linear continuity. Stabilization could then occur without transfer of information to any other substance provided that the DNA is relatively "fixed" in an environment which immobilizes either the "piece" or the broken ends. If the mechanism of stabilization is the formation of a nucleoprotein complex, this structure must be disrupted during the lysis of the bacteria with sodium lauryl sulfate or during the centrifugation because such a complex would have a much lower density than that observed. If the mechanism of stabilization were due to the formation of a multistranded hybrid with the bacterial DNA this should have been found as a species with a hybrid density. Again, the possibility of disruption of such an hypothetical hybrid during isolation of the DNA or during its centrifugation is not excluded.

Setlow & Setlow (1960) suggested that phage DNA after injection into bacteria becomes single stranded. If we assume that a large molecule becomes unwound without simultaneous synthesis (i.e. without accepting a new strand), we should expect an increase, not a decrease, in the rate of ^{32}P inactivation from a factor of 1:10 (Hershey, Kamen, Kennedy & Gest, 1950) to a factor of 1:1 for each separated strand.

It is clear that enzyme formation and stabilization of parental DNA occur very early after infection, before any evidence of DNA replication is apparent. These observations are in agreement with evidence obtained from several other laboratories and emphasize the importance of studying the biochemical and genetic events occurring in this early phase of bacteriophage infection.

The authors wish to thank Miss Patti Barnes and Miss Mary Jane Van Bibber for their contributions to these experiments.

REFERENCES

Astrachan, L. & Volkin, E. (1959). *Biochim. biophys. Acta*, **32**, 449.
Bello, L. J., Van Bibber, M. J. & Bessman, M. J. (1961). *J. Biol. Chem.* **236**.
Bessman, M. J. (1959). *J. Biol. Chem.* **234**, 2735.
Bessman, M. J. & Van Bibber, M. J. (1959). *Biochem. Biophys. Res. Comm.* **1**, 101.
Cavalieri, L. F. & Rosenberg, B. H. (1961). *Biophys. J.* **1**, 323.
Cohen, S. S. (1947). *Cold Spr. Harb. Symp. Quant. Biol.* **12**, 35.
Cohen, S. S. (1948*a*). *J. Biol. Chem.* **174**, 281.
Cohen, S. S. (1948*b*). *J. Biol. Chem.* **174**, 295.
Cohen, S. S. & Arbogast, R. (1950*a*). *J. Exp. Med.* **91**, 619.
Cohen, S. S. & Arbogast, R. (1950*b*). *J. Exp. Med.* **91**, 637.
Delikas, N. (1961). *Virology*, **13**, 153.
Dirksen, M., Wiberg, J. J., Koerner, J. R. & Buchanan, J. M. (1960). *Proc. Nat. Acad. Sci., Wash.* **46**, 1425.
Evans, E. A., Jr. (1953). *Ann. Inst. Pasteur*, **84**, 129.
Fessler, L. I., Kelemen, M. V. & Burton, K. (1960). *Biochem. J.* **77**, 558.
Flaks, J. G. & Cohen, S. S. (1957). *Biochim. biophys. Acta*, **25**, 667.
Flaks, J. G., Lichtenstein, J. & Cohen, S. S. (1959). *J. Biol. Chem.* **234**, 1507.
Fraser, D. & Jerrel, E. A. (1953). *J. Biol. Chem.* **205**, 291.
Hershey, A. D. (1953). *J. Gen. Physiol.* **37**, 1.
Hershey, A. D., Dixon, J. & Chase, M. (1952). *J. Gen. Physiol.* **36**, 777.
Hershey, A. D., Kamen, M. D., Kennedy, J. W. & Gest, H. (1950). *J. Gen. Physiol.* **34**, 305.
Keck, K., Mahler, H. R. & Fraser, D. (1960). *Arch. Biochem. Biophys.* **86**, 85.
Koerner, J. F., Smith, M. S. & Buchanan, J. M. (1960). *J. Biol. Chem.* **235**, 2691.
Kornberg, A., Zimmerman, S. B., Kornberg, S. & Josse, J. (1959). *Proc. Nat. Acad. Sci., Wash.* **45**, 772.
Kozinski, A. W. (1961). *Virology*, **13**, 124.
Kozinski, A. W. & Szybalski, W. (1959). *Virology*, **9**, 560.
Kozloff, L. M. (1953). *Cold Spr. Harb. Symp. Quant. Biol.* **18**, 209.
Kozloff, L. M. & Putnam, F. W. (1950). *J. Biol. Chem.* **182**, 229.
Lehman, I. R., Bessman, M. J., Simms, E. S. & Kornberg, A. (1958). *J. Biol. Chem.* **233**, 163.
Meselson, M., Stahl, F. W. & Vinograd, J. (1957). *Proc. Nat. Acad. Sci., Wash.* **43**, 581.
Murakami, W. T., Van Vunakis, H. & Levine, L. (1959). *Virology*, **9**, 624.
Schmidt, G. & Thannhauser, S. J. (1945). *J. Biol. Chem.* **161**, 83.
Setlow, J. K. & Setlow, R. B. (1960). *Proc. Nat. Acad. Sci., Wash.* **46**, 791.
Somerville, R., Ebisuzaki, K. & Greenberg, G. R. (1959). *Proc. Nat. Acad. Sci., Wash.* **45**, 1240.
Stent, J. (1955). *J. Gen. Physiol.* **38**, 853.
Vidaver, G. A. & Kozloff, L. M. (1957). *J. Biol. Chem.* **225**, 335.
Volkin, E. & Astrachan, L. (1956). *Virology*, **2**, 149.

J. Mol. Biol. (1961) **3**, 756–761

An Estimate of the Length of the DNA Molecule of T2 Bacteriophage by Autoradiography

JOHN CAIRNS†

Department of Genetics, Carnegie Institution of Washington, Cold Spring Harbor, N.Y., U.S.A.

(*Received 29 June 1961*)

T2 bacteriophage, labelled with [^{3}H]thymidine or [^{3}H]thymine, is subject to suicide on storage. The efficiency of suicide from ^{3}H-decay is apparently the same as that from ^{32}P-decay.

Autoradiography of T2 DNA, labelled with [^{3}H]thymine and extracted in the presence of 1000-fold excess of cold T2, shows that the molecule can assume the form of an unbranched rod about 52 μ long. If the molecule is throughout its length a double helix in the *B* configuration, this indicates a molecular weight of 110×10^6.

1. Introduction

The decay of tritium gives rise to electrons whose mean range in autoradiographic emulsion is less than one micron (Fitzgerald, Eidinoff, Knoll & Simmel, 1951). It should therefore be possible to obtain a high resolution image of individual molecules of ^{3}H-labelled DNA by autoradiography, using the very highly labelled [^{3}H]thymine that is now available; thus DNA containing [^{3}H]thymine of specific activity 10 c/m-mol will have roughly one disintegration per micron of double helix per week and should produce a near-continuous line of grains along its length after a few weeks' exposure.

Bacteriophage T2 seemed in most respects the best material with which to launch such a procedure. Most of the precursors for T-even thymine synthesis come from the medium after infection (Weed & Cohen, 1951; Kozloff, 1953) so there should be extensive incorporation of labelled thymine given at the time of infection; T2 DNA can be extracted in a pure and homogeneous state with phenol (Mandell & Hershey, 1960), each particle providing a single molecule with a molecular weight of over 100×10^6 (Rubinstein, Thomas & Hershey, 1961); lastly a molecule of such great size is ideal for testing a method of measuring molecular length the accuracy of which is, in theory at least, independent of length.

2. Materials and Methods

Phage. T2, strain T2H (Hershey), was used throughout.

Bacteria. Escherichia coli strain S was used for the production of stocks of unlabelled phage and for phage assays. Labelled phage was prepared in the thymineless strain B^{2} (Brenner).

† Present address: The Australian National University, Canberra, Australia.

Media. Stocks of unlabelled phage were prepared in M9 (Adams, 1959) supplemented with 0·5 g/l. NaCl. All experiments on the production of phage in the presence of limited thymine or thymidine were carried out using the glucose-ammonium medium described by Hershey (1955).

E. coli strain B3 was grown in the presence of 5 μg/ml. of thymine or thymidine. Phage assays were performed using the standard methods (Adams, 1959). Dilution of phage stocks was made in 10^{-3} M-$MgCl_2$, 0·05% NaCl, 0·001% gelatin, buffered with 0·01 M-tris (2-amino-2-hydroxymethylpropane-1:3-diol) pH 7·4.

[^3H]*Thymine and* [^3H]*thymidine.* These were obtained from the New England Nuclear Corp. and from Schwartz Inc. In the case of the former source these materials are prepared by reducing 5-hydroxymethyl-uracil with tritium so that the label is confined to one hydrogen atom in the methyl group; for this reason they can be specifically designated as 5-[^{3}H]methyl-uracil and 5-[^{3}H]methyldeoxyuridine.

Preparation of labelled phage. In order to ensure extensive incorporation of [^{3}H]thymine (or thymidine) into phage it was necessary to engineer the situation so that phage would only be made if thymine was present and would then be made in an amount which was proportional to the amount of thymine present. The thymineless B3 strain of *E. coli* was used as host since this strain readily incorporates thymidine even at low concentrations, whereas the prototroph does not (Crawford, 1958). Since T2 infection causes the formation of thymidylate synthetase even in thymineless bacteria (Barner & Cohen 1959), it was necessary to block this enzyme by the addition of 5-fluorodeoxyuridine (FUDR) (Cohen, Flaks, Barner, Loeb & Lichtenstein, 1958). At the same time, uridine (UR) was added to ensure that FUDR derivatives were not incorporated into RNA. Thus the final procedure was as follows:

E. coli B3 was grown to 2×10^8 cells/ml. in glucose-ammonium medium with 5 μg/ml. thymidine, and then centrifuged and resuspended in one third volume of fresh medium without thymidine. FUDR and UR were added to give final concentrations of 10^{-5} and 10^{-4} M. Five minutes later the bacteria were infected with T2 at a multiplicity of 4. After 4 min, 0·02 ml. of these infected bacteria was added to 0·02 ml. of double strength medium (with 2×10^{-5} M-FUDR and 2×10^{-4} M-UR) and 0·02 ml. of [^{3}H]thymidine in water. The final concentrations in this growth tube were 2×10^8 B3/ml. 10^{-5} M-FUDR, 10^{-4} M-UR, 2 to 8 μg/ml. thymidine (40 to 160 μC/ml.). (When thymine was the label, the growth tube was supplemented with 10^{-3} M-deoxyadenosine.) After aeration for a further 30 min, the bacteria were lysed with chloroform and the contents of the growth tube were made up to 10 ml. with diluting fluid.

The yield of phage from such a system was 1×10^{10} phage/μg thymidine and 6 to 8×10^9 phage/μg thymine; it was slightly less with [^{3}H]thymidine and [^{3}H]thymine. These yields are 2 to 4 times less than would be expected on the basis of the known thymine content of T2 (Hershey, Dixon & Chase, 1953), but they were not lowered further by raising the concentration of FUDR. In the absence of thymine or thymidine the yield was about 5 phage per bacterium. Purified phage prepared from cold thymidine in this way had the normal optical density per infective particle at 260 mμ. Phage prepared from hot or cold thymine or thymidine showed no rise in the frequency of *r* mutants.

Extraction of phage DNA. Phage was extracted with phenol according to the method of Mandell & Hershey (1960). When labelled phage was extracted, enough cold carrier phage was added to bring the concentration up to the requisite 3×10^{12} phage/ml.; the mixture was then packed in the centrifuge, resuspended and extracted with phenol.

Autoradiography. Once the DNA had been extracted it was diluted to a suitable concentration in various salt solutions and spread in various ways upon glass microscope slides which had previously been coated with various materials. These slides were, on occasion, then coated with chrome-gelatin (0·5% gelatin, 0·05% chrome alum). They were overlaid in the usual manner with Kodak autoradiographic stripping film, AR 10, and stored at 4°C over silica gel in an atmosphere of CO_2 to prevent latent image fading (Herz, 1959). After exposure the film was developed with Kodak D19b for 20 min at 16°C.

3. Results

(a) *Suicide of ^3H-labelled phage*

Two lots of [^{3}H]thymidine and one of [^{3}H]thymine were used at various times for making labelled phage. In each case the resulting phage was diluted 10^2 to 10^4-fold, stored at 4°C and repeatedly assayed for surviving phage. Excess cold phage mixed with the hot phage and stored under the same conditions proved to be stable, as did phage prepared by the same procedure but with cold thymidine. Thus the observed

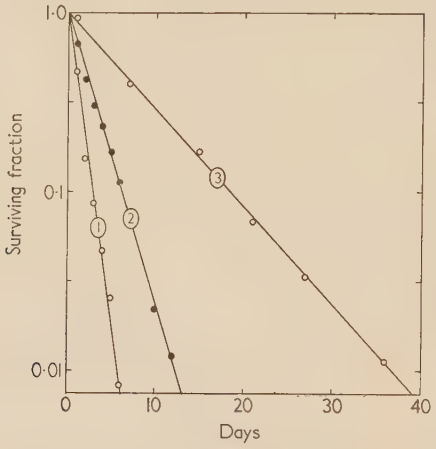

FIG. 1. The suicide of T2 labelled with (1) [^{3}H]thymine 11·2 c/m-mole. (2) [^{3}H]thymidine 5·5 c/m-mole and (3) [^{3}H]thymidine 1·8 c/m-mole.

inactivation of labelled phage was due neither to indirect effects of radiation within the storage tube nor to any innate instability of phage prepared, for example, in the presence of FUDR. Since tritium has a half-life of 12 years, no correction has to be made for decline in radioactivity during the period of storage.

TABLE 1

The suicide of T2 phage labelled with [^3H]thymine and [^3H]thymidine.

Label	sp. A (c/m-mole)	k (lethals/phage. day)	k.m-mole / c	αN† ("lethal" methyl H atoms/phage)
(1) 5-(^{3}H-methyl)-uracil	11·2	0·78	0·069	$3{\cdot}9\times10^4$
(2) 5-(^{3}H-methyl)-deoxyuridine	5·2	0·37	0·071	$4{\cdot}1\times10^4$
(3) ^{3}H-thymidine	1·8	0·13	0·072	$4{\cdot}1\times10^4$

† $\alpha N = \dfrac{\text{lethals}}{\text{disintegration}} \times \dfrac{\text{methyl H atoms}}{\text{phage}}$

$= \dfrac{\text{lethals}}{\text{phage . day}} \times \dfrac{\text{m-mole}}{\text{c}} \times \dfrac{\text{molecules}}{\text{m-mole}} \times \dfrac{\text{methyl H atoms}}{\text{molecule}} \times \dfrac{\text{Curie. day}}{\text{disintegration}}$

$= k \times \dfrac{\text{m-mole}}{\text{c}} \times 6{\cdot}02\times10^{20} \times 3 \times \dfrac{1}{3{\cdot}20\times10^{15}}$

$= 5{\cdot}64\times10^5 \times \dfrac{k.\text{m-mole}}{\text{c}}$

The results are shown in Fig. 1 and Table 1. The suicide of phage is seen to be a first order process with a rate constant (k) which is directly proportional to the specific activity (c/m-mole) of the thymine or thymidine. From this the number, αN, of "lethal" thymine methyl H atoms per phage may be calculated to be 4×10^4. Since the burst size in these experiments was around 120, the contribution of cold thymine from the pool of bacterial DNA (about 24 phage equivalents of thymine) (Hershey *et al.*, 1953; Hershey & Melechen, 1957) will have lowered the specific activity of the incorporated thymine by 20%. Correction for this raises αN to 5×10^4.

This value is not significantly different from the number of "lethal" P atoms per phage, determined from the rate of ^{32}P-suicide (Hershey, Kamen, Kennedy & Gest, 1950; Stent & Fuerst, 1955). Since one third of the bases in T2 DNA are thymine, the total number of thymine methyl H atoms equals the total number of P atoms. It follows therefore that the efficiency of inactivation by decay of ^{32}P and ^{3}H are the same. This is an unexpected result. First, ^{32}P and ^{3}H differ greatly in the energy of the electrons they emit (max. energy 1700 and 17 kev respectively). Second, the sites of their incorporation into DNA seemingly could scarcely differ more; the decay of ^{32}P, in the sugar-phosphate chain, and its conversion to sulfur must necessarily break that chain; the decay of ^{3}H, in the methyl group of thymine, and its conversion to helium need not necessarily cause chain breakage nor perhaps any lasting local alteration in the DNA at all.

Practically, these results indicate that at least 99% of the phage is fairly uniformly labelled.

(b) *Autoradiography of ^{3}H-labelled T2 DNA*

Although the production and extraction of highly-labelled DNA presented no problem, there was little prior information on how best to fix this DNA in a sufficiently extended state so that its contours could be followed by autoradiography. Electron microscopy has shown that DNA can be adsorbed from phosphate-buffered solutions of pH 5 to 6 to a variety of surfaces as straight rods many microns long (Hall & Litt, 1958; Beer, 1961) and various methods have been used to ensure that at the time of adsorption the molecules are subject to sufficient shear to align them.

In the course of several months many combinations of DNA concentrations, suspending fluids, varieties of shearing force and adsorbent surfaces were tested. Interestingly, fibres drawn from DNA at high concentration show very poor extension of the minority of molecules that are labelled. The most satisfactory method was found by accident. On testing the appearance of labelled DNA adsorbed to slides partly coated with a co-polymer of polyvinylpyridine and styrene (generously supplied by Dr. Michael Beer), numerous straight molecules were seen adsorbed to the glass on either side of the area coated with polymer; this glass had been cleaned with chromic acid, coated with DNA by drawing the slide across the surface of a solution of DNA in M/15 phosphate buffer pH 5·6, drained and rinsed with distilled water, and then coated with chrome-gelatin (to ensure that the autoradiographic film remained stuck to the slide on drying). Even here, however, there were only localized regions where the DNA was suitably extended. In most regions, the individual molecules were apparently folded back on themselves several times to form a short "rod" of densely packed grains. It seems therefore that the best method for displaying DNA molecules —at least those as long as T2 DNA—has not yet been found.

The appearance of the extended DNA is shown in Plate I. Of the 13 labelled molecules (or fragments of molecules) shown, 7 have a length between 49 and 53 μ; of the remaining 6, one (immediately over the center of the scale) seems from its grain density and length to be folded about its center. Other samples of DNA prepared on different occasions likewise showed that the maximum length, when adsorbed on to glass, was slightly more than 50 μ.

As an estimate of length and hence of molecular weight this is subject to certain errors and variables. For example:

(i) There are several configurations which the molecules might assume, giving values of 2·55 to 3·46 Å per base pair (Langridge, Wilson, Hooper, Wilkins & Hamilton, 1960). Of these the most likely, particularly in the case of T2 DNA (Hamilton *et al.*, 1959), is the *B* configuration with 3·4 Å per base pair.

(ii) Since it is the autoradiographic image and not the molecule itself which is seen, any stretching of the film between exposure and measuring will produce an apparent lengthening. This, however, seems to be a rare occurrence with stripping film.

(iii) Since the molecule is indicated as a series of grains which one may assume to be randomly placed along its length, it is simple to show for this case, where the mean number of grains (M) per molecule of length L is more than about 10, that the mode, mean and variance of observed lengths (that is, between the centres of the outermost grains) will be approximately $L(1 - 1/M)$, $L(1 - 2/M)$ and $L^2(2/M^2)$ respectively. One would therefore expect for molecules such as these, marked with 50 to 100 grains, that the length of the average molecule would be underestimated by 2 to 4%.

(iv) The resolution of the technique can best be judged by the fact that the grains appear to deviate little to either side of the apparent line of each labelled molecule. It is therefore unlikely that the length of any molecule is overestimated by more than 1μ for the reason of poor resolution.

Thus if any single length has to be selected as the most likely for T2 DNA, that length is probably 52 μ. Taking a value of 3·4 Å per base pair and 357 as the average molecular weight of a base in the sodium salt of T2 DNA, this indicates a molecular weight of 110×10^6 and a phosphorus content of $3{\cdot}0 \times 10^5$. These are slightly below the accepted values though probably not by enough to warrant, at this stage, postulating anything other than an uncomplicated double helix as the form of the T2 DNA molecule.

I am greatly indebted to Dr. A. D. Hershey for his advice and encouragement and for the hospitality of his laboratory, to Dr. Michael Beer for information and advice on spreading DNA, and to the National Institutes of Health (U.S.A.) for a post-doctoral fellowship during which this work was done.

REFERENCES

Adams, M. H. (1959). *The Bacteriophages*. New York: Interscience Publishers.
Barner, H. D. & Cohen, S. S. (1959). *J. Biol. Chem.* **234**, 2987.
Beer, M. (1961). *J. Mol. Biol.* **3**, 263.
Crawford, L. V. (1958). *Biochim. biophys. Acta*, **30**, 428.
Cohen, S. S., Flaks, J. G., Barner, H. D., Loeb, M. R. & Lichtenstein, J. (1958). *Proc. Nat. Acad. Sci., Wash.* **44**, 1004.
Fitzgerald, P. J., Eidinoff, M. L., Knoll, J. E. & Simmel, E. B. (1951). *Science*, **114**, 494.
Hall, C. E. & Litt, M. (1958). *J. Biophys. Biochem. Cytol.* **4**, 1.

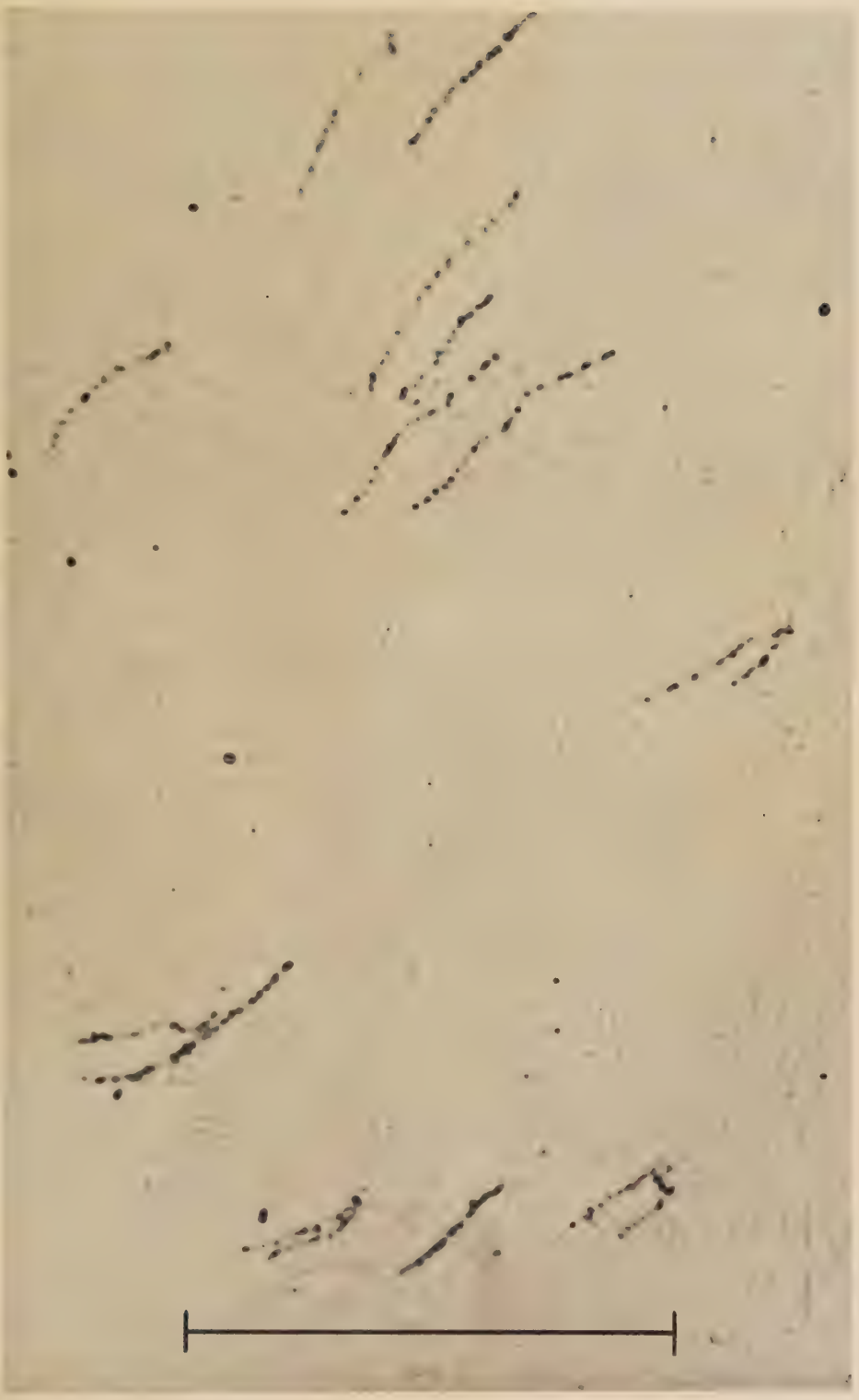

PLATE I. T2 DNA, labelled with [^{3}H]thymine (11·2 c/m-mole), extracted with phenol in the presence of 1000-fold excess of cold T2, and adsorbed to glass at a total DNA concentration of 25 μg/ml. in M/15 phosphate buffer pH 5·6. The autoradiographic exposure was 63 days. The scale shows 100 μ.

[*To face page* 760

Hamilton, L. D., Barclay, R. K., Wilkins, M. H. F., Brown, G. L., Wilson, H. R., Marvin, D. A., Ephrussi-Taylor, H. & Simmons, N. S. (1959). *J. Biophys. Biochem. Cytol.* **5**, 397.
Hershey, A. D. (1955). *Virology*, **1**, 108.
Hershey, A. D., Dixon, J. & Chase, M. (1953). *J. Gen. Physiol.* **36**, 777.
Hershey, A. D., Kamen, M. D., Kennedy, J. W. & Gest, H. (1950). *J. Gen. Physiol.* **34**, 305.
Hershey, A. D. & Melechen, N. E. (1957). *Virology*, **3**, 207.
Herz, R. H. (1959). *Lab. Investigation*, **8**, 71.
Kozloff, L. M. (1953). *Cold Spr. Harb. Symp. Quant. Biol.* **18**, 209.
Langridge, R., Wilson, H. R., Hooper, C. W., Wilkins, M. H. F. & Hamilton, L. D. (1960). *J. Mol. Biol.* **2**, 19.
Mandell, J. D. & Hershey, A. D. (1960). *Analyt. Biochem.* **1**, 66.
Rubinstein, I., Thomas, C. A. & Hershey, A. D. (1961). *Proc. Nat. Acad. Sci., Wash.* **47**, 1113.
Stent, G. S. & Fuerst, C. R. (1955). *J. Gen. Physiol.* **38**, 441.
Weed, L. L. & Cohen, S. S. (1951). *J. Biol. Chem.* **192**, 693.

J. Mol. Biol. (1961) **3**, 762–768

Mutagenesis of Bacteriophage T4 by Acridines

Alice Orgel

Department of Pathology, University of Cambridge, England

AND

S. Brenner

Medical Research Council Unit for Molecular Biology, Cavendish Laboratory, Cambridge, England

(*Received 8 August 1961*)

Induced reversion by acridines of a number of different r_{II} mutants of bacteriophage T4 has been studied. The following mutants were used: ten BD mutants (induced with bromouracil), ten SP mutants (spontaneous origin), twelve P mutants (induced with proflavin) and ten AC mutants (induced with 5 aminoacridine). All ten BD mutants were induced to revert by 5-bromodeoxyuridine while none was induced to revert either by proflavin or by 5-aminoacridine. By contrast, these acridines induced reversion of ten of the P mutants, ten of the eleven AC mutants and eight of the ten SP mutants. None of the AC, P, and SP was reverted by 5-bromodeoxyuridine. These experiments confirm the existence of at least two main classes of mutagenic effect. Mutagenesis by other acridine compounds is also reported; all have much the same spectrum of behaviour as proflavin and 5-aminoacridine, but differ greatly in their effectiveness.

1. Introduction

It has been shown that mutations can be induced in the r_{II} region of bacteriophage T4 by a variety of chemical agents including base analogues (5-bromouracil or 5-bromodeoxyuridine (BD) and 2-aminopurine (AP)), proflavin (P) and nitrous acid (NA) (Litman & Pardee, 1956; Benzer & Freese, 1958; Freese, 1959*a*; Brenner, Benzer & Barnett, 1958; Vielmetter & Wieder, 1959). Freese (1959*b*) studied the induction of reversions to standard type and found that nearly all BD, AP and NA mutants could be induced to revert by either BD or AP or both. Only 14% of spontaneous (SP) mutants and only one of 55 P mutants were base analogue revertible. The existence of these two mutually exclusive classes of mutants has led Freese (1959*b*) to suggest that there are two independent molecular mechanisms for point mutation.

In this paper we describe experiments which confirm the existence of at least two classes of mutagenic effect. We have studied the reversion induced by proflavin in different r_{II} mutants and our results are complementary to those of Freese (1959*b*); BD mutants are not induced to revert by proflavin while spontaneous and P mutants are, in general, revertible in this way. In addition, we have shown that other mutagenic acridines have a similar specificity to that of proflavin.

2. Materials and Methods

Bacteria: *Escherichia coli* strains B, BB (Berkeley), K12(λ) and B3 (thymineless).

Bacteriophages: T4Br^+ (standard type of Benzer) and r_{II} mutants. Spontaneous mutants were those of Benzer (1955), BD mutants were the N mutants of Benzer & Freese (1958) and S mutants induced in an independent experiment (A. Orgel, unpublished). P mutants were those of Brenner, Benzer & Barnett (1958). Other mutants are described in this paper.

Acridines: The English system of numbering the acridine ring has been used throughout. It is:

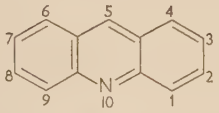

Proflavin (2,8-diaminoacridine), 5-aminoacridine, acridine yellow (2,8-diamino-3,7-dimethylacridine), acridine orange (2,8-bisdimethylaminoacridine), coriphosphine (exact structure unknown, probably mainly 2-amino-3-methyl-4,8-dimethylaminoacridine) and acridine hydrochloride were commercial preparations. 1-, 2-, 3-, and 4-aminoacridines and 2,5- and 2,7-diaminoacridines were gifts from Professor A. Albert of the Australian National University, Canberra.

(a) *Induction of reversions and mutations*

Special procedures are required to induce revertants or mutants with acridines since they prevent the maturation of phage (Foster, 1948; De Mars, Luria, Fisher & Levinthal, 1953). In order to obtain a yield of bacteriophages which have been subjected to the mutagenic action of acridines we have used lysis-inhibited cultures. A culture of *E. coli* BB was grown with aeration to 3×10^8 cells/ml. in minimal glucose-salts medium. 10 μg/ml. L-tryptophan and the acridine solution were added, the culture immediately infected with phage at a multiplicity of 5 phage per cell and aerated at 37°C. Eight minutes later the culture was superinfected with the same phage (multiplicity = 5) to produce lysis inhibition. (On strain BB both r^+ and r_{II} bacteriophages are lysis inhibiting.) After aeration at 37°C for 40 min the culture was diluted 1 : 50 into warmed glucose-salts medium to remove the inhibitory effect of the acridine. After incubation for a further 40 min at 37°C the cultures were lysed with chloroform. Control tubes were treated in exactly the same manner except that the acridine was omitted.

The lysates were plated at suitable dilutions on *E. coli* K12(λ) to obtain the numbers of revertants and on *E. coli* B for the total count. Under these conditions the burst size after treatment with acridines was 25 to 50% of that of the control tube.

The mutagenic action of 5-bromouracil was measured in liquid medium using *E. coli* strain B3 (thymineless). A culture of B3, grown to 3×10^8 cells/ml. in glucose-salts medium supplemented with thymine (2·5 μg/ml.), was centrifuged and resuspended in fresh medium. L-tryptophan (10 μg/ml.) was added and 5-bromouracil to a final concentration of 10^{-4} M. The bacteriophage was added (multiplicity = 0·01) and the culture aerated at 37°C for 2 hr. It was then lysed with chloroform. In controls, the 5-bromouracil was omitted.

Spot tests with 2-aminopurine and 5-bromodeoxyuridine were carried out as described by Freese (1959*b*).

(b) *Genetic methods*

Methods of handling the r_{II} system were those described by Benzer (1955, 1957) and Benzer & Freese (1958).

3. Results

(a) *Induction of* r_{II} *mutants by 5-aminoacridine*

5-aminoacridine (4 μg/ml.) is mutagenic, increasing the frequency of r mutants in standard type from the spontaneous background of about 10^{-4} to 0·45%. A number

of independently arising mutants induced by 5-aminoacridine were isolated, and the r_{II} mutants selected by their inability to grow on *E. coli* strain K12 (λ). Of these AC mutants, fourteen were chosen which had low spontaneous reversion frequencies (less than 10^{-6}) and which were at different sites as shown by recombination experiments. Four of these mutants were rejected; one because it was non-reverting, and three because they were at the same sites as three of the seventeen P mutants initially

TABLE 1

Reversion of r_{II} *mutants with proflavin and 5-aminoacridine*

Type	r_{II} mutant	Proportion $r^+ \times 10^{-6}$		
		No acridine	proflavin	5-aminoacridine
BD	N11	0·8	1·7	0·8
	N12	0·03	0·09	0·09
	N24	0·9	1·9	1·9
	N31	0·05	0·05	0·05
	S9	0·04	0·03	0·03
	S20	0·3	0·3	0·5
	S21	0·2	0·2	0·2
	S30	0·02	0·03	0·03
	S87	0·1	0·1	0·1
	S116	0·05	0·05	0·05
SP	*r*111	250	420	220
	*r*114	0·04	7	3
	*r*117	1·5	40	20
	*r*131	0·7	18	25
	*r*150	0·005	1	0·4
	*r*155	0·09	1·9	1·2
	*r*240	0·1	6	9
	*r*271	0·02	13	8
	*r*279	0·04	19	38
5-AA	AC1	0·02	2·7	2·6
	AC2	0·004	2·3	0·7
	AC3	0·03	9	30
	AC9	0·09	15	50
	AC11	0·01	16	28
	AC15	0·02	40	200
	AC22	0·01	2·4	1·6
	AC23	0·2	3·1	2·8
	AC25	0·02	17	28
	AC8	0·03	0·06	0·05
P	P3	0·03	30	10
	P23	0·04	11	2·8
	P43	0·02	35	200
	P53	0·04	7·8	11
	P62	0·04	15	4·2
	P73	0·2	30	20
	P79	0·1	15	10
	P83	0·07	0·9	0·4
	P59	0·36	0·35	0·38
	P14	1·8	10	3·2
	P63	1·6	15	2·2
	P19	3·8	4·9	5·2

chosen for use in this work. These coincidences of forward mutation sites suggest that 5-aminoacridine might have a spectrum of mutants similar to that of proflavin.

(b) *Induction of reversion by proflavin and 5-aminoacridine*

Ten BD mutants, ten SP mutants, twelve P mutants and ten AC mutants were studied. Spot tests showed that 5-bromodeoxyuridine induced reversion of all the BD mutants. None of the P and AC mutants was induced to revert by this base analogue. Of the SP mutants, nine were insensitive to induction and one, r_{263}, showed induced reversion. This mutant is a special case which will be discussed later.

The induction of reversion by proflavin (4 μg/ml.) and 5-aminoacridine (8 μg/ml.) was measured and Table 1 shows the induced and spontaneous reversion frequencies for each mutant. It is seen that none of the BD mutants was induced to revert by acridines, although all reverted spontaneously.

By contrast, ten of the twelve P mutants were induced to revert by acridines, the factors of increase ranging from approximately five to ten thousand. Mutants P14 and P63 were revertible by proflavin but not by 5-aminoacridine. P19, which has a fairly high spontaneous reversion frequency, and P59 do not appear to be revertible by either agent. These mutants showed no induced reversion in spot tests with 5-bromodeoxyuridine or with 2-aminopurine.

Nine of the ten AC mutants were induced to revert by proflavin and by 5-aminoacridine; the exception, AC8, was also not induced to revert by the base analogues in spot tests.

Of the spontaneous mutants, eight were acridine revertible. The extent of induced reversion was difficult to assess for r_{111} which has a very high spontaneous reversion frequency.

The spontaneous mutant r_{263} is revertible by 5-bromodeoxyuridine in spot tests. When stocks of this mutant are plated, two kinds of plaques are observed on *E. coli* K12(λ): large, apparently standard, type, and tiny plaques. These are genetically different since the characteristics of each kind of plaque are retained on picking and replating on *E. coli* K12(λ).

The mutation frequencies of the two kinds of "reversion" of r_{263} were studied with the different mutagens in liquid medium. The results are given in Table 2. It is seen that the incidence of the tiny plaques was specifically increased by the acridines which left the frequency of the large plaques unchanged. By contrast 5-bromouracil induced reversion to the large plaque type and probably did not affect the mutation

Table 2

Reversion of r_{263} *with 5-bromouracil, proflavin and 5-aminoacridine*

		Plaques in 0·1 ml. on K12 (λ)			Reversion frequency $\times 10^{-6}$	
	titre/ml.	dilution	large	tiny	large	tiny
No acridine	3×10^{7}	10^{0}	54	20	18	7
Proflavin	$8{\cdot}4\times10^{6}$	10^{0}	11	112	13	*130*
5-aminoacridine	4×10^{7}	10^{0}	35	120	9	30
No 5-BU	$9{\cdot}6\times10^{9}$	10^{-2}	206	97	21	10
5-BU	$2{\cdot}5\times10^{9}$	10^{-4}	236	2	*9400*	(80)

frequency of the tiny plaques. The latter frequency was difficult to estimate after treatment with 5-bromouracil since the tiny plaques were a small minority of the total revertants and the numbers have probably been overestimated.

(c) *Mutagenesis by other acridines*

A number of other acridines have been screened for mutagenic activity and specificity using selected P, AC, SP and BD mutants. For each of the mutagens a concentration was chosen which gave least killing of the bacteria and optimum induced frequency of reversion. The results for some mutagenic acridines are shown in Table 3 in which it can be seen that all have a similar specificity to that of proflavin and 5-aminoacridine. They induce the reversion of the AC, P, and SP mutants and leave the frequency of reversion of the BD mutants unchanged. Acridine yellow appears to exert the most powerful mutagenic effect. Coriphosphine (not included in the Table) was also tested on these mutants and gave a spectrum of reversion frequencies at a concentration of 3 μg/ml. similar to that of acridine orange. 4-aminoacridine, at a concentration of 72 μg/ml., was also found to be active, raising the reversion frequency of mutant AC15 from a spontaneous rate of $0{\cdot}02\times10^{-6}$ to 29×10^{-6}, while 3-aminoacridine at the same concentration increased the frequency in this mutant to $4{\cdot}6\times10^{-6}$. 1-aminoacridine at a concentration of 132 μg/ml. increased the reversion rate to $0{\cdot}7\times10^{-6}$.

TABLE 3

Reversion frequencies ($\times 10^{-6}$) of selected r_{II} mutants with different acridines

	Mutagen and concentration used								
r_{II} mutant	No acridine	acridine yellow 1·6 to 2 μg/ml.	2,5-di-amino-acridine 8 μg/ml.	5-amino-acridine 8 μg/ml.	proflavin 4 μg/ml.	2-amino-acridine 16 μg/ml.	2,7-di-amino-acridine 16 μg/ml.	acridine hydro-chloride 80 to 100 μg/ml.	acridine orange 16 to 20 μg/ml.
AC2	0·004	6·5	3·1	0·7	2·3	0·5	1·1	0·2	0·05
P53	0·04	3·4	35	11	7·8	2·1	1·6	1·4	0·1
P3	0·03	22	25	10	30	4·3	3·9	1·1	0·4
AC3	0·03	90	80	30	9	19	2·3	1·9	2·7
*r*271	0·02	400	160	8	13	30	8	15	2·5
*r*274	0·04	250	320	38	19	60	22	17	2·6
AC15	0·02	350	340	200	40	22	7	13	6·2
P43	0·02	300	340	200	35	22	11	8	3·4
N31	0·05	0·08	0·01	0·05	0·05	0·05	0·03	0·01	0·04
S87	0·1	0·04	0·05	0·1	0·1	0·02	0·03	0·03	0·01

Acridine yellow and 2,5-diaminoacridine were also tested on those P and AC mutants in which reversion was not induced by proflavin and 5-aminoacridine and on the two P mutants in which reversion was induced only by proflavin. The results are shown in Table 4. It is seen that the mutants P19, P59 and AC8 are not induced to revert by acridine yellow or by 2,5-diaminoacridine. The reversion frequencies of P14 and P63 are slightly increased by these agents.

Table 4

r_{II} mutant	Proportion $r^+ \times 10^{-6}$				
	No acridine	proflavin	5-amino-acridine	acridine yellow	2-5 diamino-acridine
P14	1·75	10·6	3·15	4·18	4·84
P63	1·55	14·5	2·2	7·8	6·6
P19	3·8	4·9	5·2	4·1	5·2
P59	0·36	0·35	0·38	0·64	0·27
AC8	0·03	0·06	0·05	0·02	0·07

4. Discussion

Our most definite findings are:

(1) that none of the BD mutants which were tested was induced to revert by the acridines, while all of them reverted spontaneously and were induced to revert by BD in spot tests;

(2) that most SP, P and AC mutants are induced to revert by acridines and are insensitive to reversion by base analogues;

(3) that no mutant was found to be revertible to standard type by both classes of compounds;

(4) that a few AC and P mutants are not induced to revert by either class of mutagen, although they do so spontaneously.

On this point it is possible that in the case of mutant P19, which has a fairly high spontaneous reversion frequency, reversion is indeed induced by the acridines but the number of induced revertants is not high enough to be detected above that of spontaneous revertants. This seems less likely to be true of mutants P59 and AC8, which have moderately low spontaneous reversion frequencies and yet are not reverted by either class of mutagen. Since these two mutants do revert spontaneously these cannot be gross defects, such as deletions. It is unlikely that these are double mutants, although this possibility cannot be ruled out.

The mutant r_{263} is of particular interest in that two kinds of plaques can be seen on *E. coli* K12(λ); one apparently standard type is BD-inducible, while the frequency of the other, which forms a minute plaque on *E. coli* K12(λ), is specifically increased by the acridines. It may be that the two types of "reversion" are occurring at the same site or alternatively that a partial suppressor mechanism is operating.

Our findings are thus complementary to those of Freese (1959*b*) and give further support to his suggestion that there are at least two classes of mutagens, although we have reservations about his interpretation of this result in terms of molecular mechanism (Brenner, Barnett, Crick & Orgel, 1961).

As the mechanism of acridine mutagenesis is not understood, it is not possible to give a detailed interpretation of our results. We can only point out some factors which may be important in determining the degree of induced reversion with the acridines. Acridine itself is a mutagen and its activity is generally enhanced by the presence of amino groups on the rings. This effect is particularly marked when the amino groups are on the 2- and 5-positions. Methylation of the rings in the 3,7-positions of proflavin (to give acridine yellow) markedly increases its activity while

methylation of the amino groups of proflavin (to give acridine orange) results in diminution of mutagenic effect.

The most active compounds are, in general, those with the greatest bacteriostatic activity and there is also a strong correlation with basicity, as shown in Table 5. We have also found that the most mutagenic compounds are the most effective in inhibiting the maturation of bacteriophage at low concentrations. However, factors other than bacteriostatic activity and basicity are clearly important since acridine orange is less mutagenic, and acridine yellow more mutagenic, than proflavin although all these compounds are almost completely ionized at pH 7·3 and have comparable bacteriostatic activity. Factors such as ability to penetrate into the bacterial cell, ability to form hydrogen bonds, distribution of charge on the molecules, detailed stereochemistry and degree and mechanism of binding to DNA may all affect mutagenic activity (Bradley & Wolf, 1959; Lerman, 1961).

Table 5

Acridine	Optimum concentration for mutagenesis (μg/ml.)	Basic pK in water at 37°C	% ionized as cation at pH 7·3 and 37°C	Bacteriostatic activity. Sum of "inhibitory dilutions"†
acridine yellow	1·6–2	9·8	99	21
2,5-diaminoacridine	8	11·1	100	17
6-aminoacridine	8	9·6	99	25
proflavin	4–6	9·3	99	22
2-aminoacridine	16	7·7	72	21
2,7 diaminoacridine	16	7·8	76	26
4-aminoacridine	80	5·7	2·6	9
acridine	80–100	5·3	1·0	9
3-aminoacridine	80	5·6	2·2	8
acridine orange	20	10·1	100	17
1-aminoacridine	150	4·2	0·1	4

† Albert, Rubbo, Goldacre, Davey & Stone (1945).

REFERENCES

Albert, A., Rubbo, S. D., Goldacre, R. J., Davey, M. E. & Stone, J. D. (1945). *Brit. J. Exptl. Path.* **26**, 160.

Benzer, S. (1955). *Proc. Nat. Acad. Sci., Wash.* **41**, 344.

Benzer, S. (1957). In *The Chemical Basis of Heredity*, ed. by McElroy & Glass. Baltimore: Johns Hopkins Press.

Benzer, S. & Freese, E. (1958). *Proc. Nat. Acad. Sci., Wash.* **44**, 112.

Bradley, D. F. & Wolf, M. K. (1959). *Proc. Nat. Acad. Sci., Wash.* **45**, 944.

Brenner, S., Benzer, S. & Barnett, L. (1958). *Nature*, **182**, 983.

Brenner, S., Barnett, L., Crick, F. H. C. & Orgel, A. (1961). *J. Mol. Biol.* **3**, 121.

Foster, R. A. C. (1948). *J. Bact.* **56**, 795.

Freese, E. (1959*a*). *J. Mol. Biol.* **1**, 87.

Freese, E. (1959*b*). *Proc. Nat. Acad. Sci., Wash.* **45**, 622.

Lerman, L. S. (1961). *J. Mol. Biol.* **3**, 18.

Litman, R. M. & Pardee, A. B. (1956). *Nature*, **178**, 529.

de Mars, R. I., Luria, S. E., Fisher, H. & Levinthal, C. (1953). *Ann. Inst. Pasteur*, **84**, 113.

Vielmetter, W. & Wieder, C. M. (1959). *Z. Naturf.* **14b**, 132.

J. Mol. Biol. (1961) **3**, 769–777

Optical Rotatory Dispersion of Sperm Whale Ferrimyoglobin and Horse Ferrihemoglobin†

S. Beychok and E. R. Blout

The Children's Cancer Research Foundation and Harvard Medical School, Boston 15, Massachusetts, U.S.A.

(*Received 8 August 1961*)

Optical rotatory dispersion measurements of solutions of sperm whale ferrimyoglobin and horse ferrihemoglobin have been performed at wavelengths between 225 mμ and 730 mμ. Analysis of these results indicates that both proteins in dilute aqueous solution depart considerably from the behavior observed with most native globular proteins. This departure is attributed to unusually high helix contents in solution. The helix content has been estimated to be around 80% for both proteins from b_0 values using the Moffitt equation in the wavelength range 236 to 334 mμ. The helix content has also been estimated using the intensity of the optical rotation trough at 233 mμ (Simmons, Cohen, Szent-Györgyi, Wetlaufer & Blout, 1961). This estimate yielded values of about 75% helix content for both ferrimyoglobin and ferrihemoglobin. In addition, for both proteins, two positive Cotton effects have been observed in the visible. Their inflection points correspond to prominent absorption bands. The relationship of the structure of the molecules in dilute solution to that in the wet crystal is discussed.

1. Introduction

The X-ray diffraction studies of Kendrew *et al.* (1960, 1961) on sperm whale ferrimyoglobin have demonstrated directly, for the first time, the existence of the α-helix as a major structural feature of the wet crystals of that protein. The 2 Å Fourier synthesis showed that there are eight segments of right-handed α-helix accounting for 77% of the molecule.‡ Perutz *et al.* (1960) have achieved a somewhat lower resolution with the larger molecule, horse ferrihemoglobin. While no direct demonstration of the existence of the α-helix in ferrihemoglobin has thus far been achieved, the main features of tertiary structure have been established and the close resemblance to that of ferrimyoglobin justifies the belief that in crystalline ferrihemoglobin, also, the α-helix is an important part of the molecular anatomy.

However, the structure of wet protein crystals, under conditions of high protein and electrolyte concentration, may not correspond to that which exists in relatively

† This work was supported in part by U.S. Public Health Service Grant A-2558.

‡ The figure for percentage of residues in helical segments depends, of course, on how one counts residues at junctions of helical and non-helical regions in addition to the terminal residues. We have used the system suggested by Kendrew *et al.* (1961). There are 13 junctions between helical and non-helical segments in myoglobin. It is important to realize that in the analysis of optical rotatory dispersion which follows there is no suitable treatment for either junctions or terminal residues.

dilute solution. A recent paper by Flory (1961) is especially lucid in examining the effect of concentration on the degree of crystallinity of macromolecules, and numerous other investigators have repeatedly questioned the legitimacy of inferring solution conformation from studies on crystals.

We present here some experimental results gathered for the purpose of shedding light on the question of correspondence of structure in wet crystals and in dilute solutions of ferrimyoglobin and ferrihemoglobin at low protein and electrolyte concentration. Our measurements, in this report, are confined to optical rotatory dispersion in the visible and ultraviolet. A subsequent communication (Beychok, de Lozé & Blout, to be published) will describe results obtained with different techniques as well as our experiences with the denatured forms of these proteins.

2. Experimental

Horse ferrihemoglobin, prepared according to the method of Steinhardt & Zaiser (1953), was kindly supplied by Drs. J. Steinhardt and R. Ona. Samples of crystalline sperm whale ferrimyoglobin were kindly provided by Dr. J. C. Kendrew and by Professor F. R. N. Gurd. Both samples were freed of salts by prolonged dialysis, initially against dilute phosphate buffer at pH 6·8, then against water. The dialysed solutions were divided into equal portions, one of which was lyophilized and the other stored in the freezing compartment of the refrigerator. Optical rotatory dispersion measurements did not show reproducible differences between the two samples or between lyophilized and frozen stocks. Concentration determinations of stock solutions were made by drying to constant weight at 105°C.

Optical rotations were measured with a model 200, Rudolph photoelectric polarimeter, using a General Electric AH-6 water-cooled high pressure mercury lamp, and an Engelhard-Hanovia no. 510B xenon-mercury compact arc, as light sources. Solvent blanks were measured at every wavelength at which solution readings were taken. Below 355 mμ, fused quartz cells of 0·1, 0·5, 1·0 and 5·0 cm were used. If, after complete adjustment of the optical system, the solvent blank varied by more than 0·004° from 236 to 700 mμ, then the solvent and/or the cell was rejected.

It is, of course, apparent that in spectral regions where the rotation is changing rapidly with wavelength, care must be taken to use the smallest slit compatible with reliable measurement. If, in addition, the absorbance is varying greatly with wavelength, then anomalies in rotation may be encountered at large slits. Whenever low spectral purity is suspected, it is imperative that a concentration dependence of observed rotation be measured in these spectral regions without compensating changes in path length. We have, in this fashion, assured ourselves that at optical densities below 2·0 and slits no greater than 0·8 mm, observed rotations at all wavelengths reported here were proportional to the product of concentration and path length.†

The temperature at which the measurements were made was 24·5 ± 1°C, with the actual variation during the course of a given experiment less than 0·5°C. Our instrument utilizes the method of symmetric angles for determination of the extinction angle. The symmetric angle used in our experiments was 3·5°.

3. Results

The specific rotations of ferrimyoglobin and ferrihemoglobin are shown at wavelengths from 225 to 730 mμ in Figs. 1(a) and 1(b) (different scales) for the ultraviolet and visible, respectively. The salient features of the figures are these:

1. The rotations for both proteins are, as anticipated, very similar.

† The point shown in Fig. 1(a) at 225 mμ could be obtained only by using a wider slit.

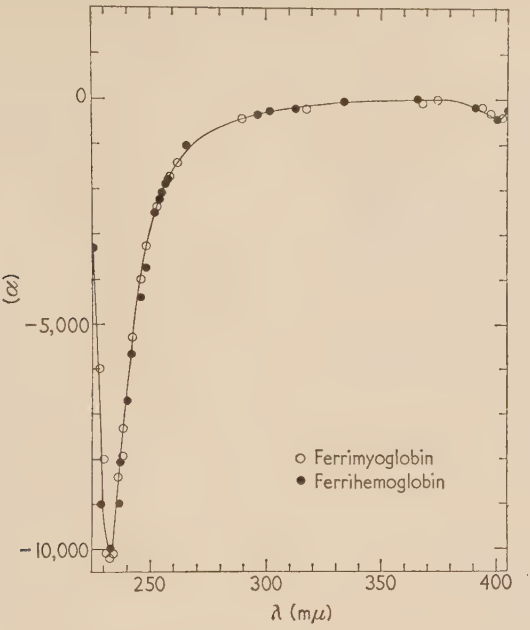

FIG. 1(a). Specific rotations in the ultraviolet, calculated on the basis of weight per cent protein, of solutions of ferrihemoglobin and ferrimyoglobin at pH 6·6 to 24·5°C with no added electrolyte.

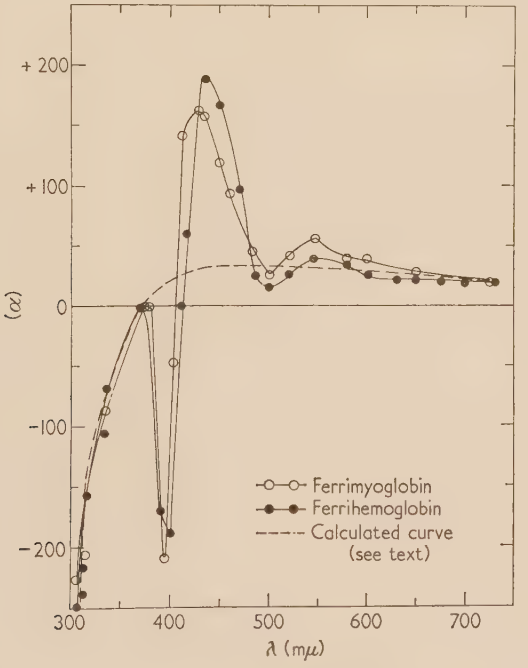

FIG. 1(b). Specific rotations in the near ultraviolet, calculated on the basis of weight per cent protein, and visible of ferrihemoglobin and ferrimyoglobin solutions at pH 6·6 to 6·8 at 24·5°C with no added electrolyte. The dashed line is constructed from Moffitt-Yang parameters as described in the text.

2. There are two Cotton effects in the visible, both positive in sign (Lowry, 1935) with inflection points that correspond to prominent heme absorption bands. (We were unable to detect a third Cotton effect corresponding to the 630 mμ absorption band. While this does not necessarily mean that the transition is optically inactive, it does exclude an important contribution to the observed rotation at any wavelength arising from that particular excitation.)

3. The specific rotations are positive at all wavelengths from 410 to 730 mμ.

4. The rate of change of rotation with wavelength below 334·1 mμ is very steep compared to that observed with most globular proteins and quite comparable to the behavior observed with highly helical macromolecules such as poly-γ-benzyl-L-glutamate (Karlson, Norland, Fasman & Blout, 1960), poly-L-methionine, tropomyosin, paramyosin and poly-L-glutamic acid (Simmons *et al.*, 1961).

5. There is an apparent negative Cotton effect with a minimum at 233 mμ. The influence of this band on the dispersion at higher wavelengths is still undetermined. However, investigations with certain well-characterized polypeptides and fibrous proteins (Simmons *et al.*, 1961) have shown that the value of the residue rotation at 233 mμ provides a good estimate of helix content, and that the Cotton effect disappears with the destruction of helix.

It might appear that no. 3 is a natural consequence of no. 2, but we will show below that this is not the case and that the *sustained* positive rotation is, in fact, the result of transitions in the far ultraviolet.

The usual analysis of the rotatory dispersive behavior of proteins (Schellman, 1958) takes advantage of the fact that native globular proteins obey the simple single-term Drude equation

$$[\alpha]_\lambda = \frac{A}{\lambda^2 - \lambda_c^2} \qquad (1)$$

at wavelengths above 350 mμ. In equation (1), $[\alpha]_\lambda$ is the specific rotation at wavelength λ, and both A and λ_c are empirical constants. This equation obviously is not obeyed above 350 mμ for myoglobin and hemoglobin because of the presence of optically active absorption bands in the visible. However, a plot of $[\alpha]\lambda^2$ versus $[\alpha]$ below 350 mμ (linear, if equation (1) is obeyed) is shown in Fig. 2 and is not linear. Since Schellman (1958) and Jirgensons (1961) have noted that certain proteins obey equation (1) in the visible and not in the ultraviolet, we may not reliably infer from Fig. 2 that myoglobin and hemoglobin are atypical. We can, however, bring other evidence to bear which will establish that the rotatory dispersive behavior observed here is different from that of other globular proteins examined thus far.

We note, most clearly in Fig. 1(b), that the rotation between 360 and 370 mμ is very nearly zero. The two Cotton effects above these wavelengths, since both are positive in sign, can only be contributing negative or zero rotation at 360 mμ. Since the observed rotation at this wavelength is zero, it follows immediately that the partial rotation at 360 mμ due to all absorption bands below 236 mμ is zero or positive. Consequently if we were able to subtract the full contribution of the heme absorption bands in the visible, the remaining rotation would display either a maximum at 360 mμ or a change in sign of rotation in this wavelength region, positive rotations appearing above these wavelengths and negative below. In either event, a single term Drude expression would not suffice to describe the observed dispersion. This kind of behavior is just that which has been observed with helical polyamino acids (Blout, 1960; Schellman & Schellman, 1961).

We have chosen, for reasons stated below, to represent our data with the Moffitt-Yang equation (Moffitt & Yang, 1956)

$$[m']_\lambda = [\alpha]_\lambda \cdot \frac{3}{n^2+2} \cdot \frac{M_0}{100} = \frac{a_0\lambda_0^2}{\lambda^2-\lambda_0^2} + \frac{b_0\lambda_0^4}{(\lambda^2-\lambda_0^2)^2} \quad (2)$$

n which $[m']$ is the effective residue rotation at wavelength λ, $[\alpha]_\lambda$ is the specific otation at wavelength λ, M_0 is the mean residue weight of the protein, n is the refractive index of the solvent at wavelength λ and a_0, b_0 and λ_0 are constants. With λ_0 aken as 212 mμ, b_0 (both in sign and magnitude) has proved to be remarkably haracteristic of the conformation of helical synthetic polypeptides (Blout, 1960;

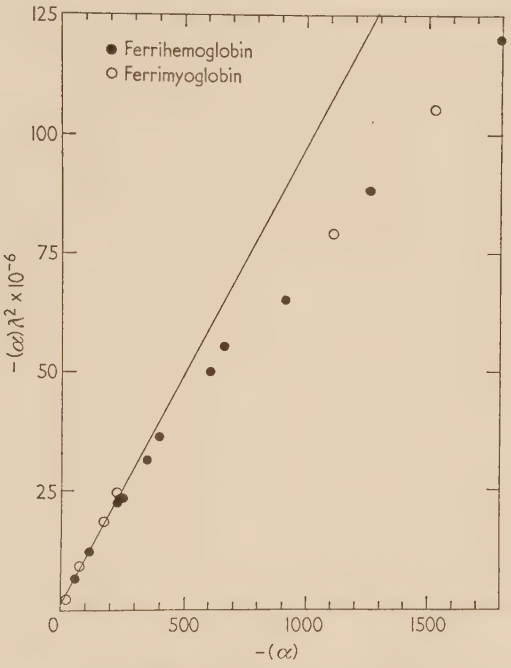

Fig. 2. Modified Drude plot of data obtained at wavelengths from 334·1 mμ to 258 mμ.

chellman & Schellman, 1961) and of the muscle proteins, but largely insensitive o solvent changes when these do not affect the conformation. A value between - 630 and — 660 for b_0 is commonly observed with completely helical molecules of ght-handed screw sense; random coils give values close to zero. The assumption hat non-helical regions of proteins make no contribution to b_0 then permits calculation f the fraction of residues in the helical conformation (provided only one sense of elix is present). This is a serious assumption, since the amorphous regions in native roteins are not random. We will comment further on this point in a later section f the paper.

The data of Fig. 1(a), at wavelengths from 236 to 334·1 mμ† are re-plotted according o equation (2) in Fig. 3. Using $\lambda_0 = 212$ mμ, values of b_0 for myoglobin of — 509

† Note that the frequency range covered (29,900 cm^{-1} to 42,400 cm^{-1}) in these experiments is tually greater than the range normally utilized for optical rotatory dispersion, i.e. 17,300 cm^{-1} 27,400 cm^{-1} (365 mμ to 578 mμ).

and for hemoglobin of < 520 were obtained.† Use of the assumption in the preceeding paragraph gives 77 to 81% and 79 to 83% right-handed helix, respectively. We note that equation (2) is fitted by the rotatory dispersion data for poly-γ-benzyl-L-glutamate at wavelengths from 578 to 237 mμ (Karlson *et al.*, 1960), using $\lambda_0 = 212$ mμ.‡

With the constants a_0 (+ 321) and b_0 (− 520) of equation (2) as determined from the intercept and slope of Fig. 3, and using a value of 212 mμ for λ_0 we have constructed a dispersion curve for hemoglobin extending to 730 mμ. This calculated curve is the dashed line in Fig. 1(b). Clearly, this represents the partial rotation

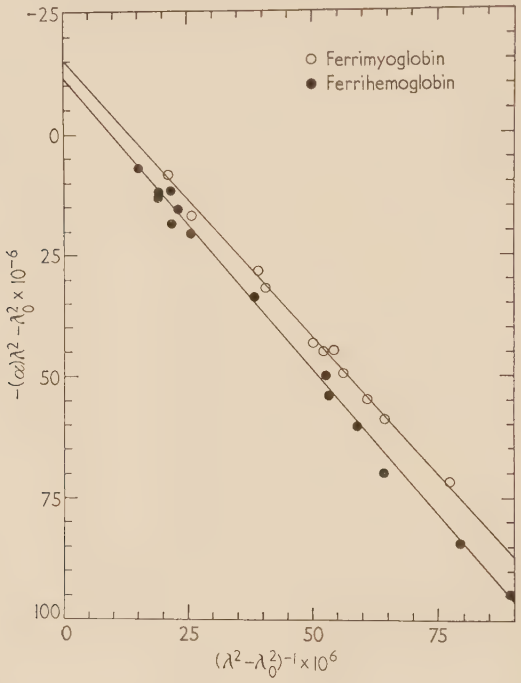

FIG. 3. Results of Fig. 1(a) plotted according to Moffitt-Yang, using equation (2) of text. Wavelengths are in millimicrons.

which is due to chromophores in the far ultraviolet. The curve crosses zero degrees at 370 mμ and nearly coincides with the experimentally observed rotations at wavelengths above 600 mμ.

We are, of course, aware of the possible contribution to b_0 from excitations other than those of the hydrogen-bonded peptide groups, particularly those due to heme absorption bands below 233 mμ. The existence of optically active heme absorption bands is virtually assured in the far ultraviolet in view of the Cotton effects observed

† The values of b_0, and of a_0 given below were calculated from the slopes and intercepts, respectively, of plots identical to those of Fig. 3 except that a small correction was applied to each wavelength for the dispersion of the refractive index of water. Neglect of this correction in the wavelength region 334·1 to 240 mμ introduces a possible maximum error of 2·6% in the calculation of b_0. The values of b_0 and a_0 given in the text make use of this correction.

‡ Our confidence in the application of equation (2) to the frequency range utilized herein is considerably strengthened by the strict obedience to it of poly-γ-benzyl-L-glutamate in a frequency range broader than but including that employed here. In a subsequent paper (Beychok, de Loze & Blout, to be published) we will comment on the usefulness of equation (2) in the ultraviolet.

in the visible, although the partial rotations resulting from such bands may not, in fact, exhibit an anomalous frequency dependence. It may be relevant here to point out that the hemoglobin Cotton effect at 406 mμ approximately doubles in size as the added electrolyte concentration is raised from zero to 0·2 M in sodium chloride. Whether this implies that the magnitude of heme Cotton effects in the far ultraviolet also increases as salt concentration is changed is not known, but we can assert that the b_0 remains constant under conditions of changing electrolyte concentration.

The most reassuring observation, in this connection, is the size of the rotation trough at 233 mμ. Estimates of helix content of certain synthetic polypeptides and fibrous proteins based on the value of the effective residue rotation at 233 mμ are in good agreement with b_0 results and it has been stated that the agreement is observed because both parameters reflect the helical conformation (Simmons *et al.*, 1961). Calculations of the data of Fig. 1(a) according to the method of these investigators, using $\Delta[R']_{233} = 11{,}000°$ as the difference between helical and random conformations, yields a value of about 75% helix content for both ferrimyoglobin and ferrihemoglobin. Since the Cotton effect at 225 mμ is related to the helical polypeptide conformation, the satisfactory agreement between the two estimates for ferrihemoglobin makes it exceedingly unlikely that contributions from far ultraviolet transitions of the heme have an important influence on the dispersion between 236 and 334·1 mμ.

4. Discussion

The assumption that the amorphous regions (including junctions between helical and non-helical regions) in these proteins contribute nothing to b_0 is a serious one. In many proteins—perhaps in all native proteins—the non-helical segments are almost certainly characterized by fixed orientations of the peptide links. It is true that most native globular proteins, in aqueous solutions, give values of b_0 less than − 250, with a large number having values near, or lower than, − 100 (Jirgensons, 1961). Nonetheless, the ease with which they can be crystallized, their compactness and biological specificity all militate against the belief that substantial portions of these molecules exist as random coils possessing a high degree of conformational freedom.

In this connection, it should be remembered that the source of anomalous frequency dependence of the dispersion, as formulated by Moffitt & Yang (1956), resides in the interaction of the instantaneous electric moments of one peptide bond with those of its neighbours. In the helix, certain fixed phase relationships of the vectors representing transition moments obtain in the excited states of the peptide chromophores. If the planes of the peptide bonds, albeit fixed, are not related to one another in a specific sense, then the dispersion due to transitions in that plane will be simple if, indeed, the transitions are optically active at all.

The lack of a satisfactory theoretical treatment of optical rotatory dispersion of proteins prevents our drawing firm conclusions about the significance of the dextrorotation observed in the visible with ferrihemoglobin and ferrimyoglobin (after subtraction of the heme Cotton effects). Positive rotations have been found with synthetic helical polyamino acids in the visible in non-aqueous media, but water solutions of helical rod-like fibrous proteins show a small negative rotation. Inspection of equation (2) reveals that the magnitude of the coefficient a_0 becomes increasingly important at longer wavelengths. It is now well established that while the term b_0

is solvent independent for a given molecule, a_0 varies markedly with the solvent. Thus, we may reasonably anticipate that the rotatory dispersion of a segment of helix in the hydrophobic interior of a folded molecule will be different from that of its counterpart which is fully exposed to solvent. This difference, whether it reflects the rotation due to the α-carbons, the peptide chromophores, or both, will be felt only in the a_0 term when the Moffitt-Yang equation is employed. There is substantial evidence that ferrihemoglobin in its native state is organized in such a fashion that many of its residues are not accessible to hydrogen ions and, by inference, to water. On the strictly empirical grounds set forth in a preceding section, we are justified in using b_0 for estimates of helix content even in the absence of a proper assessment of specific solvent effects on a_0. Such effects may be quite different in the case of compactly folded globular proteins of high helix content than in extended rods of equally high helix content. Whatever the reasons for the observed rotatory behavior we simply emphasize that our demonstration of an atypically dominant helical character in these two proteins in no way depends on the finding of visible dextrorotation.

We conclude with a brief comment on the question of the degree of crystallinity as a function of concentration. Flory (1961) has pointed out that the statistical advantage which the random state in polymers enjoys at high dilution is diminished at large concentrations by virtue of competition for space. This is particularly important when the polymer is obliged to conform to the regular array of the crystal. Without questioning the generality of Flory's argument, we may point out that we are dealing here with particles known to possess a high degree of molecular organization even in dilute solution, with low asymmetry observed independent of contacts with other particles (Beychok & Steinhardt, 1960). This is not to say that a given segment of helical residues does not undergo conversion to a non-helical region with increasing dilution. However, calculation of the probability of such an event must take into account its effect upon all side chain interactions in the crystal and those which can occur after the transition. A calculation of this kind is not possible at this time.

The results presented here indicate helix contents of 75 to 80% for ferrimyoglobin and ferrihemoglobin at high dilution. The helix content of myoglobin is comparable to that observed in wet crystals of the same protein. Evidently, the helical structure found in the crystals is also characteristic of the molecules at high dilutions. We will, in the near future (Beychok, de Lozé & Blout, to be published), report experiments utilizing the technique of deuterium exchange of amide hydrogens which, in large measure, confirm our analysis of the rotatory dispersion results presented here.

Note added in proof

Urnes, Imahori & Doty (*Proc. Nat. Acad. Sci., Wash.*, in the press) have examined the rotatory dispersion of ferrimyoglobin in the ultraviolet. Their conclusions, arrived at by an analysis somewhat different from that presented above, are in essential agreement with ours insofar as helix content in solution is concerned.

REFERENCES

Beychok, S. & Steinhardt, J. (1960). *J. Amer. Chem. Soc.* **82**, 2756.

Blout, E. R. (1960). *Optical Rotatory Dispersion* by C. Djerassi, p. 238. New York: McGraw-Hill.

Flory, P. (1961). *J. Polymer. Sci.* **49**, 105.

Jirgensons, B. (1961). *Die Makro. Chemie*, **44-46**, 123.

Karlson, R. H., Norland, K. S., Fasman, G. D. & Blout, E. R. (1960). *J. Amer. Chem. Soc.* **82**, 2268.

Kendrew, J. C., Dickerson, R. E., Strandberg, B. E., Hart, R. G., Davies, D. R., Phillips, D. C. & Shore, V. C. (1960). *Nature*, **185**, 422.
Kendrew, J. C., Watson, H. C., Strandberg, B. E., Dickerson, R. E., Shore, V. C. & Phillips, D. C. (1961). *Nature*, **190**, 666.
Lowry, T. M. (1935). *Optical Rotatory Power*. London: Longmans, Green.
Moffitt, W. & Yang, J. T. (1956). *Proc. Nat. Acad. Sci., Wash.* **42**, 596.
Perutz, M. F., Rossmann, M. G., Cullis, A. F., Muirhead, H., Will, G. & North, A. C. T. (1960). *Nature*, **185**, 416.
Schellman, J. A. (1958). *C.R. Lab. Carlsberg*, **30**, 363.
Schellman, J. A. & Schellman, C. G. (1961). *J. Polymer. Sci.* **49**, 129.
Steinhardt, J. & Zaiser, E. (1953). *J. Amer. Chem. Soc.* **75**, 1599.
Simmons, N. S., Cohen, C., Szent-Györgyi, A. G., Wetlaufer, D. B. & Blout, E. R. (1961). *J. Amer. Chem. Soc.* in the press.

KKK*

J. Mol. Biol. (1961) **3**, 778–783

On Configurations of High-Polymer Ribonucleic Acid Macromolecules as Revealed by Electron Microscopy

N. A. Kisselev, L. P. Gavrilova and A. S. Spirin

Institute of Crystallography, Academy of Sciences of the U.S.S.R., and A. N. Bakh Institute of Biochemistry, Academy of Sciences of the U.S.S.R., Moscow, U.S.S.R.

(*Received 9 August 1961*)

Infectious tobacco mosaic virus RNA and *E. coli* ribosomal RNA were studied by electron microscopy. Depending on the ionic strength, temperature and pH of the solutions from which the specimens had been prepared, three different configurations of the high-polymer RNAs were revealed: a coil (from solutions of high ionic strength at room temperature), a rod of a diameter about 30 Å (from solutions of low ionic strength at room temperature) and an unfolded thread (from heated or acidified solutions). The observation of these configurations under corresponding conditions lends direct support to the proposed earlier models of macromolecular structure of high-polymer RNA and its configurational transitions as well as to the idea that the macrostructural principles are common to both viral and ribosomal protein-free RNAs in solution.

1. Introduction

In a previous paper (Spirin, 1960) some problems of macromolecular structure of isolated protein-free RNAs in solution were considered and RNA configurations under various conditions were discussed on the basis of available physical and physico-chemical data. The consideration of macromolecular organization of RNA in solution led to the conclusion that there could exist three types of RNA configurations interrelated by reversible transitions: (a) an unfolded (uncoiled) single-stranded polynucleotide chain; (b) a compact rod; (c) a compact coil (Spirin, 1960). According to this, an unfolded single-stranded polynucleotide chain of RNA occurs in solutions at high temperatures or in a completely salt-free aqueous medium as well as in all other cases where H-bonds between purine and pyrimidine bases of the chain are broken or cannot exist; under these conditions, high-polymer RNA is believed to be a more or less straightened continuous thread without secondary and tertiary structure. RNA as a compact rod exists, according to these concepts, in solutions of low ionic strength at low temperature; the same single polynucleotide chain forms a rod because of coiling and H-bonding between adjacent sections of the chain resulting in short double-stranded regions oriented perpendicularly with respect to the long axis of the rod. Finally, a compact RNA coil is formed at high ionic strength when there are possibilities for additional H-bonding between distant sections of the chain; the particle comes to be as if "cross-linked" and hence transforms into a coil with

preservation of the former secondary structure. The proposed principles of RNA macrostructure in solution were supposed to be common to high-polymer RNAs of different origin, both viral and ribosomal.

The object of this study was to test these structural concepts by direct electron microscope observations on the shapes and sizes of high-polymer RNA macromolecules under different conditions.

2. Materials and Methods

Infectious tobacco mosaic virus (TMV) RNA and ribosomal *E. coli* RNA preparations were used. The RNA preparations were obtained by phenol deproteinization of the TMV or the *E. coli* ribosomes respectively, with the subsequent additional purification from possible depolymerization products by precipitating with 1·5 M-saline. All the RNA preparations exhibited a sharp increase of specific viscosity upon heating (thermal unfolding) (Gavrilova, Spirin & Belozersky, 1959; Spirin, 1961). The TMV RNA displayed a single monodisperse peak on sedimentation patterns and had a molecular weight of about 2×10^6. Sedimentation patterns of the ribosomal *E. coli* RNA showed two components corresponding to molecular weights of about $1{\cdot}1 \times 10^6$ and $0{\cdot}6 \times 10^6$.

The preparations were dissolved in ammonium acetate buffer pH 7. Four different solutions of RNA were used for preparing specimens: (1) in buffer of ionic strength 0·075 to 0·15 at room temperature; (2) in buffer of ionic strength 0·0003 to 0·00075 at room temperature; (3) in buffer of ionic strength 0·00075 heated to 70°C; (4) in the same buffer acidified with acetic acid (up to 10%), at room temperature. The RNA concentration varied from 0·0001 to 0·005% in different experiments.

When preparing specimens for electron microscopy the solution was deposited onto the surface of freshly cleaved mica with a spray gun. In the experiments with the acidified solution (solution 4), the acetic acid was added 30 sec before spraying of the solution onto mica. In the case of the heated RNA solution (solution 3) the preparations were deposited in two ways: (a) by spraying the heated (70°C) RNA solution onto heated mica inside a thermostatted chamber; (b) by immersing heated mica into the heated (70°C) RNA solution. The latter was used to diminish fragmentation of the RNA particles which occurs on spraying.

The single-step carbon replica technique (Bradley, 1956) was used. The RNA specimens were shadow-cast with a platinum-palladium alloy at a shadow-to-height ratio of 7 : 1 to 10 : 1 and then backed with carbon. The error in estimating the shadow-casting angle was about ± 10 to 13%. After shadow-casting and carbon-backing the carbon-metal films were stripped from the mica by floating them off on water. The floated films were picked up over conventional grids and examined with the electron microscope JEM-5G using an instrumental magnification of 18,000 to 27,000.

3. Results

(a) *RNA particles from solution of high ionic strength*

Plate I shows electron micrographs of RNA prepared from solutions of high ionic strength at room temperature (solution 1). Plate I(a) shows particles of TMV RNA which appear as flattened coils. Approximately half of the observed particles have a diameter of about 400 Å; the remainder includes aggregates and also comparatively small coils, apparently fragments. The latter may be a result of spraying. The height of the 400 Å diameter coils is about 25 to 32 Å as estimated from shadow length. The volume of these particles, which appear to be flattened coils lying on the supporting surface, is about 2×10^6 Å^3 if calculated from the formula $\pi r^2 h/2$. This value seems to be in good agreement with the molecular volume of the intact virus RNA (molecular weight 2×10^6).

Particles of *E. coli* ribosomal RNA prepared under the same conditions can be seen in Plate I(b). Just as in the case of the virus RNA, coil-like particles are observed under conditions of high ionic strength. The sizes of the coils, however, are different: if aggregates are not taken into account the particles observed here are smaller than those of the virus RNA. Most of the coils have a diameter of about 200 Å and a height of 25 to 30 Å, which correspond to a particle volume of about 5×10^5 Å^3. There are also coils of a somewhat larger diameter, 250 to 300 Å; from this and the height of 25 to 30 Å their particle volume can be calculated to be of about 10^6 Å^3. Besides these two sorts of coils there are both aggregates and much smaller particles which may be fragments of the RNA molecules. The two principal sorts of coils, with particle volumes of about 5×10^5 Å^3 and 10^6 Å^3, seem to correspond to the two high-molecular components of ribosomal RNA.

(b) *RNA particles from solution of low ionic strength*

Micrographs of RNA particles prepared from solutions of low ionic strength at room temperature are presented in Plate II.

As one can see, both the viral RNA particles (Plate II(a)) and the ribosomal ones (Plates II(b) and (c)) appear as rods. In both cases the heights of the rods are 25 to 30 Å as estimated from shadow lengths; the height along the rod is not quite uniform but somewhat variable within these limits. The virus RNA rods (Plate II(a)) and the ribosomal ones (Plates II(b) and (c)) are practically indistinguishable in appearance, except for their lengths.

The length of the rods is rather variable, which may be a result of fragmentation of the RNA particles upon spraying. Therefore it is the maximum length of the rods which is of special interest. The longest rods of the TMV RNA are found to be about 2500 Å in length (Plate II(a)). If calculated as a product $25\times30\times2500$ Å^3 the rod volume will be of about 2×10^6 Å^3; this value seems to correspond to the particle volume of the intact TMV RNA.

The longest ribosomal RNA rods (Plates II(b) and (c)) are about 1000 to 1200 Å in length; from this their volume can be calculated as about 10^6 Å^3. Therefore, the 1000 to 1200 Å length seems to be consistent with the molecular volume of the larger component of ribosomal RNA. The maximum in the length distribution, however, corresponds to the length of 600 Å. This dimension leads to a particle volume of about 5×10^5 Å^3 and may correspond to the smaller component of the *E. coli* ribosomal RNA.

Discussing the RNA micrographs in Plate II, it should be noted in the first place that the finding of RNA molecules as rod-like particles is of great interest in itself. It is completely consistent with the earlier proposal about the rod-like shape for high-polymer RNA in solution under low ionic strength and at room temperature, as well as with the proposed scheme of the configurational transitions of RNA in solution (Spirin, 1960).

Moreover, the dimensions of the rods observed (height 25 to 30 Å) seem to be compatible with the proposed scheme of tertiary structure of the rod-like RNA molecules. According to this scheme, short helical DNA-like regions are arranged mainly perpendicularly to the long axis of the particle, and their linear piling forms the rod (Dvorkin & Spirin, 1960; Spirin, 1960). When such rod-like particles are deposited onto the surface of the film for electron microscopy, the heights of the rods should be determined by the diameter of the double polyribonucleotide helical

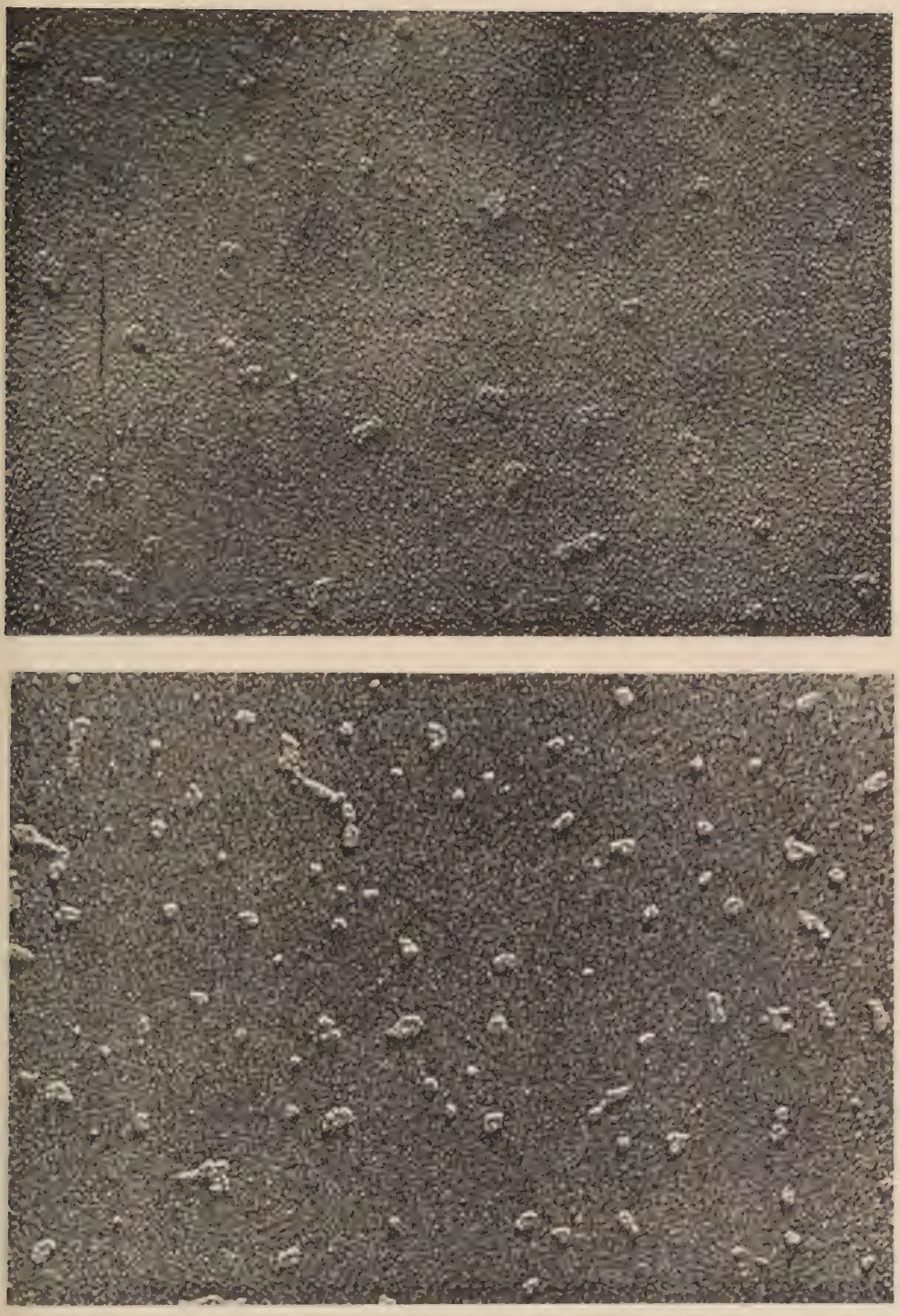

PLATE I(a). TMV RNA from solution of ionic strength 0·1 (coils). Shadow-to-height ratio 7·6 : 1. Magnification 100,000×.

(b) Ribosomal *E. coli* RNA from solution of ionic strength 0·15 (coils). Shadow-to-height ratio 8·6 : 1. Magnification 100,000×.

[*To face page* 780

(a)

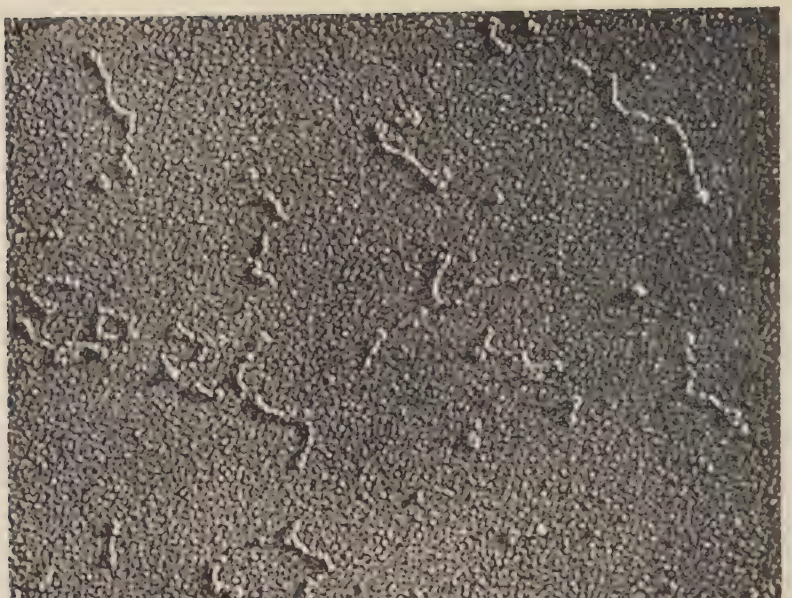

(b)

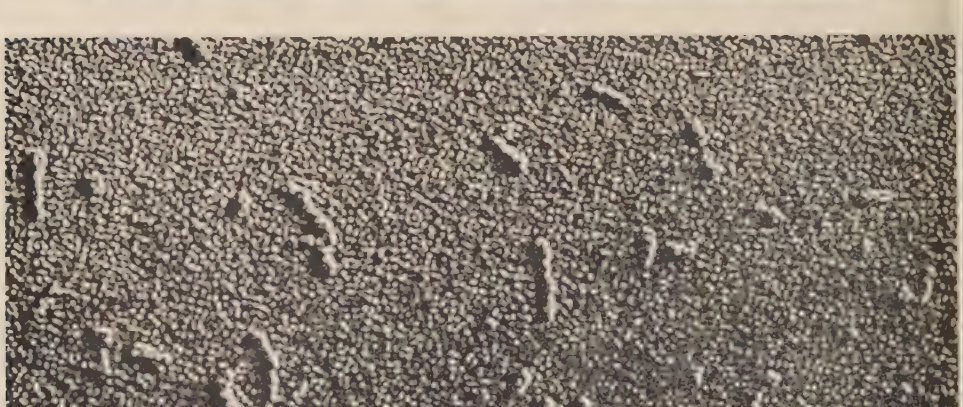

(c)

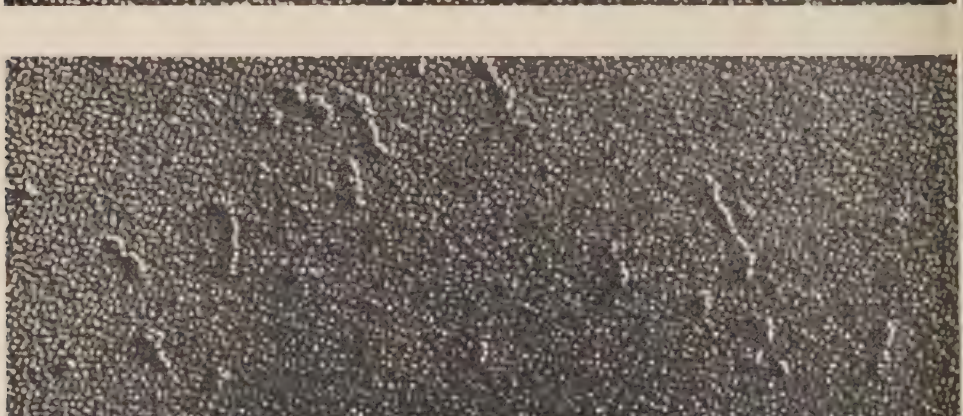

PLATE II(a). TMV RNA from solution of ionic strength 0·0003 (rods). Shadow-to-height ratio 9·0 : 1. Magnification 100,000×.

(b) and (c). Ribosomal *E. coli* RNA from solution of ionic strength 0·0003 (rods). Shadow-to-height ratio 9·5 : 1. Magnification 100,000×.

Plate III(a). TMV RNA from solution of ionic strength 0·0001 (extended rods). Shadow-to-height ratio 9·0 : 1. Magnification 100,000×.

(b) TMV RNA from heated solution of ionic strength 0·00075 (a thread). Shadow-to-height ratio 9·6 : 1. Magnification 100,000×.

(c) Ribosomal *E. coli* RNA from acidified solution (threads). Shadow-to-height ratio 9·5 : 1. Magnification 100,000×.

regions where the regions are lying on the film, and by the length of the regions where they are standing upright. The diameter of a double polyribonucleotide helix of the AU-complex type is known to be about 26 Å in the dry state; the length of one turn of the helix is about 30 Å. Consequently, the experimentally determined heights of the rod-like particles are consistent with the dimensions which should characterize the RNA molecules formed by the piling of the short double-helical regions of average length of about one turn.

The starting-point in the consideration of the tertiary structure of the rod-like RNA particles is the suggestion that it is *adjacent* sections along the same *single-stranded* polynucleotide chain that interact with each other resulting in short helical regions. Electron microscopic observations on the RNA specimens prepared from solutions of very low ionic strength may be expected to lend support to this manner of formation of the rod-like particles. Under these conditions configurations intermediate between the rod-like and thread-like ones should exist, and the compact rods should be able to transform into a more loose and expanded state. Plate III(a) seems to show this state. On the lengthened RNA molecules there are alternating very thin parts which might be attributed to the single-stranded polynucleotide regions, and much thicker "nodules" and 30 Å regions which may characterize the helical regions formed by coiling up the single-stranded polynucleotide sections on themselves (see Plate III(a)). Heating or acidifying such solutions results in still more extended configurations that can be considered as threads with occasional "nodules" or "rod-like" parts which seem to be the stable double-helical regions which do not "melt" (see Plates III(b) and (c)).

(c) *RNA particles in the unfolded configurations*

It has been found earlier that upon heating, high-polymer RNA molecules become unfolded (uncoiled) and transform from compact particles into extended single-stranded threads (Gavrilova *et al.*, 1959; Spirin, 1960, 1961). This thermal unfolding goes on in parallel with the "melting" of the secondary structure (despiralization of the short helical regions) (Spirin, Gavrilova, Bresler & Mossevitsky, 1959). The transition is completely reversible unless thermal degradation of the polynucleotide chain takes place. The high-molecular RNA particle as a whole is unfolded into a single continuous chain, and no dissociation into "subunits" is found (Spirin *et al.*, 1959; Spirin, 1960, 1961). Further evidence for this transformation is found in the electron micrographs of RNA specimens prepared from solutions heated to 70°C. Under these conditions RNA molecules can be revealed as very long thin threads with a height mainly of about 7 Å (Plate III(b)).

It should be noted, however, that it is rather difficult to obtain completely unfolded continuous long threads by this method. In most cases, configurations intermediate between the threads and coils are revealed, as well as a great number of fragments. We have therefore used another method for unfolding RNA, acidifying solutions with acetic acid. The ribosomal RNA threads obtained by this method are shown in Plate III(c). Their prevalent height of about 7 Å is compatible with a single-stranded polynucleotide chain.

Besides providing direct support for the earlier proposed scheme of configurational transitions, the electron micrographs presented here are of interest in that they can confirm the continuity of the polynucleotide chain of the high-polymer RNA molecules. This should be especially emphasized in the case of ribosomal RNA, as there are still

some tendencies in the literature to consider it to consist of many subunits. The longest threads of ribosomal RNA have a length of 18,000 Å; this would correspond to one continuous polynucleotide chain of the larger component of ribosomal RNA. Threads of another size are found which are about 10,000 Å long; they may correspond to the continuous chain of the smaller component.

4. Discussion

The data presented here show that the same high-polymer RNA can be revealed by electron microscopy to exist in three different configurations: a coil, a rod, or an unfolded thread, depending on conditions of ionic strength, temperature and pH of solutions used for preparing specimens. These observations are in excellent accordance with previous proposals (Spirin, 1960).

It should be noted that these different RNA configurations were separately observed earlier by various workers. Hart (1955) observed TMV RNA in the form of a rod-like structure, or a "fibril" of a diameter 30 to 40 Å. Later Hall (1958) obtained fine micrographs of animal high-polymer RNA molecules that appeared as rods of a height of about 30 Å; these rods seem to be equivalent to the rods found by us. Recently Beer, Highton & McCarthy (1960) reported that RNA "fibrils" with a diameter of about 30 Å were revealed upon disintegration of *E. coli* ribosomes. On the other hand, a number of workers have observed RNA in the form of thread-like single-stranded structures. Schuster, Schramm & Zillig (1956) presented micrographs of TMV RNA where single-thread structures could be occasionally distinguished. Hart (1958) succeeded in obtaining micrographs of the extended single-stranded polynucleotide chain of TMV RNA, and at that time it was a forcible argument in favour of single-stranded RNA configuration and the continuity of its chain. Recently Danon, Marikovsky & Littauer (1961) managed to reveal RNAs of different origin as threads of a diameter about 10 Å. At high ionic strength these authors observed aggregation of RNA molecules as well as typical coil-like particles ("flat granules"). Littauer, Danon & Marikovsky (1960) have also published micrographs of *E. coli* RNA where structures with a diameter 10 to 13 Å, presumably intermediate between threads and rods ("granular threads"), could be observed.

Thus, different workers have observed one or other of the RNA configurations, depending on the conditions they used. In this work it is the same RNA that has been shown to display the different configurations, a coil, a rod and an unfolded thread. Each of them is shown to be determined by conditions of solution from which a specimen has been prepared.

We wish to thank Professor B. K. Vainshtein, in whose laboratory the electron microscope observations were made, for his interest during the course of this study, and Professor A. N. Belozersky for his support and encouragement.

REFERENCES

Beer, M., Highton, P. J. & McCarthy, B. J. (1960). *J. Mol. Biol.* **2**, 447.
Bradley, D. E. (1956). *J. Appl. Phys.* **27**, 1399.
Danon, D., Marikovsky, Y. & Littauer, U. Z. (1961). *J. Biophys. Biochem. Cytol.* **9**, 253.
Dvorkin, G. A. & Spirin, A. S. (1960). *Doklady Akad. Nauk S.S.S.R.* **135**, 987.
Gavrilova, L. P., Spirin, A. S. & Belozersky, A. N. (1959). *Doklady Akad. Nauk S.S.S.R.* **126**, 1121.

Hall, C. E. (1958). Proceedings IV International Congress of Biochemistry, Vienna, **9**, 90.
Hart, R. G. (1955). *Proc. Nat. Acad. Sci., Wash.* **41**, 261.
Hart, R. G. (1958). *Biochim. biophys. Acta*, **28**, 457.
Littauer, U. Z., Danon, D. & Marikovsky, Y. (1960). *Biochim. biophys. Acta*, **42**, 435.
Schuster, H., Schramm, G. & Zillig, W. (1956). *Z. Naturf.* **11b**, 339.
Spirin, A. S. (1960). *J. Mol. Biol.* **2**, 436.
Spirin, A. S. (1961). *Biokhimiya*, **26**, 511.
Spirin, A. S., Gavrilova, L. P., Bresler, S. E. & Mossevitsky, M. I. (1959). *Biokhimiya*, **24**, 938.

J. Mol. Biol. (1961) **3**, 784–786

Letters to the Editor

The Fine Structure of α-Keratin

1. Introduction

The combination of sectioning techniques with electron microscopy has played a major role in revealing the microfibrillar framework of α-keratins (Birbeck & Mercer, 1957; Rogers, 1959*a*,*b*; Dobb, Nott & Sikorski, 1960). The microfibrils have been reported to be 60 to 80 Å in diameter, of indeterminate length and embedded in a matrix of apparently amorphous protein rich in cystine. Wide variations in the way in which the microfibrils pack have been observed (Rogers, 1959*b*), ranging from near-hexagonal packing to layers or sheet-like formations and totally irregular close-packing. Some arrangements were found to be characteristic of particular keratins. In the earlier study the presence of substructure within each microfibril was observed in some electron micrographs, but the infrequency of its appearance and lack of contrast precluded any useful interpretation being made. It was evident that a more satisfactory delineation of intra-microfibrillar organization largely depended upon the utilization of additional "electron staining."

2. Methods

The α-keratin fibres (Australian fine merino wool, human hair, porcupine quill tip) were stained in bulk by initial partial reduction of the cystine content with 0·5 M-thioglycollic acid at pH 5·6 for 24 hr followed by washing with water, a procedure which enhances the extent of reaction of the matrix on subsequent treatment with 1% OsO_4 for 72 hr (Rogers, 1959*b*). Following the osmic treatment, the fibres were embedded in Araldite (Glauert, Rogers & Glauert, 1956; Rogers, 1959*b*) and sections cut with a diamond knife on a Siroflex microtome.

The sections were post-stained with aqueous solutions of lead salts, especially saturated lead hydroxide (Watson, 1958) for up to 1 hr, and supported on a collodion net, stabilized with carbon.

Electron micrographs of regions of keratin sections centred over holes in the supporting net were taken with a Siemens Elmiskop I at an instrumental magnification of 80,000, using double condenser illumination and selected 30 μ objective apertures. Provided that micrographs were taken rapidly at low beam intensity, the Siemens cooling attachment for reducing the rate of contamination of specimens offered no improvement in resolution.

3. Results

An increase in contrast between the relatively unstained microfibrils and surrounding electron-dense matrix (Plate I), additional to that obtained by the usual bulk-staining procedure with OsO_4, was produced by post-staining with lead hydroxide. As a result the diameters of microfibrils can be measured with more accuracy and

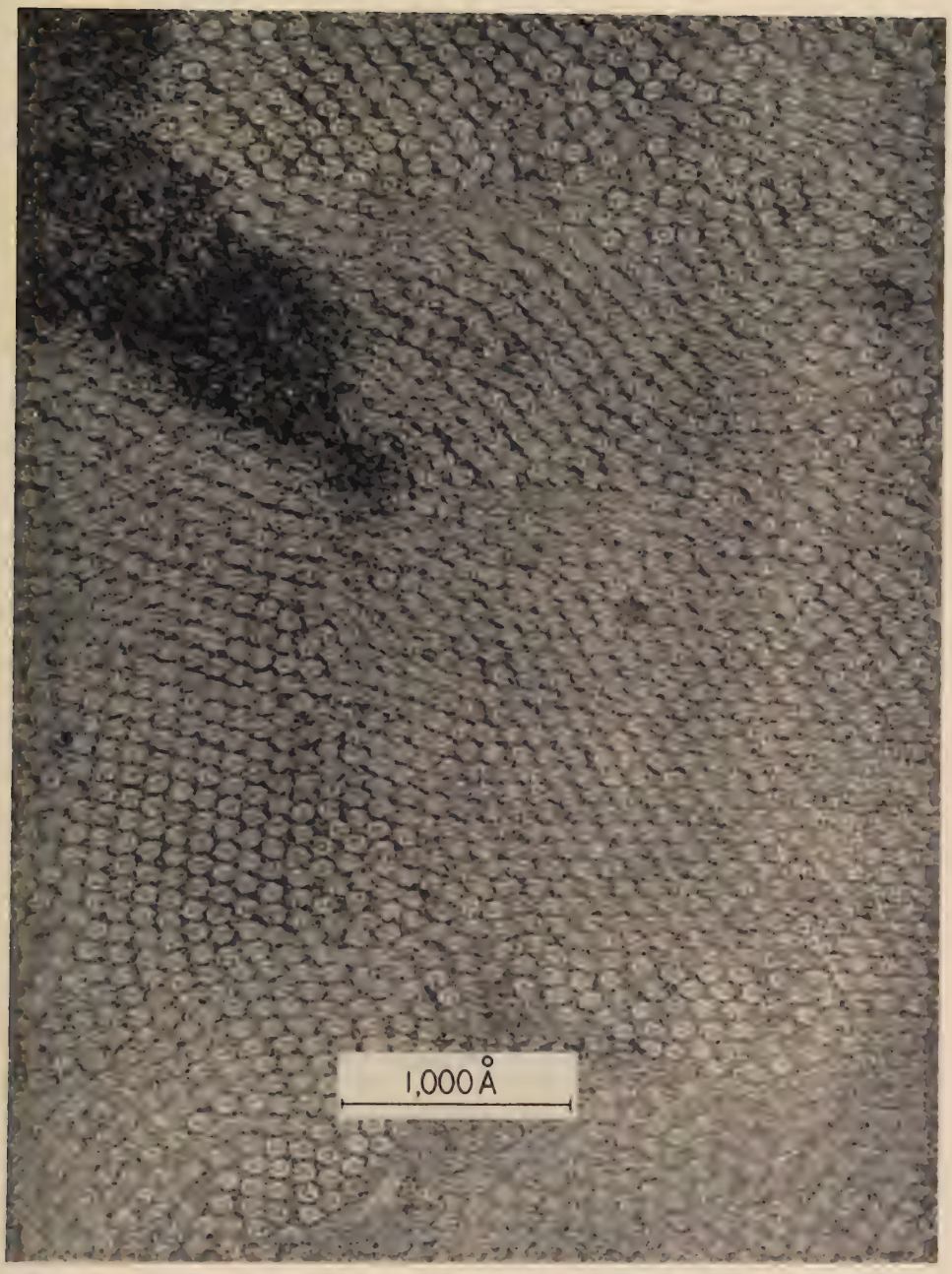

PLATE I. Cross-section of an α-keratin fibre (Australian fine merino wool) showing portion of a cortical cell in the paracortex. The matrix is more densely stained than the microfibrils. Regions of particularly regular packing of microfibrils are evident and, in addition, relatively unstained protofibrils within the microfibrils can be seen. Portion of nuclear remnant at upper left. × 300,000.

[*To face page* 784

PLATE II(a). As in Plate I but showing the protofibrils more clearly. Within a microfibril a number of unstained protofibrils form the periphery and are separated by a stained interstitial area from a central unstained region consisting of one or possibly two protofibrils. $\times 800{,}000$.
The delineation is imperfect but the number and arrangement is close to "9 + 2" and this is well demonstrated by making repetitive prints from selected fields. Insert, negative print. $\times 1{,}600{,}000$.

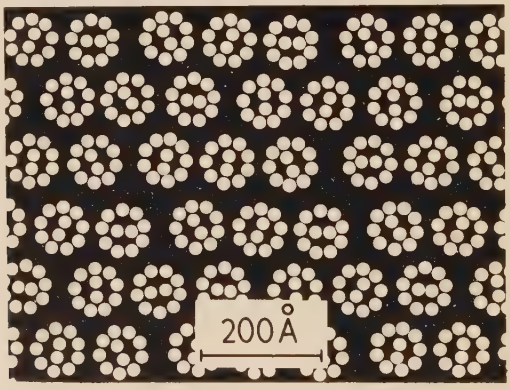

PLATE II(b). Schematic representation of the fine structure of α-keratin as visualized by electron-microscopy and incorporating the postulated flagella-like "9+2" arrangement of protofibrils. The orientation of protofibrils of neighbouring microfibrils has been randomized as it is not known whether there is any preferred orientation. The interstitial region between protofibrils is represented by black, like the matrix, but denotes a similarity in properties only in so far as the "electron staining" is concerned.

their packing arrangements in different keratins readily studied. Measurements have shown that microfibril diameters are approximately 80 Å and certainly not as low as 60 Å. The measurement of diameters is still complicated by the difficulty of defining the boundary between a microfibril and the matrix that surrounds it.

The frequent appearance of microfibrillar sheets, with intervening layers of matrix, in electron micrographs of cross-sections of α-keratins was observed in earlier work (Rogers, 1959*b*). Moreover the isolation of sheets of microfibrils from wool by Jeffrey, Sikorski & Woods (1955) favoured the view that the electron micrographs of sections revealed the existence of microfibrillar sheets *in situ*. Nevertheless the possibility remained that the sheet-like appearances from the study of accurate cross-sections could be solely due to the tilting of the microfibrils with respect to the fibre axis. It is now certain from the present study, however, that such appearances do in fact arise from a closer juxtaposition of microfibrils within the sheets and are not entirely the result of tilting.

It can be observed in Plates I and II(a) that a high concentration of lead has entered each microfibril and become bound to preferred sites, revealing a composite structure consisting of filamentous subunits relatively unstained by lead (henceforth to be referred to as protofibrils) each of the order of 20 Å in diameter. By observing sections cut parallel with the fibre axis the filamentous nature of the subunits was confirmed. Since the section thickness is about three times the diameter of a microfibril, poorer delineation of substructure is obtained owing to the image overlap of neighbouring microfibrils in this orientation.

It can be seen from Plate II(a) that protofibrils are arrayed peripherally around a stained central region containing an unstained core, the total arrangement bearing a strong resemblance to the structural organization of animal flagella. In such flagella, which are larger structures than keratin microfibrils, the occurrence of the basic "9 + 2" arrangement of subfibrils is well known (Fawcett & Porter, 1954; Bradfield, 1955; Gibbons & Grimstone, 1960) and from evidence recently adduced (Astbury, Beighton & Weibull, 1955) it is possible that this organization extends to bacterial flagella as well.

Although it is not possible to ascertain the exact number of protofibrils in a microfibril of α-keratin from electron micrographs obtained to date, it is close to "9 + 2." This was more convincingly illustrated when repetitive prints were made (McLachlan, 1958) of individual microfibrils showing the best delineation of substructure (insert, Plate II(a)). Thus a tentative interpretation of the electron micrographs describing the fine structure of α-keratin is given in Plate II(b).

Bacterial flagella yield X-ray diffraction patterns of the α-type and are regarded as having close structural ties with the *k-m-e-f* group of fibrous proteins as well as sharing the property of contractility (Astbury *et al.*, 1955). It is of profound significance for the elucidation of the structure of α-keratin that we now have direct evidence from electron microscopy of a structural organization at the macromolecular level which is common to α-keratin and animal flagella and possibly bacterial flagella as well.

Since the component α-helices of a microfibril are not arranged in an irregularly close-packed manner, but organized into protofibrils, it follows that each protofibril is probably a compound helix of the coiled-coil type already suggested for α-keratin (Pauling & Corey, 1953; Crick, 1953). For a protofibril about 20 Å in diameter, a triple helix (Fraser & MacRae, 1961) is indicated. It follows too from the proposed

"9 + 2" arrangement of protofibrils that since approximately 40 protein chains are required to fill a microfibril on the basis of a density of 1·32 g cm^{-3} for dry keratin, there must be several interstitial chains filling the space between the protofibrils. It is into this region that the lead penetrates, whereas the organized chains of the protofibrils would be expected to be inaccessible.

Very little can be said as to the nature of the reaction between α-keratin and lead hydroxide. In this connection we have found that the staining effect is not elicited unless the keratin has been bulk-stained by reduction and treatment with OsO_4. Reduction alone is not sufficient. Furthermore, the lead may be removed, as judged by the disappearance of contrast and substructure, by treatment of the stained grids with dilute (0·01 N) acids or by a chelating agent (0·1 M-ethylenediaminetetra-acetic acid). Both the staining with lead and its removal occur only in areas unirradiated by the electron beam (Gibbons & Bradfield, 1956), an effect which is useful for investigating potential "electron stains". The ready removal of lead indicates that it is electrostatically bound to the proteins of the matrix and the interstices of the microfibrils. The saturated lead hydroxide solution employed in the present work had a pH of 9·3, but at higher pH values reaction with the cystines of the keratin might be expected to become significant, with the formation of lead sulphide the colloidal nature of which would preclude the delineation of substructures described here.

Division of Protein Chemistry
C.S.I.R.O. Wool Research Laboratories
343 Royal Parade, Parkville N2, Melbourne
Victoria, Australia

B. K. Filshie
G. E. Rogers

Received 19 June 1961

REFERENCES

Astbury, W. T., Beighton, E. & Weibull, C. (1955). *Symp. Soc. Exp. Biol.* **9**, 282.
Birbeck, M. S. C. & Mercer, E. H. (1957). *J. Biophys. Biochem. Cytol.* **3**, 202.
Bradfield, J. R. G. (1955). *Symp. Soc. Exp. Biol.* **9**, 306.
Crick, F. H. C. (1953). *Acta Cryst.* **6**, 689.
Dobb, M. G., Nott, J. A. & Sikorski, J. (1960). Proceedings of Second European Regional Conference on Electron Microscopy, Delft.
Fawcett, D. W. & Porter, K. R. (1954). *J. Morphol.* **94**, 221.
Fraser, R. D. B. & MacRae, T. P. (1961). *J. Mol. Biol.* **3**, 640.
Glauert, A. M., Rogers, G. E. & Glauert, R. H. (1956). *Nature*, **178**, 803.
Gibbons, I. R. & Bradfield, J. R. G. (1956). Proceedings of First European Regional Conference on Electron Microscopy, Stockholm.
Gibbons, I. R. & Grimstone, A. V. (1960). *J. Biophys. Biochem. Cytol.* **7**, 697.
Jeffrey, G. M., Sikorski, J. & Woods, H. J. (1955). *Proc. Int. Wool Text. Res. Conf. Aust. F,* 130.
McLachlan, D. (1958). *Proc. Nat. Acad. Sci., Wash.* **44**, 948.
Pauling, L. & Corey, R. B. (1953). *Nature*, **171**, 59.
Rogers, G. E. (1959*a*). *J. Ultrastructure Res.* **2**, 309.
Rogers, G. E. (1959*b*). *Ann. N.Y. Acad. Sci.* **83**, 378.
Watson, M. L. (1958). *J. Biophys. Biochem. Cytol.* **4**, 727.

J. Mol. Biol. (1961) 3, 787–789

Über die Strahlensensibilisierende Wirkung des 5-Bromuracils†

5-Bromouracil and 5-bromodeoxyuridine are hardly altered by u.v.-irradiation (in water or in ice). On the other hand 5-bromouracil, which is incorporated in deoxyribonucleic acid, is dehalogenated to a great extent. The amount of thymine dimer formed in bacterial DNA by u.v.-irradiation decreases after incorporation of 5-bromouracil.

Bestrahlt man Bakterien mit UV-Licht der Wellenlänge 254 mμ, so findet man nach Hydrolyse der mit Thymin-[2-^{14}C] markierten Desoxyribonucleinsäure (DNS) eine zweite radioaktive Verbindung, die ein Dimeres des Thymins darstellt (Wacker, Dellweg & Weinblum, 1960). Die Menge Thymin-Dimeres hängt von der eingestrahlten UV-Dosis ab und nähert sich einem Grenzwert, der je nach Bakteriengattung verschieden ist (Wacker, Dellweg & Lodemann, 1961). Es war nun von Interesse festzustellen, wie in der DNS an Stelle von Thymin eingebautes 5-Bromuracil (BU) strahlenchemisch verändert wird und weiterhin, wie sich der teilweise Ersatz von Thymin durch BU in der DNS auf die Dimerisierung des Thymins auswirkt.

Bestrahlt man eine wässrige Lösung von BU (10^{-4} M) mit $1{,}5\times10^5$ erg/mm^2 UV-Licht der Wellenlänge 254 mμ, so wird dabei das BU nicht nachweisbar verändert. 5-Bromuracildesoxyribosid wird mit der gleichen Dosis zu etwa 3% in Uracildesoxyribosid umgewandelt. Bei Bestrahlung der eingefrorenen Lösungen erhält man das gleiche Ergebnis. Daraus ergibt sich, daß BU im Gegensatz zu Thymin und Uracil unter der Einwirkung von UV-Licht nicht dimerisiert. Eingebaut in die DNS wird jedoch überraschenderweise BU bei Bestrahlung entweder der Bakterien oder der aus ihnen isolierten DNS mit der gleichen UV-Dosis zu 56% (Bakterien) bzw. 72% (DNS) (siehe Abb. 1) verändert. Die Menge des in der DNS umgewandelten BU hängt von der eingestrahlten Dosis ab. Wird sie auf $5{,}8\times10^5$ erg/mm^2 erhöht, so werden 83% (Bakterien) BU verändert.—Es ist anzunehmen, daß ein großer Teil des isolierten, aus BU entstandenen radioaktiven Uracils in der Bakterien-DNS nach der UV-Bestrahlung in einer anderen Form vorgelegen hat (z. B. dimerisiert, in Form eines Wasseradduktes oder auch in Form eines Mischdimeren, wenn sich in Nachbarschaft zu Uracil Thymin befand), da die Uracilphotoprodukte unter den verwendeten Hydrolysebedingungen nicht stabil sind (Wacker, Weinblum, Träger & Moustafa, 1961).

Bei Bestrahlung von *Enterococcus* Stei mit $1{,}7\times10^5$ erg/mm^2 UV-Licht (λ 254 mμ) dimerisieren 10,5% der Thyminmoleküle in der Bakterien-DNS, was man dadurch einfach nachweisen kann, daß man die Bakterien mit 2 μg Thymin-[2-^{14}C]/ml. Nährmedium (Spezif. Aktivität 10 mc/mM) kultiviert. Befinden sich im Nährmedium noch zusätzlich 16 μg BU/ml., wodurch etwa 20% Thymin in der DNS durch BU ersetzt werden (Weygand & Wacker, 1952), so werden bei Bestrahlung mit der gleichen UV-Dosis nur noch 6,8% Thymin dimerisiert und bei einem weiteren Ersatz des Thymins durch BU von 35% (2 μg Thymin-[2-^{14}C]/ml. und 64 μg BU/ml.) sinkt die Ausbeute des Thymin-Dimeren auf 4,7%.

† 5. Mitteilung der Reihe "Strahlenchemische Veränderungen der Nucleinsäuren".

Bei *E. coli* 15 T⁻ lassen sich mit $1{,}7 \times 10^5$ erg/mm² UV-Licht 7,7% Thymin dimerisieren. In Anwesenheit von 2 μg Thymin-[2-^{14}C]/ml. und 16 μg BU/ml. wodurch etwa 35% der Thymin-Moleküle durch BU ersetzt werden, sinkt die Menge Thymin-Dimeres bei gleicher UV-Dosis auf 6% ab. Es sei hier hinzugefügt, daß bei *Enterococcus* Stei, dessen Basenverhältnis $(G+C)/(A+T) = 0{,}69$ beträgt, maximal 17% der Thyminmoleküle unter der Einwirkung des UV-Lichtes dimerisieren (Wacker *et al.*, 1961), und bei *E. coli* 15 T⁻ mit einem Basenverhältnis von 1,0 maximal 10%. Überträgt man die Ergebnisse der UV-Bestrahlung des Dinucleotides Thymidylyl-(3′ → 5′)-thymidin (TpT) (Wacker *et al.*, 1961) auf die Nucleinsäure, so ergibt sich, daß maximal etwa 1/3 der benachbarten Thyminmoleküle innerhalb einer DNS-Kette dimerisieren.

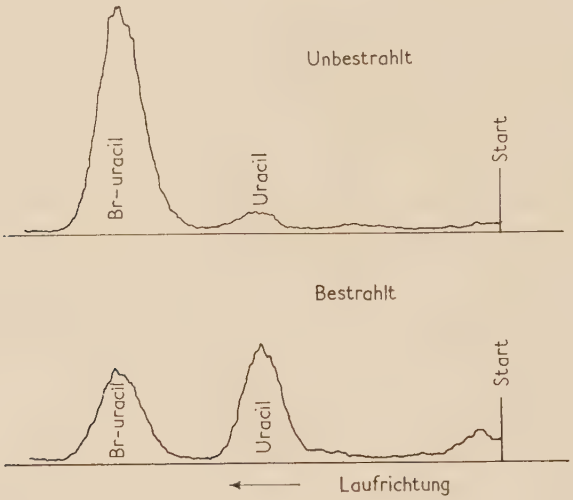

Abb. 1. Dehalogenierung von 5-Bromuracil in der Bakterien-DNS durch UV-Bestrahlung. Papierchromatographie des Perchlorsäure-Hydrolysates von *Enterococcus* Stei in *n*-Butanol/Wasser (86 : 14). 2 μg 5-Bromuracil-[2-^{14}C]/ml. Nährmedium, Spezif. Aktivität 10 mc/m-M. UV-Dosis $1{,}5 \times 10^5$ erg/mm². (Wie aus der Papierchromatographie der unbestrahlten Bakterien hervorgeht, wird BU zu ca. 5% von den Bakterien dehalogeniert und in Uracil überführt.) Ordinate: Radioaktivität in Imp/min.

Wir konnten nun kürzlich zeigen (Wacker, 1961), daß ein Zusammenhang zwischen der Menge des Thymin-Dimeren und der Überlebensrate von Bakterien nach UV-Bestrahlung besteht. Bei 18% Überlebenden bei *E. coli* 15 T⁻ finden wir 0,059% Thymin-Dimeres, bei 0,5% Überlebenden 0,094% Thymin-Dimeres. In Modellversuchen der Photoreaktivierung fanden wir ferner (Wacker, 1961), daß sichtbares Licht und Hefeenzym, die Bedingungen also, unter denen eine Photoreaktivierung stattfindet, Thymidin-Dimeres etwa zu 10% spalten. Diese Befunde weisen darauf hin, daß die letale Wirkung des UV-Lichtes mit der Dimerisierung des Thymins zusammenhängen kann, wobei aber noch unklar ist, ob hierbei allein die Menge Thymin-Dimeres unabhängig von dem Ort, an dem die Dimerisierung erfolgt, entscheidend ist, oder ob eine Dimerisierung zwischen den beiden DNS-Ketten ausschlaggebend ist. In scheinbarem Gegensatz zu dieser Annahme steht die Tatsache, daß nach Einbau von BU in die DNS die Menge Thymin-Dimeres zurückgeht, gleichzeitig aber die UV-Empfindlichkeit der Zelle wesentlich zunimmt (Greer &

Zamenhof, 1957; Szybalski, 1959). Berücksichtigt man aber, daß BU in der DNS sehr leicht durch UV-Licht dehalogeniert wird, Uracil aber kein Baustein der DNS ist, ferner, daß dabei auch einzelständig entstehende Uracilmoleküle durch UV-Licht unter Wasseraddition weiterreagieren können (was bei einem einzelständigen Thymin nicht der Fall ist), so sieht man, daß das Ausmaß der Störungen in einer BU-haltigen DNS-Kette (falscher Baustein, Dimerisierung, Mischdimerisierung, Wasseraddition) weit größer ist, als in einer DNS, die kein BU enthält.

Wir danken Frl. Andrea Gerstenberger und Frl. Ute Güngerich für die Mithilfe bei den Versuchen, dem Verband der Chemischen Industrie—Fonds der Chemie—und dem Bundesminister für Atomkernenergie und Wasserwirtschaft für die Unterstützung der Arbeit.

REFERENCES

Greer, S. & Zamenhof, S. (1957). Abstr. Papers 131st Meeting, Amer. Chem. Soc. 3c.
Szybalski, W. (1959). *Animal Cell Information Service*, **1**, 5.
Wacker, A. (1961). XI^{e} Reunion Annuelle Col de Voza, Soc. de chimie physique.
Wacker, A., Dellweg, H. & Lodemann, E. (1961). *Angew. Chem.* **73**, 64.
Wacker, A., Dellweg, H. & Weinblum, D. (1960). *Naturwissenschaften*, **47**, 477.
Wacker, A., Weinblum, D., Träger, L. & Moustafa, Z. H. (1961). *J. Mol. Biol.* **3**, 790.
Weygand, F. & Wacker, A. (1952). *Z. Naturf.* **7b**, 26.

Institut für Therapeutische Biochemie
der Universität Frankfurt am Main
Germany

Adolf Wacker
Hanswerner Dellweg
Dieter Weinblum

Received 4 August 1961

J. Mol. Biol. (1961) **3**, 790–793

Photochemische Reaktionen von Uracil und Uridin†

On u.v.-irradiation of uracil and uridine a water addition-product and a dimer are formed in each case. When a mixture of uracil and thymine is irradiated a mixed dimer can be isolated, which consists of uracil and thymine. The formation, isolation and stability of the irradiated compounds are discussed. The irradiation products of uracil and uridine are not growth factors for the uracil-deficient mutant *E. coli* 63–86.

Durch spektralphotometrische Untersuchungen entdeckten Sinsheimer & Hastings (1949) die reversible photochemische Umwandlung des Uracils und Uridins. Mit Hilfe der Papierchromatographie bestätigte Moore (1958) die Wasseranlagerung an die 5.6-Doppelbindung des Uracilmoleküls (Shugar & Wierzchowski, 1957). Für 1.3-Dimethyluracil haben Wang, Apicella & Stone (1956) ebenfalls den Beweis der reversiblen Wasseranlagerung unter UV-Bestrahlung erbracht. Durch Verwendung ^{14}C-markierten Uracils und Uridins konnten wir kürzlich u. a. zeigen (Wacker, Träger & Weinblum, 1961), daß beide Verbindungen bei Bestrahlung mit UV-Licht der Wellenlänge 254 mμ dimerisieren, wie dies erstmals Beukers & Berends (1960) für Thymin gefunden haben (vergl. hierzu auch Wang, 1961). Nachfolgend berichten wir ausführlicher über die photochemischen Veränderungen des Uracils und Uridins.

Bestrahlt man wässrige Lösungen von Uracil-[2-^{14}C] flüssig oder eingefroren, so bilden sich in Abhängigkeit von der eingestrahlten Dosis UV-Licht (und von der Konzentration der Lösung) zwei Verbindungen A und B, die sich papierchromatographisch (siehe Abb. 1) im Lösungsmittelsystem *n*-Butanol/Wasser (86 : 14) trennen lassen (R_F-Werte Verbindung A 0,04; B 0,18; Uracil 0,31). Wie aus Abb. 1 hervorgeht, bildet sich bei einer kleineren UV-Dosis mehr A, bei einer größeren mehr B. Höhere Uracil-Konzentrationen begünstigen die Bildung von A, niedrigere die von B. Das Absorptionsspektrum der Verbindungen A und B zeigt kein Maximum bei 258 mμ, woraus man schließen kann, daß das Uracil unter Absättigung der 5.6-Doppelbindung reagiert hat. Durch Hitze (100°C, 15 min) wird A sehr wenig, B zum größten Teil in Uracil verwandelt. Durch UV-Bestrahlung der wässrigen Lösungen wird A in Uracil überführt, B dagegen nicht verändert. Gegenüber Säuren und Alkalien sind beide Verbindungen wenig beständig. Nach ihrem R_F-Wert in *n*-Butanol/Wasser (86 : 14) (Moore, 1958) und ihren physikalisch-chemischen Eigenschaften ist die Verbindung B mit dem Wasseradditionsprodukt des Uracils identisch. Die Verbindung A zeigt all die Eigenschaften einer dimeren Verbindung analog der des Thymins (Beukers & Berends, 1960; Wacker, Dellweg & Lodemann, 1961). Offenbar ist das Uracil-Dimere mit dem von Rörsch, Beukers, Ijlstra & Berends (1958) beschriebenen 1. irreversiblen Photoprodukt des Uracils identisch.

Das gleiche Verhalten wie Uracil zeigt Uridin. Bestrahlt man eine wässrige Lösung von Uridin-[2-^{14}C] (Spezif. Aktivität 0,28 mc/mM; Konz. 5×10^{-4} M) mit verschiedenen Dosen UV-Licht ($7{,}2 \times 10^4$ erg/mm^2; $5{,}8 \times 10^5$ erg/mm^2), so erhält man

† 4. Mitteilung der Reihe "Strahlenchemische Veränderungen der Nucleinsäuren"; 3. Mitteilung: Wacker, Träger & Weinblum (1961).

mit der kleinen Dosis 27% Dimeres und 27% Wasseranlagerungsprodukt, mit der großen Dosis 19% Dimeres und 58% Wasseranlagerungsprodukt. Wird die Uridinlösung in gefrorenem Zustand bestrahlt, so ist die Dimerisierung im Vergleich zur Wasseraddition begünstigt. R_F-Werte im Lösungsmittelsystem *n*-Butanol/Wasser (86 : 14): Uridin 0,17; Wasseradditionsprodukt des Uridins 0,09; Uridin-Dimeres 0,02. Die Stabilität des Wasseranlagerungsproduktes und der dimeren Verbindung gegenüber Hitze, UV-Licht, Säure und Alkali ist ähnlich wie beim Uracil.

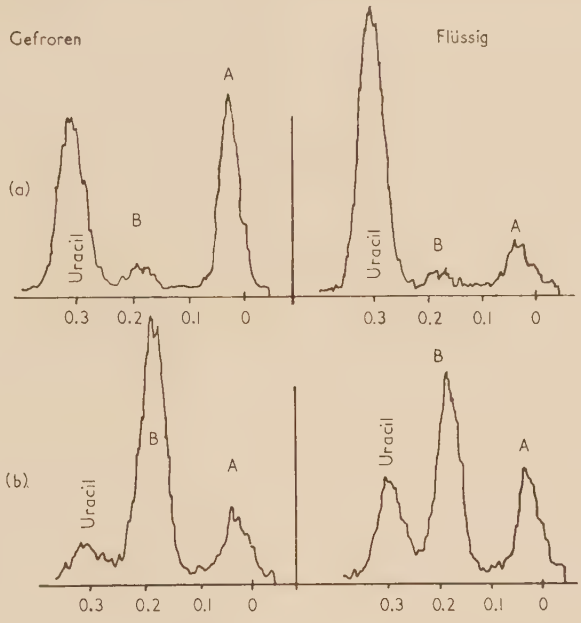

Abb. 1. Bildung von Uracil-Dimeren (A) und Uracil-Wasseradditionsprodukt (B) in Abhängigkeit von der UV-Dosis und vom Zustand der bestrahlten Lösung.

Chromatogramme von UV-bestrahltem Uracil-[2-^{14}C] (Spezif. Aktivität 2 mc/mM). Konzentration 10^{-3} M.

(a) UV-Dosis $5{,}4 \times 10^4$ erg/mm^2
(b) UV-Dosis $8{,}6 \times 10^5$ erg/mm^2

Abszisse: R_F-Wert im Lösungsmittelsystem *n*-Butanol/Wasser (86 : 14)

Ordinate: Radioaktivität Imp/min.

Bestrahlt man in Eis eine 5×10^{-4} molare Lösung von Thymin-[2-^{14}C] und Uracil-[2-^{14}C] mit einer UV-Dosis von $5{,}4 \times 10^4$ erg/mm^2 und chromatographiert anschließend die Reaktionsmischung, so erhält man das in Abb. 2(c) wiedergegebene Bild. Eluiert man die photochemisch entstandenen Verbindungen und bestrahlt ihre wässrigen Lösungen mit UV-Licht (Dosis $5{,}4 \times 10^4$ erg/mm^2), so erhält man bei der Verbindung mit dem kleinsten R_F-Wert nur Uracil zurück, bei der Verbindung mit dem nächsthöheren R_F-Wert in äquimolaren Mengen Thymin und Uracil. Die Verbindung mit dem R_F-Wert 0,13 ist mit dem Thymin-Dimeren identisch. Daraus ergibt sich eindeutig, daß die Verbindung mit dem R_F-Wert 0,09 ein Mischdimeres von Thymin und Uracil darstellt, dessen mögliche Bildung Beukers & Berends (1961) diskutiert haben (vgl. hierzu Marmur & Grossmann, 1961).

Bestrahlt man eine wässrige Lösung von Uridin (UR), Guanylyluridin (GpU) und Adenylyladenosin (ApA) (je 0,4 μmol/ml.) mit UV-Licht ($5{,}8 \times 10^5$ erg/mm^2), so beträgt der Abfall von der Ausgangsextinktion am jeweiligen Maximum bei UR 86%, bei GpU 15% und bei ApA 0%. Erhitzt man die bestrahlten Lösungen (100°C, 10 min), so steigt die Extinktion der Lösungen bei UR um 33% und bei GpU um 13% an. Vergleicht man diese Ergebnisse mit den oben mitgeteilten Beständigkeiten der

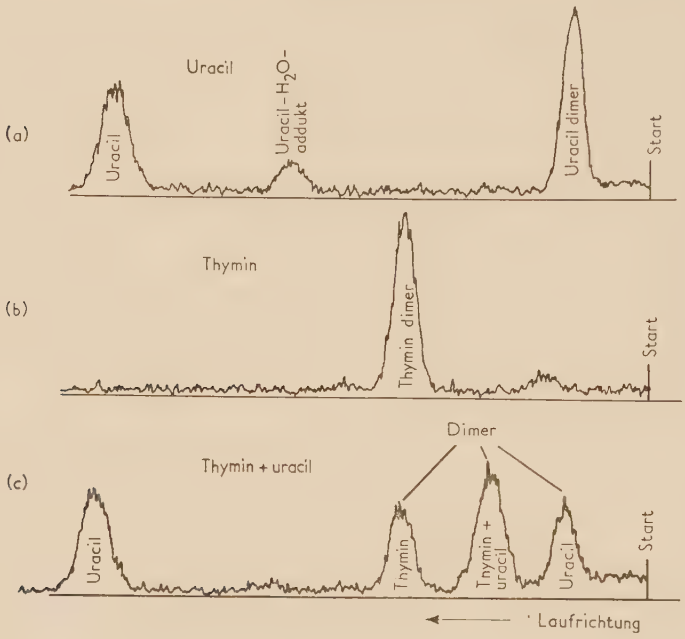

Abb. 2. Bildung von Thymin-Uracil-Mischdimeren.

UV-Bestrahlung einer eingefrorenen Lösung von 5×10^{-4} M-Thymin-[2-^{14}C] (Spezif. Aktivität 2 mc/mM) und 5×10^{-4} M-Uracil-[2-^{14}C] (Spezif. Aktivität 2 mc/mM). UV-Dosis $5{,}4 \times 10^4$ erg/mm^2. Chromatogramme im Lösungsmittelsystem *n*-Butanol/Wasser (86 : 14).

(a) Uracil-Bestrahlungsprodukte
(b) Thymin-Bestrahlungsprodukte
(c) Bestrahlungsprodukte aus der Thymin/Uracil-Mischung

Ordinate: Radioaktivität Imp/min.

dimeren Verbindung des Uridins und des Wasseradditionsproduktes des Uridins, so ergibt sich hieraus, daß im Dinucleotid GpU das Uracilmolekül bei der UV-Bestrahlung lediglich Wasser anlagert, jedoch nicht dimerisiert. Zu dem gleichen Ergebnis kam auch D. Shugar (persönliche Mitteilung) bei der UV-Bestrahlung anderer Uracil-haltiger Nucleotide.

Die Wasseradditionsprodukte von Uracil und Uridin und die dimeren Verbindungen des Uracils und Uridins sind für die Uracil-Mangelmutante *E. coli* 63–86, die entweder Uracil oder Uridin zum Wachstum benötigt, keine Wuchstoffe mehr.

Wir danken Herrn Dr. H. Witzel für die freundliche Überlassung der Dinucleotide, dem Verband der Chemischen Industrie—Fonds der Chemie—und dem Bundesminister für Atomkernenergie und Wasserwirtschaft für die Unterstützung der Arbeit.

REFERENCES

Beukers, R. & Berends, W. (1960). *Biochim. biophys. Acta*, **41**, 550.
Beukers, R. & Berends, W. (1961). *Biochim. biophys. Acta*, **49**, 181.
Marmur, J. & Grossmann, L. (1961). *Proc. Nat. Acad. Sci., Wash.* **47**, 778.
Moore, A. M. (1958). *Canad. J. Chem.* **36**, 281.
Rörsch, A., Beukers, R., Ijlstra, J. & Berends, W. (1958). *Rec. Trav. Chim.* **77**, 423.
Shugar, D. & Wierzchowski, K. (1957). *Biochim. biophys. Acta*, **23**, 657.
Sinsheimer, R. L. & Hastings, R. (1949). *Science*, **110**, 525.
Wacker, A., Dellweg, H. & Lodemann, E. (1961). *Angew. Chem.* **73**, 64.
Wacker, A., Träger, L. & Weinblum, D. (1961). *Angew. Chem.* **73**, 65.
Wang, S. Y. (1961). *Nature*, **190**, 690.
Wang, S. Y., Apicella, M. & Stone, B. R. (1956). *J. Amer. Chem. Soc.* **78**, 4180.

Institut für Therapeutische Biochemie
der Universität Frankfurt am Main
Germany

Adolf Wacker
Dieter Weinblum
Lothar Träger
Zeinab H. Moustafa

Received 4 August 1961

J. Mol. Biol. (1961) **3**, 794–795

Recommendations for the Nomenclature of Hemoglobins

Chain Nomenclature

There is now general agreement on the naming of the peptide chains of the major components of normal human adult and fetal hemoglobins as the α, β and γ chains; e.g. adult hemoglobin is written as $\alpha_2^A\beta_2^A$ and fetal hemoglobin as $\alpha_2^A\gamma_2^F$. The superscripts A and F refer to the fact that the particular chain is the one found in the human adult and fetal hemoglobins. It is recommended that this practice be continued and that the symbols α, β and γ, without superscripts, be reserved for those occasions when reference is being made to, for example, α chains in general.

Information concerning the structure of the chains of hemoglobin A_2 is now sufficient to indicate that one of the chains is identical with the α^A chain, while the second differs in a number of residues from the three foregoing chains. In addition there is evidence (Cepellini, 1959) to indicate that the genetic control of this unique chain is independent of the genes for the α, β and γ chains. It is therefore recommended that this chain be designated as δ^{A_2}; Hb A_2 is then written as $\alpha_2^A\delta_2^{A_2}$. Again, one could refer simply to δ chains in the general case.

The simplest method of naming the tryptic peptides of a chain is to number them in the order in which they occur in the chain, beginning with the N-terminus. The symbol for the chain is included as a part of the designation. The letters Tp are included to identify that these are the peptides obtainable by tryptic digestion. For example, the third tryptic peptide of the α chain would be αTpIII in this system. Where a lysyl bond is not attacked under the conditions used, the symbol for the resultant "dipeptide" or "double peptide" would contain the numbers appropriate to both tryptic peptides, e.g. αTpI,II. From the published structure of the α and β chains (Braunitzer *et al.* 1961; Hill & Konigsberg, 1961) and from the amino acid composition, it is evident that the α chain will contain the tryptic peptides αTpI to αTpXIV and the β chain the tryptic peptides βTpI to βTpXV. It so happens that the tryptic "peptides" αTpVIII and βTpVIII are lysine. In addition, the present methods of tryptic cleavage do not break the bond separating the expected tryptic peptides αTpXII and αTpXIII, nor the bond between the expected peptides βTpX and βTpXI. In view of the possibility that these bonds might be split in some experiments at a later date, it is felt that the numbering system should correspond with the theoretical number of tryptic peptides.

When the complete sequence of the chains is determined beyond question and is published, then a more specific designation involving residue numbers should be adopted. Thus, βTpI can be designated as βTpl-8.

Nomenclature of the Abnormal Hemoglobins

An ideal nomenclature system for the abnormal hemoglobins would provide for adequate designation of the chemical structure at each stage of the investigation. The following system is an attempt to meet this requirement.

When only the chain in which the abnormality resides is known, then the hemoglobin may be written as $\alpha_2^A\beta_2^S$, or $\alpha_2^A\beta_2^{D\text{Punjab}}$. When the abnormality has been

located in a particular tryptic peptide, as by finger printing, then the designation should be, for example, $\alpha_2^A\beta_2^{TpI}$. When the amino acid composition of the tryptic peptide indicates a particular amino acid substitution, then this will be indicated as $\alpha_2^A\beta_2^{TpI(Glu\rightarrow Val)}$ for Hb S. Finally, when the amino acid interchange has been located at a particular residue position in the chain, the fully descriptive formula, as in the case of Hb S, would be in the form: $\alpha_2^A\beta_2^{6Val}$.

Presumably, for use in formulae describing experiments such as reassociation, it will be necessary to define in a given paper a one-letter designation for a particular hemoglobin. For example, the formula $\alpha_2^I\beta_2^S$ could be used, provided that wherever possible the individual hemoglobins have been defined, as for example, Hb I as $\alpha_2^{16Asp}\beta_2^A$ and Hb S as $\alpha_2^A\beta_2^{6Val}$.

It is strongly urged that no further letters be assigned to abnormal hemoglobins. Newly discovered hemoglobins, prior to their chemical identification, should be known by the letter designation of the previously described hemoglobin whose electrophoretic mobility they most nearly resemble. To the letter should be attached a subscript indicating the geographic origin of the new hemoglobin.

Proposals similar to the above originated during the Hemoglobin Structure Workshop held in Boston, December 14 to 16, 1960. These proposals have been modified at the suggestion of other workers in the protein structure field. In their present form they represent a compromise between the views of these two groups.

Children's Hospital Medical Center & P. S. Gerald
Harvard Medical School
Boston, Massachusetts, U.S.A.

Division of Biochemistry, Department of Biology V. M. Ingram
Massachusetts Institute of Technology
Cambridge, Massachusetts, U.S.A.

Received 10 August 1961

REFERENCES

Braunitzer, G., Hilschmann, N., Rudloff, V., Hilse, K., Liebold, B. & Muller, R. (1961). *Nature*, **190**, 480.

Cepellini, R. (1959). In *Biochemistry of Human Genetics*, ed. by G. E. Wolstenholme & C. M. O'Connor, p. 133. London: J. & A. Churchill.

Hill, R. & Konigsberg, W. (1961). *J. Biol. Chem.* **236**, PC7.

Index to Volume 3

Acridine mutagenesis in bacteriophage T4, a theory of its mechanism, 762
Acridines, interaction with DNA, 18
Adult and foetal horse haemoglobins, a comparison, 112
Albertsson, P. Å. (see Lif, T.), 727
Allison, W. S. (see Grossman, L.), 47
Arginine biosynthesis, control in strains of *E. coli* not repressible by arginine, 439
Ascoli, F., Botré, C. & Liquori, A. M., Irreversible changes of ionic activities following thermal denaturation of sodium deoxyribonucleate, 202
Atwater, J., Huehns, E. R. & Shooter, E. M., Haemoglobin I_2, a further variant of haemoglobin A_2, 707
Autoradiography, used to estimate the length of the DNA molecule of T2 bacteriophage, 756
8-azaguanine, effect of ribosomal RNA in *B. cereus*, 693

Bacillus cereus ribosomal RNA, effect of 8-azaguanine, 693
Bacteriophage, an estimate by autoradiography of the length of the DNA molecule in T2, 756
— a relative molecular weight series derived from the nucleic acid of T2, 458
— densities of transducing lambda, 393
— DNA, electron microscopy of molecules with denatured regions, 699
— DNA released from T2 and T4, 277
— DNA subunits in the phage precursor pool, 267
— λ, a mutation affecting the DNA content and its lysogenizing properties, 399
— multiplicity reactivation with a trypsin-sensitive factor after heat disruption, 125
— physical characterization of the DNA molecules from T2 and T4, 277
— single polynucleotide chains derived from T2 and T4, 289
— stabilization to ^{32}P decay and onset of DNA replication in T4, 409
— T2 DNA, reaction with formaldehyde, 47
— T4, multiplicity reactivation after the decay of incorporated radioactive phosphorus, 61
— T4, theory of mutagenesis by acridines, 762
— T4, the nature of "deletion" mutants in the *r*II region, 684
— T4B, some remarks on morphology, 225
Barnett, L. (see Brenner, S.), 121
Bautz, E. (see Freese, E.), 133
Bautz-Freese, E. (see Freese, E.), 133
Beer, M., Electron microscopy of unbroken DNA molecules, 263
— & Thomas, C. A., Jr., The electron microscopy of phage DNA molecules with denatured regions, 699
— & Zobel, C. R., Electron stains II. Electron microscopic studies on the visibility of stained DNA molecules, 717
Benzer, S. (see Nomura, M.), 684
Berns, K. I. (see Thomas, C. A., Jr.), 277
— & Thomas, C. A., Jr., A study of single polynucleotide chains derived from T2 and T4 bacteriophage, 289
Bessman, M. (see Kozinski, A.), 746
Beychok, S. & Blout, E. R., Optical rotatory dispersion of sperm whale ferrimyoglobin and horse ferrihemoglobin, 769
Blout, E. R. (see Beychok, S.), 769
Bonar, L. C. (see Glimcher, M. J.), 541
Botré, C. (see Ascoli, F.), 202
Bradbury, E. M., Price, W. C. & Wilkinson, G. R., Infrared studies of molecular configurations of DNA, 301
Brenner, S. (see Orgel, A.), 762

— Barnett, L., Crick, F. H. C. & Orgel, A., The theory of mutagenesis, 121
5-Bromouracil, radiation-sensitizing action, 787
Bromouracil-substituted mammalian DNA, separation of light and heavy strands, 668
Brown, D. M. & Schell, P., The reaction of hydroxylamine with cytosine and related compounds, 709
Burgi, E. & Hershey, A. D., A relative molecular weight series derived from the nucleic acid of bacteriophage T2, 458

Cairns, J., An estimate of the length of the DNA molecule of T2 bacteriophage by autoradiography, 756
Cell-free system to study the specificity of haemoglobin synthesis, 241
Cesari, M., (see Luzzati, V.), 566
Chloroplasts, correlation of structure with function in *Spinacea oleracea*, 1
Chun, E. H. L. & Littlefield, J. W., The separation of light and heavy strands of bromouracil-substituted mammalian DNA, 668
Clegg, J. B. (see Williams, J.), 532
Cohen, J. A. (see Daems, W. Th.), 225
Coincidence and protein structure, 532
Collagen, molecular structure, 483
D, L-Copoly-γ-benzyl glutamate, regularity in chain configuration, 507
Crick, F. H. C. (see Rich, A.), 483
— (see Rich, A.), 71
— (see Brenner, S.), 121
Cross-β structure and the 1700 cm^{-1} band, 480
Cummings, D. J. (see Hanawalt, P. C.), 156
Cytosine and related compounds, reaction with hydroxylamine, 709

Daems, W. Th., van de Pol, J. H. & Cohen, J. A., Some remarks on the morphology of bacteriophage T4B, 225
Daniel, E. J. (see Glimcher, M. J.), 541
Davies, D. R. (see Rich, A.), 71
Davison, P. F. (see Levinthal, C.), 674
Deletion mutants in the rII region of bacteriophage T4, 684
Dellweg, H. (see Wacker, A.), 787
Dental enamel, molecular structure of the protein matrix, 541
Deoxyguanylate kinase formation in *E. coli*, a comparison with parental DNA replication, 746
Deoxyribonucleate, sodium, irreversible changes of ionic activities following thermal denaturation, 202
Deoxyribonucleic acid, a mutation affecting the content and lysogenizing properties in bacteriophage λ, 399
— a procedure for isolation from micro-organisms, 208
— adsorption in a polarized water-mercury interface, temperature dependence, 357
— bacteriophage, physical characteristics from T2 and T4, 277
— comparison of parental replication and deoxyguanylate kinase formation in *E. coli*, 746
— degradation under hydrodynamic shearing forces, 674
— electron microscopy of unbroken molecules, 263
— infrared studies of molecular configurations, 301
— interaction with acridines, 18
— interaction with proflavine, a small angle X-ray scattering study, 634
— lithium salt, an X-ray diffraction study of the *C* form, 547
— low-angle X-ray studies in solution, 185
— mammalian, separation of light and heavy strands when bromouracil-substituted, 668
— molecule, an estimate by autoradiography of its length in T2 bacteriophage, 756
— molecules, electron microscopic studies on visibility when stained, 717
— normal replication cycle, 144, 156
— of bacteriophage, electron microscopy of molecules with denatured regions, 699
— phage subunits in the phage precursor pool, 267

Deoxyribonucleic acid, preparations from animal tissues, equilibrium sedimentation and density gradients, 711
— reaction with formaldehyde, 47
— replication, the effect of thymine deficiency and the normal replication cycle, 144
— the formation of hybrid molecules and their use in studies of DNA homologies, 595
— stabilization to ^{32}P decay and onset of replication in T4 bacteriophage, 409
— structure in the water-mercury interface, 229
— thermal renaturation, 585
— transfer from parent to progeny in a tissue culture line of human carcinoma of the cervix (strain HeLa), 101
Deoxyribonucleic acids, ultraviolet spectrum, 119
— variation and heterogeneity in base composition, 31
Doty, P. (see Marmur, J.), 585
— (see Schildkraut, C, L.), 595

Echols, H., Garen, A., Garen, S. & Torriani, A., Genetic control of repression of alkaline phosphatase in *E. coli*, 425
Electron microscopy, of phage DNA molecules with denatured regions, 699
— of unbroken DNA molecules, 263
— used to reveal the configurations of high polymer RNA macromolecules, 778
Electron microscopic studies on the visibility of stained DNA molecules, 717
Elliott, G. F. & Lowy, J., Low-angle X-ray reflections from living molluscan muscles, 41
Ennis, H. L. & Gorini, L. Control of arginine biosynthesis in strains of *Escherichia coli* not repressible by arginine, 439
Enzyme synthesis, effect of ^{32}P decay, 219
Equilibrium sedimentation in density gradients of DNA preparations from animal tissues, 711
Escherichia coli, comparison of parental DNA replication and deoxyguanylate kinase formation, 745
— control of arginine biosynthesis in strains not repressible by arginine, 439
— genetic control of repression of alkaline phosphatase, 425
— synthesis of β-galactosidase in the presence of thiouracil, 166

Ferrihemoglobin from horse, optical rotatory dispersion, 769
Ferrimyoglobin from sperm whale, optical rotatory dispersion, 769
Filshie, B. K. & Rogers, G. E., The fine structure of α-keratin, 784
Finch, J. T. (see Klug, A.), 87
Foetal and adult horse haemoglobins, a comparison, 112
Fontaine, F. (see Fredericq, E.), 11
Formaldehyde, reaction with nucleotides and T2 bacteriophage DNA, 47
Formamide-treated nucleic acid, infrared spectra, 241
Fraser, R. D. B. & MacRae, T. P., The molecular configuration of α-keratin, 640
Fredericq, E., Oth, A. & Fontaine, F., The ultraviolet spectrum of deoxyribonucleic acids and their constituents, 11
Freese, E., Bautz-Freese, E. & Bautz, E., Hydroxylamine as a mutagenic and inactivating agent, 133
Frick, G. (see Lif, T.), 727
Fuller, W., Two-stranded helical configurations for ribonucleic acid, 175

β-Galactosidase synthesis by *E. coli* in the presence of thiouracil, 166
Garen, A. (see Echols, H.), 425
Garen, S. (see Echols, H.), 425
Gavrilova, L. P. (see Kisselev, N. A.), 778
Genetic control of repression of alkaline phosphatase in *E. coli*, 425
Genetic regulatory mechanisms in the synthesis of proteins, 318
Gerald, P. S. & Ingram, V. M., Recommendations for the nomenclature of hemoglobins, 794
Glauser, S. C. (see Stockell, A.), 112

Glimcher, M. J., Bonar, L. C. & Daniel, E. J., The molecular structure of the protein matrix of bovine dental enamel, 541
Gorini, L. (see Ennis, H. L.), 439
Grossman, L., Levine, S. S. & Allison, W. S., The reaction of formaldehyde with nucleotides and T2 bacteriophage DNA, 47

Haemoglobin A_2, a further variant, haemoglobin I_2, 707
— polypeptide chains, 257
Haemoglobin G_2, polypeptide chains, 257
Haemoglobin I_2, a further variant of haemoglobin A_2, 707
Haemoglobin from horse, optical rotatory dispersion, 769
Haemoglobins of horse, a comparison of foetal and adult, 112
Haemoglobins, recommendations for nomenclature, 794
Haemoglobin synthesized in a cell-free system, factors determining specificity, 241
Hamers-Casterman, C. (see Hamers, R.), 166
Hamers, R. & Hamers-Casterman, C., Synthesis by *Escherichia coli* of an abnormal β-galactosidase in the presence of thiouracil, 166
Hamilton, L. D. (see Marvin, D. A.), 547
Hanawalt, P. C. (see Maaløe, O.), 144
— Maaløe, O., Cummings, D. J. & Schaechter, M., The normal DNA replication cycle II, 156
Harriman, P. D. (see Pratt, D.), 409
Harris, J. I. & Hindley, J., The protein subunit of tobacco mosaic virus, 117
Hart, R. G., Surface structure of tobaccco mosaic virus, 701
HeLa cell culture from human carcinoma of the cervix, transfer of DNA from parent to progeny, 101
Helical forms and transitions in poly-γ-benzyl-L-glutamate, 566
α-Helices, sidechain-sidechain interaction between L- and D- forms of polypeptide chains, 705
Helices, further remarks concerning rate of uncoiling, 473, 475
Hershey, A. D. (see Burgi, E.), 458
Hindley, J. (see Harris, J. I.), 117
Holmes, K. C. (see Klug, A.), 87
Horiuchi, S. (see Horiuchi, T.), 703
Horiuchi, T., Horiuchi, S. & Novick, A., A temperature-sensitive regulatory system, 703
Huehns, E. R. (see Atwater, J.), 707
— & Shooter, E. M., The polypeptide chains of haemoglobin A_2 and haemoglobin G_2, 257
Hydroxylamine, as a mutagenic and inactivating agent, 135
— reaction with cytosine and related compounds, 709
— reaction with TMV RNA, 447

Infrared studies of molecular configurations of DNA, 301
Infrared spectra of formamide-treated nucleic acids, 741
Ingram, V. M. (see Gerald, P. S.), 794
Ionic activities, changes following thermal denaturation of sodium deoxyribonucleate, 202

Jacob, F. & Monod, J., Genetic regulatory mechanisms in the synthesis of proteins, 318

Kellenberger, G., Zichichi, M. L. & Weigle, J. J., A mutation affecting the DNA content of bacteriophage λ and its lysogenizing properties, 399
α-Keratin, fine structure, 784
— molecular configuration, 640
Kiho, Y. & Watanabe, I., The role of a trypsin-sensitive factor in multiplicity reactivation with heat-disrupted phage, 125
Kisselev, N. A., Gavrilova, L. P. & Spirin, A. S., On configurations of high polymer ribonucleic acid macromolecules as revealed by electron microscopy, 778
Kit, S., Equilibrium sedimentation in density gradients of DNA preparations from animal tissues, 711

Klug, A., Holmes, K. C. & Finch, J. T., X-ray diffraction studies on ribosomes from various sources, 87
Kozinski, A. W. & Bessman, M., The kinetics of parental deoxyribonucleic acid replication, deoxyguanylate kinase formation and ^{32}P inactivation of the parental virus in *E. coli* infected with bacteriophage T4, 746
— & Uchida, H., Phage DNA subunits in the phage precursor pool, 267
Kuhn, W., Remark concerning the rate of uncoiling of helices of two or more strands, 473
Kyogoku, Y., Tsuboi, M., Shimanouchi, T. & Watanabe, I., Infrared spectra of formamide-treated nucleic acids, 741

λ (see bacteriophage), 393, 399
Lamfrom, H., Factors determining the specificity of haemoglobin synthesized in a cell-free system, 241
Lerman, L. S., Structural considerations in the interaction of DNA and acridines, 18
— (see Luzzati, V.), 634
Levine, S. S. (see Grossman, L.), 47
Levinthal, C. & Davison, P. F., Degradation of deoxyribonucleic acid under hydrodynamic shearing forces, 674
Lif, T., Frick, G. & Albertsson, P. Å., Fractionation of nucleic acids in aqueous polymer two-phase systems, 727
Liquori, A. M. (see Ascoli, F.), 202
Littlefield, J. W. (see Chun, E. H. L.), 668
Longuet-Higgins, H. C. & Zimm, B. H., Further remarks concerning the rate of uncoiling of helices of two or more strands, 475
Lowy, J. (see Elliott, G. F.), 41
Luzzati, V., Cesari, M., Spach, G., Masson, F. & Vincent, J. M., La structure du poly-L-γ-glutamate de benzyle en solution. Configuration en hélice différente de l'hélice α et transitions entre formes hélicoïdales, 566
— Masson, F. & Lerman, L. S., Interaction of DNA and proflavine: a small-angle X-ray scattering study, 634
— Nicolaieff, A. & Masson, F., Structure de l'acide desoxyribonucleique en solution: étude par diffusion des rayons X aux petits angles, 185
— Witz, J. & Nicolaieff, A., Détermination de la masse et des dimensions des protéines en solution par la diffusion centrale des rayons X mesurée à l'échelle absolue: exemple du lysozyme, 367
— — La structure de la sérum albumine du boeuf en solution à pH 5,3 et 3,6: étude par diffusion centrale absolue des rayons X, 379
Lysogenizing properties and DNA content of a mutation in bacteriophage λ, 399
Lysozyme, study of the structure in solution by low-angle X-ray scattering, 367

Maaløe, O. & Hanawalt, P. C., Thymine deficiency and the normal DNA replication cycle I, 144
— (see Hanawalt, P. C.), 156
MacRae, T. P. (see Fraser, R. B. D.), 640
Marmur, J. (see Schildkraut, C. L.), 595
— A procedure for the isolation of deoxyribonucleic acid from micro-organisms, 208
— & Doty, P., Thermal renaturation of deoxyribonucleic acids, 585
Marvin, D. A., Spencer, M., Wilkins, M. H. F. & Hamilton, L. D., The molecular configuration of deoxyribonucleic acid III. X-ray diffraction study of the *C* form of the lithium salt, 547
Masson, F. (see Luzzati, V.), 185, 566, 634
McFall, E., Effects of ^{32}P decay on enzyme synthesis, 219
Mercuripapain, a new crystalline form, 110
Micro-organisms, a procedure for the isolation of DNA, 208
Miller, I. R., The structure of DNA and RNA in the water-mercury interface, 229
— Temperature dependence of the adsorption of native DNA in a polarized water-mercury interface, 357
Molecular weight series derived from the nucleic acid of bacteriophage of T2, 458

Monod, J. (see Jacob, F.), 318
Moustafa, Z. H. (see Wacker, A.), 790
Muirhead, H. (see Stockell, A.), 112
Multiplicity reactivation of phage after heat disruption, 125
Muscle, X-ray diffraction studies on large scale molecular structure, in insects, 618
Muscles, molluscan, low-angle X-ray reflections, 41
Mutagenesis, of bacteriophage T4 by acridines, theory, 762
— theory of its mechanisms, 121
Mutagenic action of hydroxylamine, 133
Mutation affecting the DNA content of bacteriophage λ and its lysogenizing properties, 399
Mutch, M. O. (see Williams, J.), 532
Myoglobin, from sperm whale, optical rotatory dispersion, 769
Myoglobins, comparative studies on tryptic digests, 362

Nagashima, N. (see Tsuboi, M.), 705
Nicolaieff, A. (see Luzzati, V.), 185, 367, 379
Nomura, M. & Benzer, S., The nature of the "deletion" mutants in the *r*II region of phage T4, 684
Novick, A. (see Horiuchi, T.), 703
Nucleic acid of T2 bacteriophage, a relative molecular weight series, 458
Nucleic acids, fractionation in aqueous polymer two-phase systems, 727
— infrared spectra when formamide-treated, 741
Nucleotides, reaction with formaldehyde, 47

Okamoto, T. (see Takanami, M.), 476
Oota, Y. (see Otaka, E.), 693
Optical rotatory dispersion of sperm whale ferrimyoglobin and horse ferrihemoglobin, 769
Orgel, A. (see Brenner, S.), 121
— & Brenner, S., Mutagenesis of bacteriophage T4 by acridines, 762
Osawa, S. (see Otaka, E.), 693
Otaka, E., Osawa, S. & Oota, Y., The effect of 8-azaguanine on the ribonucleic acid of the ribosomes in *Bacillus cereus*, 693
Oth, A. (see Fredericq, E.), 11
Oxidation-reduction, a new mechanism applied to the epimerization of uridine diphospho-galactose and uridine diphosphoglucose, 318

^{32}P decay, effects on enzyme synthesis, 219
— stabilization to and onset of replication of T4 bacteriophage, 409
Park, R. B. & Pon, N. G., Correlation of structure with function in *Spinacea oleracea* chloroplasts, 1
Perutz, M. F. (see Stockell, A.), 112
Phage (see bacteriophage), 267
Phosphatase, alkaline, genetic control of repression in *E. coli*, 425
van de Pol, J. H. (see Daems, W. Th.), 225
Polyadenylic acid, molecular structure, 71
Poly-γ-benzyl-L-glutamate, structure in solution and transitions between different helical forms, 566
Polymer two-phase systems, used for fractionation of nucleic acids, 727
Polynucleotide chains derived from T2 and T4 bacteriophage, 289
Polypeptide chains of haemoglobin A_2 and haemoglobin G_2, 257
Polypeptide chains, sidechain-sidechain interaction between L- and D- forms of α-helices, 705
Pon, N. G. (see Park, R. B.), 1
Pratt, D., Stent, G. S. & Harriman, P. D., Stabilization to ^{32}P decay and onset of DNA replication of T4 bacteriophage, 409
Price, W. C. (see Bradbury, E. M.), 301
Proflavine, interaction with DNA, a small angle X-ray scattering study, 634

Protein structure and coincidence, 532
Protein synthesis, genetic regulatory mechanisms, 318

Radiation-sensitizing action of 5-bromouracil, 787
Radioactive phosphorus decay in phage T4, multiplicity reactivation, 61
Regulatory system, temperature sensitive, 703
Replication of DNA, 144, 156
Resilin, a rubber-like protein, molecular interpretation and elasticity, 648
— thermodynamic properties, 520
Ribonucleic acid, configuration by electron microscopy, 778
— soluble, effect of urea and heat treatments on activity, 476
— two-stranded helical configurations, 175
— structure in the water-mercury interface, 229
— of *B. cereus* ribosomes, effect of 8-azaguanine, 693
— of TMV, reaction with hydroxylamine, 447
Ribosomes, *B. cereus*, effect of 8-azaguanine on RNA, 693
— X-ray diffraction studies, 87
Rich, A. & Crick, F. H. C., The molecular structure of collagen, 483
— Davies, D. R., Crick, F. H. C. & Watson, J. D., The molecular structure of polyadenylic acid, 71
Richie, D. A. (see Symonds, N.), 61
Robichon-Szulmajster, H. de., Sur un nouveau mécanisme d'oxydo-réduction, appliqué à la réaction d'epimérization: uridinediphosphogalactose ⇌ uridinediphosphoglucose, 253
Rogers, G. E. (see Filshie, B. K.), 784

Schaechter, M. (see Hanawalt, P. C.), 156
Schell, P. (see Brown, D. M.), 709
Schildkraut, C. L., Marmur, J. & Doty, P., The formation of hybrid DNA molecules and their use in studies of DNA homologies, 595
Schuster, H., The reaction of tobacco mosaic virus ribonucleic acid with hydroxylamine, 447
Serum albumin, study of structure in solution by low-angle X-ray scattering, 379
Shimanouchi, T. (see Kyogoku, Y.), 741
Shooter, E. M. (see Huehns, E. R.), 257
— (see Atwater, J.), 707
Simon, E. H., Transfer of DNA from parent to progeny in a tissue culture line of human carcinoma of the cervix (strain HeLa), 101
Spach, G. (see Luzzati, V.), 566
Spencer, M. (see Marvin, D. A.), 547
Spinacea oleracea chloroplasts, correlation of structure with function, 1
Spirin, A. S. (see Kisselev, N. A.), 778
Stent, G. S. (see Pratt, D.), 409
Stockell, A., A new crystalline form of mercuripapain, 110
— Comparative studies on tryptic digests of myoglobins, 362
— Perutz, M. F., Muirhead, H. & Glauser, S. C., A comparison of adult and foetal horse haemoglobins, 112
Sueoka, N., Variation and heterogeneity of base composition of deoxyribonucleic acids; a compilation of old and new data, 31
Symonds, N. & Richie, D. A., Multiplicity reactivation after the decay of incorporated radioactive phosphorus in phage T4, 61

T2 (see bacteriophage), 47, 277, 289, 458, 756
T4 (see bacteriophage), 61, 277, 289, 409, 684, 762
T4B (see bacteriophage), 225
Takanami, M., Okamoto, T. & Watanabe, I., Effect of urea and heat treatments on the activity of soluble ribonucleic acid, 476
Temperature-sensitive regulatory system, 703
Thermal denaturation of sodium deoxyribonucleate, changes in ionic activities, 202

Thiouracil, causing the synthesis by *E. coli* of an abnormal β-galactosidase, 166
Thomas, C. A., Jr. (see Beer, M.), 699
— (see Berns, K. I.), 289
— & Berns, K. I., The physical characterization of DNA molecules released from T2 and T4 bacteriophage, 277
Thymine deficiency and the normal DNA replication cycle I, 144
Tobacco mosaic virus, protein subunit, 117
— ribonucleic acid, reaction with hydroxylamine, 447
Torriani, A. (see Echols, H.), 425
Träger, L. (see Wacker, A.), 790
Trypsin-sensitive factor in multiplicity reactivation of heat disrupted phage, 125
Tryptic digests of myoglobins, comparative studies, 362
Tsuboi, M. (see Kyogoku, Y.), 741
— & Wada, A., On the 1700 cm^{-1} band of the cross-β structure, 480
— Wada, A. & Nagashima, N., Sidechain-sidechain interaction between the α-helices of L- and D- polypeptide chains, 705

Uchida, H. (see Kozinski, A. W.), 267
Ultraviolet spectrum of DNA, 11
Urea, effect on activity of soluble RNA, 476
Uridine and uracil, photochemical reactions, 790
Uridinediphosphogalactose and uridinediphosphoglucose epimerization, a new mechanism, 253

Vincent, J. M. (see Luzzati, V.), 566

Wacker, A., Dellweg, H. & Weinblum, D., Über die strahlensensibilisierende Wirkung des 5-Bromuracils, 787
— Weinblum, D., Träger, L. & Moustafa, Z. H., Photochemische reaktionen von Uracil und Uridin, 790
Wada, A. (see Tsuboi, M.), 480, 705
— Regularity in the chain configuration of D,L-copoly-γ-benzyl glutamate, 507
Watanabe, I. (see Kiho, Y.), 125
— (see Kyogoku, Y.), 741
— (see Takanami, M.), 476
Watson, J. D. (see Rich, A.), 71
Weigle, J. J. (see Kellenberger, G.), 399
— Densities of transducing lambda bacteriophages, 393
Weis-Fogh, T., Thermodynamic properties of resilin, a rubber-like protein, 520
— Molecular interpretation of the elasticity of resilin, a rubber-like protein, 648
Weinblum, D. (see Wacker, A.), 787, 790
Wilkins, M. H. F. (see Marvin, D. A.), 547
Wilkinson, G. R. (see Bradbury, E. M.), 301
Williams, J., Clegg, J. B. & Mutch, M. O., Coincidence and protein structure, 532
Witz, J. (see Luzzati, V.), 367, 379
Worthington, C. R., X-ray diffraction studies on the large-scale molecular structure of insect muscle, 618

X-ray diffraction studies, on the large-scale molecular structure of insect muscle, 618
— study on the *C* form of lithium DNA, 547
X-ray low-angle scattering study, of DNA interaction with proflavine, 634
— of lysozyme, 367
— of beef serum albumin, 379
— of DNA in solution, 185
X-ray studies of ribosomes, 87

Zimm, B. H. (see Longuet-Higgins, H. C.), 475
Zichichi, M. L. (see Kellenberger, G.), 399
Zobel, C. R. (see Beer, M.), 717

Journal of Theoretical Biology

Chief Editor: J. F. Danielli

VOLUME I, 1961

Number 4, December

FISHER, SIR RONALD, A Model for the Generation of Self-Sterility Alleles

SUGITA, MOTOYOSI, Functional Analysis of Chemical Systems *in vivo* using a Logical Circuit Equivalent

ROSS ASHBY, W. AND RIGUET, J., The Avoidance of Over-Writing in Self-Organizing Systems

FUKUDA, NUBUO AND SUGITA, MOTOYOSI, Mathematical Analysis of Metabolism using an Analogue Computer: I. Isotope Kinetics of Iodine Metabolism in the Thyroid Gland

JOSEPHSON, ROBERT K., REISS, RICHARD F. AND WORTHY, R. M., A Simulation Study of a Diffuse Conducting System based on Coelenterate Nerve Nets

STEINBERG, CHARLEY AND STAHL, FRANK, The Clone-Size Distribution of Mutants arising from a Steady-State Pool of Vegetative Phage

RESCIGNO, A. AND SEGRE, G., The Precursor–Product Relationship

WARNER, DONALD T., Proposed Molecular Models: II. Conformations of Staphylomycin and other Polypeptides and a Possible Relation to the Structure of Water,

NAFATLIN, L. AND SPENCER HARRISON, M., Ion-Exchange Mechanisms in the Membranous Labyrinth: a Suggested Basis for the Sudden Attacks in Ménière's Disease

GAUSE, G. F., The Biological Designing of Antimetabolites for Malignant Growth

PERRET, C. J. AND LEVEY, H. C., The Theory of Uncatalysed Linear Expanding Systems

Note of Acknowledgment—
Evolution and the Theory of Games, R. C. LEWONTIN

The price of this volume is 121*s.* 6*d.* ($17.00) *or* 86*s.* ($12.00)
for private subscription

ACADEMIC PRESS, LONDON AND NEW YORK

IN STACK
3 Apr '63 D
3 AP 63 F
64 F
BRARY LOAN

CONTENTS

KIT, S., Equilibrium Sedimentation in Density Gradients of DNA Preparations from Animal Tissues 711

BEER, M. and ZOBEL, C. R., Electron Stains II : Electron Microscopic Studies on the Visibility of Stained DNA Molecules 717

LIF, T., FRICK, G. and ALBERTSSON, P. Å., Fractionation of Nucleic Acids in Aqueous Polymer Two-Phase Systems 727

KYOGOKU, Y., TSUBOI, M., SHIMANOUCHI, T. and WATANABE, I., Infrared Spectra of Formamide-treated Nucleic Acids 741

KOZINSKI, A. W. and BESSMAN, M. J., The Kinetics of Parental Deoxyribonucleic Acid Replication, Deoxyguanylate Kinase Formation and ^{32}P-Inactivation of the Parental Virus in *Escherichia Coli* Infected with Bacteriophage T4 746

CAIRNS, J., An Estimate of the Length of the DNA Molecule of T2 Bacteriophage by Autoradiography 756

ORGEL, A. and BRENNER, S., Mutagenesis of Bacteriophage T4 by Acridines 762

BEYCHOK, S. and BLOUT, E. R., Optical Rotatory Dispersion of Sperm Whale Ferrimyoglobin and Horse Ferrihemoglobin 769

KISSELEV, N. A., GAVRILOVA, L. P. and SPIRIN, A. S., On Configurations of High Polymer Ribonucleic Acid Macromolecules as Revealed by Electron Microscopy 778

Letters to the Editor—

The Fine Structure of α-Keratin, B. K. FILSHIE and G. E. ROGERS . 784

Über die Strahlensensibilisierende Wirkung des 5-Bromuracils, A. WACKER, H. DELLWEG and D. WEINBLUM 787

Photochemische Reaktionen von Uracil und Uridin, A. WACKER, D. WEINBLUM, L. TRÄGER and Z. H. MOUSTAFA . . . 790

Recommendations for the Nomenclature of Hemoglobins, P. S. GERALD and V. M. INGRAM 794

Printed in Great Britain at the Aberdeen University Press